

AN ABSTRACT OF THE THESIS OF

GARY BRUCE GRIGGS for the Ph. D.  
(Name of student) (Degree)  
in Oceanography presented on November 8, 1968  
(Major) (Date)

Title: CASCADIA CHANNEL: THE ANATOMY OF A DEEP-SEA  
CHANNEL

Abstract approved: \_\_\_\_\_

**Redacted for Privacy**

Dr. L. D. Kulm

Cascadia Channel is the most extensive deep-sea channel known in the Pacific Ocean and extends across Cascadia Abyssal Plain, through the Blanco fracture zone, and onto Tufts Abyssal Plain. The channel is believed to be over 2200 km in length and has a gradually decreasing gradient of about 1:1000, except where it is interrupted by an axial depression. Maximum relief of the channel reaches 300 m on the abyssal plain, and 1100 m in the mountains of the fracture zone. The right (north and west) bank is consistently about 30 m higher than the left (south and east). This difference in height is explained by the development of levees along the right side of the upper channel, but may be due to structural factors along the remainder of the course. A number of tributaries enter Cascadia Channel which give rise to an extensive submarine drainage system.

Turbidity currents have been depositing thick, olive green silt sequences throughout upper and lower Cascadia Channel during Holocene time. The sediment is derived primarily from the Columbia River and is transported to the channel through Willapa Canyon. A cyclic alternation of the silt sequences and thin layers of hemipelagic gray clay extends for at least 650 km along the axis of the channel. Similar Holocene sequences, which are thinner and finer-grained, occur on the walls and levees of the upper channel and indicate that turbidity currents have risen high above the channel floor to deposit their characteristic sediments. A thin surficial covering of Holocene sediment along the middle channel floor demonstrates the erosional or non-depositional nature of the turbidity currents in this area.

The Holocene turbidity current deposits are graded texturally and compositionally, and contain Foraminifera from neritic, bathyal, and abyssal depths which have been size sorted. A sequence of sedimentary structures occurs in the deposits similar to that found by Bouma in turbidites exposed on the continent. Graded, parallel laminated, cross-laminated, and pelitic intervals have all been recognized. There is a sharp break in the textural and compositional properties of each graded bed. The coarser-grained, more positively skewed basal zone of each bed probably represents deposition from the traction load. The finer-grained, organic-rich upper portion of each graded bed represents deposition from the suspension

load. Individual turbidity current sequences are thinnest in the proximal environments (upper channel) and thickest in the distal environments (lower channel). The uniform sequences along the lower channel can be correlated over at least 140 km. Turbidity current recurrence intervals are shorter in the upper channel (400 to 500 yrs) than in the lower channel in Cascadia Basin (500 to 600 yrs), and on Tufts Abyssal Plain (825 to 1500 yrs). Each flow recorded near shore evidently did not extend the entire length of the channel. Based on the distribution of the turbidity current deposits and the occurrence of submarine levees it has been determined that individual flows reach heights of at least 117 m and spread laterally to the west as far as 17 km from the channel axis. Flow velocities calculated from the equation of Middleton range from 5.8 m/sec along the upper channel to 3.3 m/sec along the lower portion. A turbidity current with an average velocity of 4 m/sec would take about two days to travel the entire length of the surveyed portion of Cascadia Channel.

Pleistocene sediments of Cascadia Channel and the adjacent areas have recorded a different set of climatic and depositional conditions. Pleistocene turbidity currents were much more extensive areally than the Holocene flows, and deposited sediment which was coarser and cleaner. The pronounced levees bordering the upper channel are due chiefly to overflow during the Pleistocene.

Gravels have been found up to 740 km from shore along the axis of Cascadia Channel and apparently were transported to the abyssal environment by the more competent Pleistocene turbidity currents. Sections of glacial marine sediment cored along the axis and wall of the channel indicate ice bergs from the Cordilleran glacier complex floated as far south as  $44^{\circ}10'N$ . during the late Pleistocene. The distribution of these sediments demonstrates that the late Pleistocene surface circulation in this area was similar to the present-day pattern. The northeast Pacific Gyral may have been farther north during the Pleistocene, but it is very unlikely that it was south of its present position.



Cascadia Channel: The Anatomy  
of a Deep-Sea Channel

by

Gary Bruce Griggs

A THESIS

submitted to

Oregon State University

in partial fulfillment of  
the requirements for the  
degree of

Doctor of Philosophy

June 1969

APPROVED:

Redacted for Privacy

---

Professor of Oceanography  
in charge of major

Redacted for Privacy

---

Chairman of Department of Oceanography

Redacted for Privacy

---

Dean of Graduate School

Date thesis is presented November 8, 1968

Typed by Opal Grossnicklaus for Gary Bruce Griggs

## ACKNOWLEDGMENTS

I would like to express sincere gratitude to Dr. L. D. Kulm, my major professor, for introducing me to the deep-sea environment and for guiding me through the study. His interest and time, as well as his critical review of the manuscript are especially appreciated.

Discussions and assistance from Dr. William H. Taubeneck, Dr. Gerald A. Fowler, Dr. Karl Wolf, Dr. June Pattullo, Dr. Aaron C. Waters, and Dr. John C. Crowell, are appreciated. Thanks are extended to Eric Crecelius and Roger Paul for laboratory assistance, to Michael King for help with drafting, and to Gail Lowell for assistance with computer programming.

Many stimulating discussions held with Dr. John R. Duncan and David W. Allen were especially helpful. Appreciation is also extended to the staff members and students of the Department of Oceanography, Oregon State University, and to the personnel of the R/V Yaquina who helped with the collection of data at sea.

For the constant inspiration and assistance of my wife, Linda, through the entire course of the study, I am very grateful. I also would like to thank my parents for their encouragement throughout the many years of education which culminates in this dissertation.

This research was made possible through the financial support of the National Science Foundation (Grants GP-5076 and GA-1246)

and the Office of Naval Research (Contract Nonr 1286(10) and by the use of shipboard and laboratory facilities of the Department of Oceanography. A graduate fellowship from the National Science Foundation from 1966 to 1968 supplied personal financial support.

## TABLE OF CONTENTS

INTRODUCTION	1
SUBMARINE PHYSIOGRAPHY	6
Cascadia Abyssal Plain and Adjacent Areas	6
Cascadia Channel	8
Bathymetry Procedures	8
Longitudinal Development of Cascadia Channel	10
Development of Channel Morphology	13
COLLECTION AND ANALYSIS OF DATA	19
Sample Collection	19
Core Processing	19
Sample Analysis	22
STRATIGRAPHY	26
Mt. Mazama Volcanic Ash	26
Planktonic Foraminifera-Radiolaria Abundance	27
Paleoclimatology	31
Stratigraphic Variations	39
SEDIMENT TYPES	41
Olive Green Silt	43
Gray Clay	47
Terrigenous Sand-Silt	50
Gravels	53
Pebbly Clays	54
Foraminiferal Ooze	56
PHYSIOGRAPHIC DISTRIBUTION OF SEDIMENTS	58
Upper Channel	58
Middle Channel	61
Lower Channel	64
Channel Walls	66
Channel Banks and Levees	70
Vancouver Sea Valley and Astoria Fan Tributaries	73
Cascadia Abyssal Plain	75
Summary of Sediment Distribution	75

## TABLE OF CONTENTS (CONTINUED)

DEPOSITIONAL PROCESSES	79
Holocene Turbidity Currents--Empirical Data	79
Foraminiferal Distribution	81
Mt. Mazama Ash Distribution	83
Textural and Structural Variations	84
Correlation of Flows	92
Flow Periodicity	95
Holocene Turbidity Currents--Flow Reconstruction	100
Flow Dimensions	100
Geometry of Deposits	103
Velocity Determinations	104
Pleistocene Turbidity Currents	107
Ice Rafting	110
Eolian Transportation	113
Slumping and Sliding	113
Pelagic and Hemipelagic Deposition	114
MINERALOGY, PETROLOGY AND PROVENANCE OF SEDIMENTS	115
Clay Mineralogy	115
Olive Green Silts	115
Gray Clays	117
Pebbly Clays	122
Sand Mineralogy	122
Suite I	123
Suite II	125
Suite III	125
Pebble Petrology	126
Gravels	126
Pebbly Clays	127
SEDIMENT DISPERSAL	130
Pleistocene	130
Holocene	136
CHANNEL ORIGIN	141
CONCLUSIONS AND GEOLOGIC HISTORY	144
BIBLIOGRAPHY	150

## TABLE OF CONTENTS (CONTINUED)

LEGEND FOR APPENDICES	159
APPENDIX 1. Piston core station locations	160
APPENDIX 2. Radiocarbon age determinations	162
APPENDIX 3. Texture and coarse fraction composition of sediment samples	163
APPENDIX 4. Percent by weight of organic carbon and calcium carbonate in sediment samples	177
APPENDIX 5. Heavy mineral composition for the sand fraction of sediment samples	179
APPENDIX 6. Quantitative analyses of chlorite, illite and montmorillonite from X-Ray diffraction records	180
APPENDIX 7. Channel dimensions on cross-sectional profiles	181
APPENDIX 8. Sedimentation rates and percentage of core consisting of coarse material	182

## LIST OF FIGURES

<u>Figure</u>	<u>Page</u>
1. Submarine and continental physiography in the vicinity of Cascadia Channel	4
2. Precision Depth Recorder track lines and bathymetry in the vicinity of Cascadia Channel	9
3. Gradient and longitudinal variation in relief and depth to banks of Cascadia Channel	12
4. Piston core location map for Cascadia Channel and tributaries.	20
5. Flow sheet for core processing and sample analysis	21
6. Distribution of volcanic ash from Mt. Mazama on the continent and in the marine environment	28
7. Summary and correlation of late Pleistocene and Holocene glacial chronology, floral and faunal stratigraphy, and sea level rise	30
8. Faunal stratigraphy of selected cores from the axis of Cascadia Channel and its tributaries	37
9. Faunal stratigraphy of selected cores from walls and banks of Cascadia Channel	38
10. Lithology of olive green silt sequence in various channel environments	44
11. Vertical variation in texture and composition of typical olive green silt sequence from Cascadia Channel	45
12. Texture and composition of olive green silt sequences	46
13. Texture and composition of gray clay	49
14. Texture and composition of selected terrigenous sand-silt sequences	51



# LIST OF FIGURES (CONTINUED)

<u>Figure</u>		<u>Page</u>
15.	Texture and coarse fraction composition of terrigenous sand-silts, gravels, pebbly clays, and foraminiferal oozes	52
16.	X-Radiographs of Pleistocene pebbly clays	55
17.	Physiographic divisions of Cascadia Channel	59
18.	Lithology of cores from upper Cascadia Channel	60
19.	Lithology of cores from middle Cascadia Channel	62
20.	Longitudinal stratigraphic correlation of cores from axis of middle Cascadia Channel	63
21.	Lithology of cores from lower Cascadia Channel	65
22.	Lithology of cores from lower Cascadia Channel (Blanco fracture zone)	67
23.	Lithology of cores from walls of Cascadia Channel	69
24.	Lithology of cores from banks and levees of Cascadia Channel	71
25.	Lithology of cores from Vancouver Sea Valley and Astoria Fan tributaries	74
26.	Holocene and Pleistocene sediment facies along the axis of Cascadia Channel	77
27.	Olive green silt sequence from lower Cascadia Channel axis illustrating textural and microfaunal variations	82
28.	Complete turbidite sequence and turbidity current sequences from Cascadia Channel	85
29.	Histograms of thicknesses of individual Holocene turbidity current sequences along Cascadia Channel axis	90

## LIST OF TABLES

<u>Table</u>	<u>Page</u>
1. Recognized deep-sea channels of the world's oceans and their characteristics	3
2. Summary of Cascadia Channel morphology	14
3. Sediment types and their characteristics	42
4. Recurrence intervals for Holocene turbidity currents	96
5. Dimensions of Holocene turbidity currents in Cascadia Channel	102
6. Holocene turbidity current velocities	106
7. Comparisons between Pleistocene and Holocene turbidity current deposits in Cascadia Basin	108
8. Comparative clay mineralogy of Cascadia Basin and Columbia River sub-basin sediments	121
9. Average percentage composition of heavy mineral suites	124
10. Comparative lithologies of bedrock in areas scoured by glaciers, and erratics contained in glacial deposits	128

# CASCADIA CHANNEL: THE ANATOMY OF A DEEP-SEA CHANNEL

## INTRODUCTION

Submarine canyons, fans, abyssal plains, and deep-sea channels are all integral parts of an enormous system which is continually shaping large areas of the earth's submerged surface. The erosion, transportation, and deposition of large volumes of sediment are the major processes acting in these areas. Most of this sediment is terrestrial material brought to the marine environment by rivers. It commonly becomes unstable at the site of deposition and may begin to flow downslope within a submarine canyon. When the sediment emerges from the mouth of a canyon, it may move as a sheet flow, eventually developing a fan or an abyssal plain. The flow may also be partly channelized due to structural features, and processes of erosion and/or deposition may produce a deep-sea channel.

The first element in this sediment transport system, the submarine canyon, has been studied intensively on continental margins around the world (Shepard and Dill, 1966). Many of the major deep-sea fans have also been studied in some detail (Menard, 1960; Menard, Smith and Pratt, 1965; Wilde, 1965; Nelson, 1968). The distribution and morphology of many of the abyssal plains are well known; however, the sedimentation picture is not as well understood, although a large amount of information has been collected. Deep-sea

channels often tie submarine canyons, deep-sea fans, and abyssal plains together and provide a connecting link between the continents and the deep ocean floor often hundreds of kilometers away.

Deep-sea channels have been found in all of the world's oceans (Table 1) but have not been studied in a detailed manner. Most of the studies concerning channel origin and sedimentation have been based on a small number of channel profiles and short sediment cores. Recently, however, acoustic reflection profiling has provided new information on channel structure and development (Hamilton, 1967). The determination of the processes taking place in a deep-sea channel and on the adjoining abyssal plain and their spatial and temporal importance are the principal objectives of this study. The lateral, longitudinal, and vertical extent of the sedimentary deposits in the deep-sea channels, as well as their internal characteristics, must be determined in order to reconstruct these processes. The origin and historical development of deep-sea channels and their relationships to the extensive abyssal plains are questions to be ultimately answered.

Cascadia Channel, because of its proximity to the coastline, is an excellent location in which to investigate in detail the characteristics of a deep-sea channel, and its relationship to two abyssal plains (Figure 1). Cascadia Channel is the most prominent and extensive deep-sea channel known in the Pacific Ocean. It originates

Table 1. Recognized deep-sea channels of the world's oceans and their dimensions and characteristics

Canyon or Channel	Length (km)	Max. Width (km)	Max. Depth (m)	Cross-sectional shape	Bank Relief	Levees	Longitudinal gradient	Reference
INDIAN OCEAN								
Bengal Abyssal Plain channels	750	7.5	75	U-shaped				Dietz (1953)
ATLANTIC OCEAN								
Outer channel of Hudson canyon	>240		600	broad leveed channel	right (south) bank higher	right bank		Pratt (1967)
Northwest Atlantic Mid-ocean Canyon	2200	8	180	steep walls flat floor	right (west) bank 18 to 27 m higher		1:2250	Ewing <u>et al.</u> (1953)
Outer Congo Canyon	>800	8	1100	V to flat bottom		in outer reaches 8 to 32 km wide	outer portion 1:600	Heezen <u>et al.</u> (1954)
Iberia-Biscay inter-plain channel		16	155	V to flat bottom			1:1500 to 1:2500	Laughton (1960)
PACIFIC OCEAN								
Outer channels of Monterey Canyon	270	4.5	230			west bank to height of 27 m		Dill <u>et al.</u> (1954) Menard (1960)
Surveyor Channel	>500	5	220				1:330	Gibson (1960)
Baker Channel		6.5	200	V with flat floor	right (west) bank higher in outer channel	west bank		Hurley (1960)
Scott Channel		7.5	200	V with irregular floor	right (northwest) bank higher	either side		Hurley (1960)
Moresby Channel		13	200	V-shaped	right (northwest) bank higher	either side		Hurley (1960)
Cascadia Channel	2200	9.3	300	U-shaped with flat floor	right (north & west) bank 6 to 70 m higher	right bank, 7.5 km wide, 28 m high	Ave. 1:1000 1:600 - 1:4000	this study

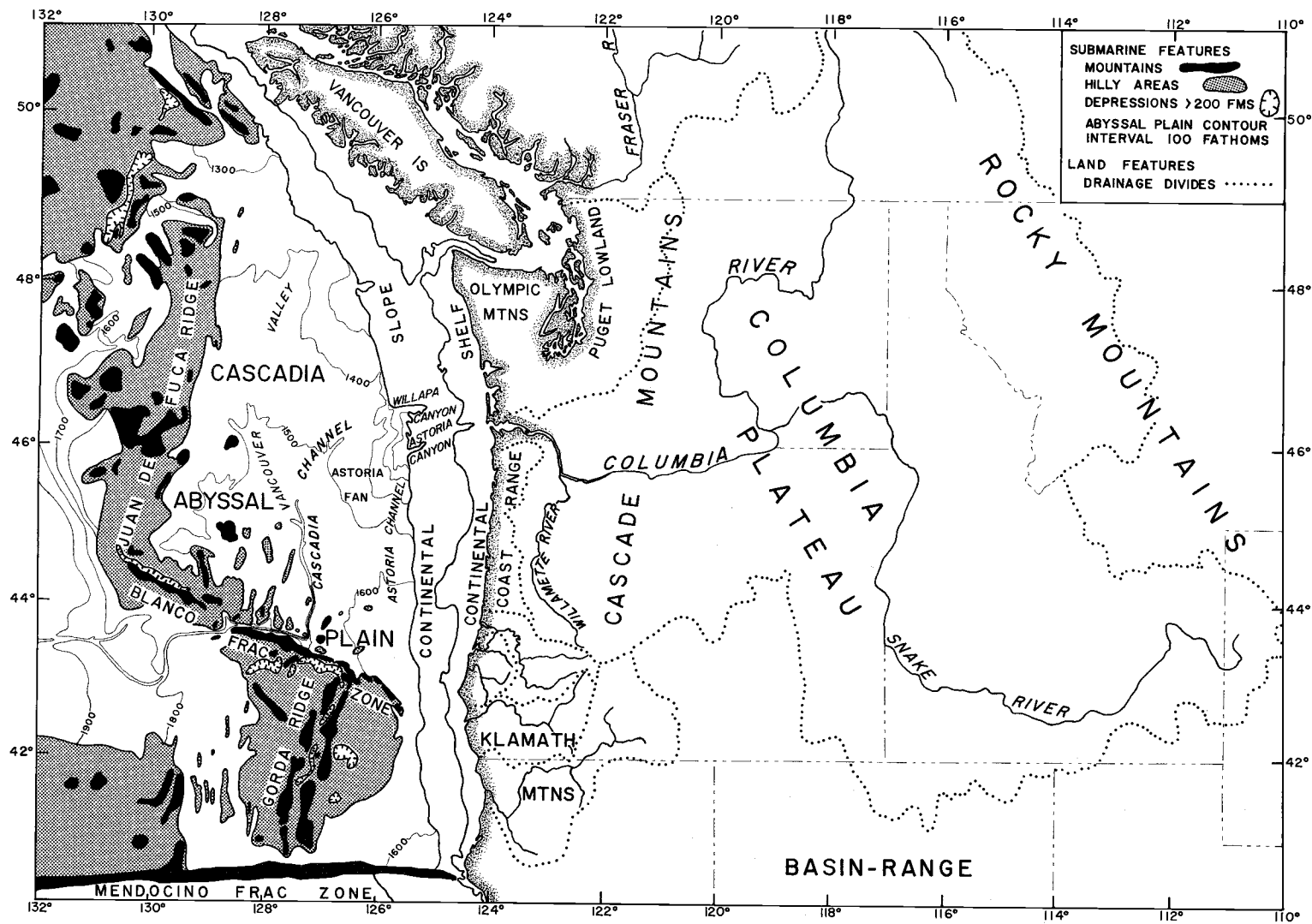


Figure 1. Submarine and continental physiography in the vicinity of Cascadia Channel

at the base of the continental slope off Oregon and Washington where several seachannels have merged. After crossing the southern portion of Cascadia Abyssal Plain, it passes through Blanco fracture zone and emerges onto Tufts Abyssal Plain where its course is less well known. Its total length is believed to be about 2200 km. (Hurley, 1960).

Cascadia Channel was first studied by Menard (1955) and later by Hurley (1960) in more detail. Royse (1964), Carlson (1967), and Nelson (1968) have studied submarine canyons and fans on the continental margin which connect with or are adjacent to Cascadia Channel. The sedimentation and stratigraphy of Cascadia Abyssal Plain and the adjacent areas has recently been studied by Duncan (1968) and serves as a foundation for this study.

## SUBMARINE PHYSIOGRAPHY

### Cascadia Abyssal Plain and Adjacent Areas

The northeastern Pacific Ocean has the most extensive system of abyssal plains in the entire Pacific Ocean Basin. Menard (1955) has attributed this to the accessibility of these areas to turbidity currents, as contrasted with those areas which are inaccessible due to physiographic barriers such as mountain chains, basins, or troughs. Cascadia Abyssal Plain partially fills a basin which lies off the coasts of Oregon, Washington, and Vancouver Island (Figure 1). It is bordered on the west by the submarine ridges and seamounts of the Juan de Fuca Rise, and on the south by Blanco fracture zone. These features act both as barriers to bottom transported material moving westward or southward across the plain, and as local sources of sediment. The plain is bounded on the north and east by the continental margin, which consists of the continental shelf and slope and two coalescing deep-sea fans. Nitinat Fan fills the northeast corner of the basin and is probably related to the Fraser River and possibly Nitinat and Fraser Canyons (Hurley, 1960). Astoria Fan, which has its apex at the mouth of Astoria Canyon, lies just offshore from the Columbia River mouth. This fan fills much of the eastern portion of the basin and merges into the abyssal plain. The continental margin bordering Cascadia Abyssal Plain is indented with a number



of submarine canyons, of which Astoria, Willapa, and Fraser canyons are the largest.

The floor of Cascadia Abyssal Plain has a consistent slope direction to the south, parallel to the continental margin rather than perpendicular to it as is more usual. The slope of the plain varies from 1:500 to 1:2000 with an average of about 1:800. The original definition of an abyssal plain required a slope less than 1:1000 (Heezen and Ericson, 1954), and therefore no agreement has been reached regarding the name of this flat area (McManus, 1964; 1967). Hamilton's (1967) recent reflection profiling survey of this area depicts a basin with an irregular volcanic basement. The region has been filled and partially leveled, primarily by turbidity current sedimentation, except at the base of the slope where submarine fans have developed. The southern portion of the plain is very flat and is characterized by buried seamounts whose peaks protrude through the smooth plain.

Several large channels cross Cascadia Abyssal Plain. Astoria Channel, the smaller of the two, is an extension of Astoria Canyon (Nelson, 1968) which crosses Astoria Fan and the eastern plain. Cascadia Channel, with its tributaries, is more extensive and traverses the southern half of Cascadia Abyssal Plain, passes through Blanco fracture zone and emerges onto Tufts Abyssal Plain.

## Cascadia Channel

### Bathymetry Procedures

A detailed bathymetric survey of Cascadia Channel and its tributaries was made in order to accurately determine the physiography of this prominent feature. Over 3000 km of Precision Depth Recorder (Times Facsimile Corporation Mark V) sounding tracks were made in the vicinity of the channel during Oregon State University cruises from 1965 to 1967 (Figure 2). Seventy-five channel crossings were made at an average interval of about ten kilometers. Loran A was used for positioning of all sounding lines, with fixes at 15 to 30 minute intervals (4.5 to 9 km). The bathymetric data was manually digitized from the PDR records, key punched, and plotted using an X-Y plotter coupled to an CDC 3300 computer. Unfortunately, all previous bathymetry in the area under investigation has been recorded in fathoms. In order to simplify the reporting of the data and to conform to the metric system, all depths were plotted and contoured in meters (Plate 1). Some interpolation was therefore necessary to relate the channel system to adjacent areas contoured in fathoms (Royse, 1964; Carlson, 1967; Nelson, 1968).

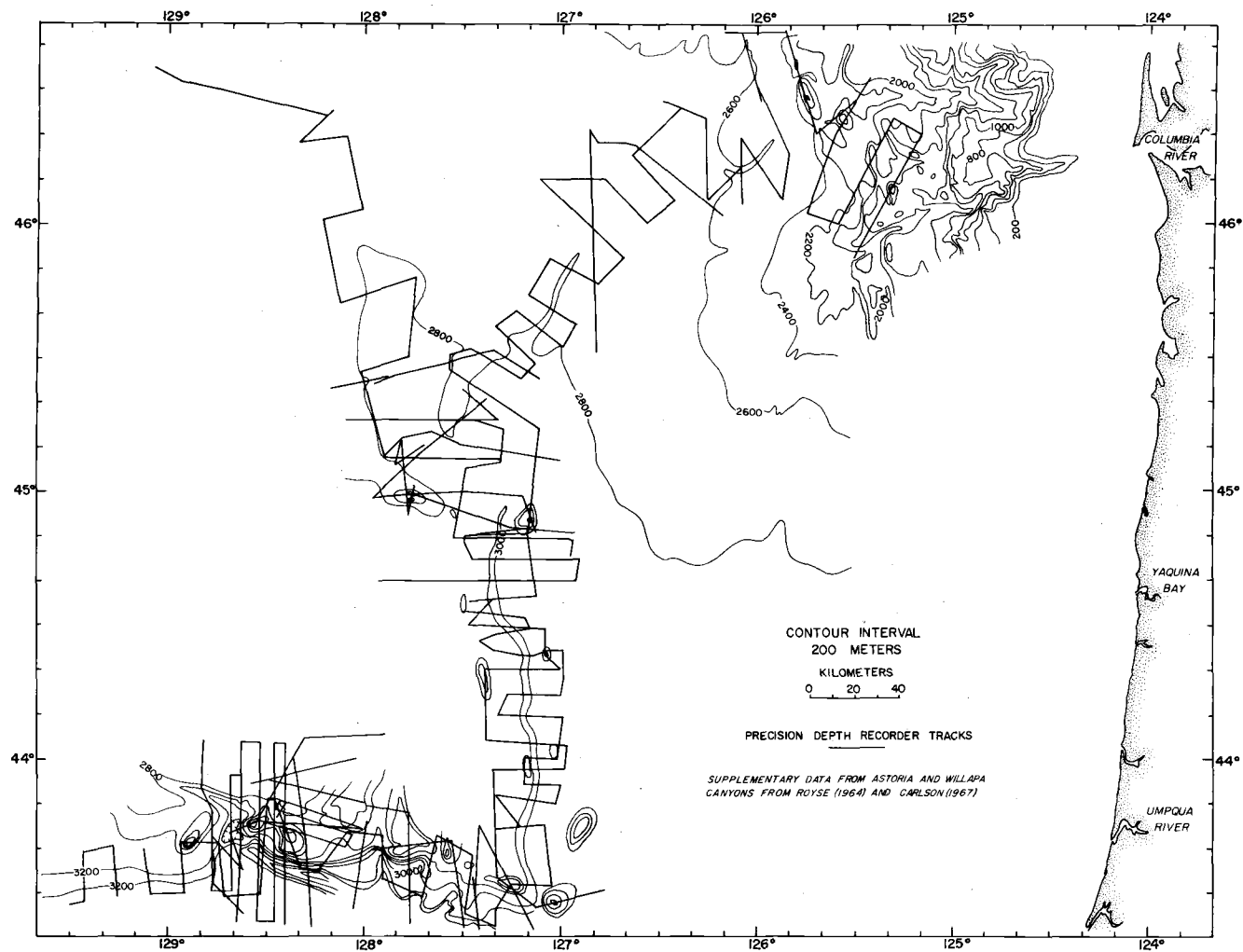


Figure 2. Precision Depth Recorder track lines and bathymetry in the vicinity of Cascadia Channel

### Longitudinal Development of Cascadia Channel

Cascadia Channel originates between Nitinat and Astoria Fans where Willapa Sea Channel and a second large channel merge (designated as the upper channel). The large unnamed channel originates at the apex of Nitinat Fan and trends south along the base of the slope for about 110 km where it turns to the southwest and joins Willapa Sea Channel. The latter appears to connect directly with Willapa Canyon through a gap in the hilly region at the base of the continental slope. The canyon lies about 28 km north of Astoria Canyon and heads 30 km off the Washington coast at a depth of about 200 m (Royse, 1964). Several of its tributaries seem to be offshoots or distributaries of Astoria Canyon, which heads 16 km west of the Columbia River mouth at a depth of about 100 m (Carlson, 1967). Astoria Canyon winds its way across the shelf and slope for about 120 km, and then turns sharply to the south to connect with Astoria Channel.

From its origin at a depth of about 2750 m, Cascadia Channel extends southwest for about 120 km in the furrow between Astoria and Nitinat Fans, and then turns to the south. A smaller channel, which crosses the southern part of Nitinat Fan, joins Cascadia Channel along the upper reaches of its course. From this point, the main channel trends almost due south for the next 220 km, meandering somewhat but confined to a zone about 20 km wide. A series of

seamounts on the east and west are apparently responsible for this lateral confinement. Two small channels, which cross the outer portion of Astoria Fan, enter from the east along this segment of Cascadia Channel. Vancouver Sea Valley, the largest channel tributary, joins the main channel from the northwest in this region. This valley extends northwestward for about 400 km forming the western boundary of Nitinat Fan, and heads near the base of the continental slope off Vancouver Island. The portion of Cascadia Channel which lies between its origin and Vancouver Sea Valley is designated the middle channel while the section which crosses southern Cascadia Abyssal Plain and passes through Blanco fracture zone will be referred to as the lower channel.

Cascadia channel makes a right angle turn to the west at  $43^{\circ} 30'N$ . and enters the Blanco fracture zone; it extends westward for about 150 km, confined between the submarine ridges and mountains of the fracture zone. In the mountains its course is sinuous, and several small, south trending channels enter the main channel from the north. Emerging from the fracture zone, Cascadia Channel turns south and then west again to begin its course across Tufts Abyssal Plain, where it is poorly known (Hurley, 1960).

The gradient of Cascadia Channel decreases gradually from about 1:625 at the base of the continental slope to 1:4000 on Tufts Abyssal Plain. It has an average gradient of about 1:1000 (Figure 3,

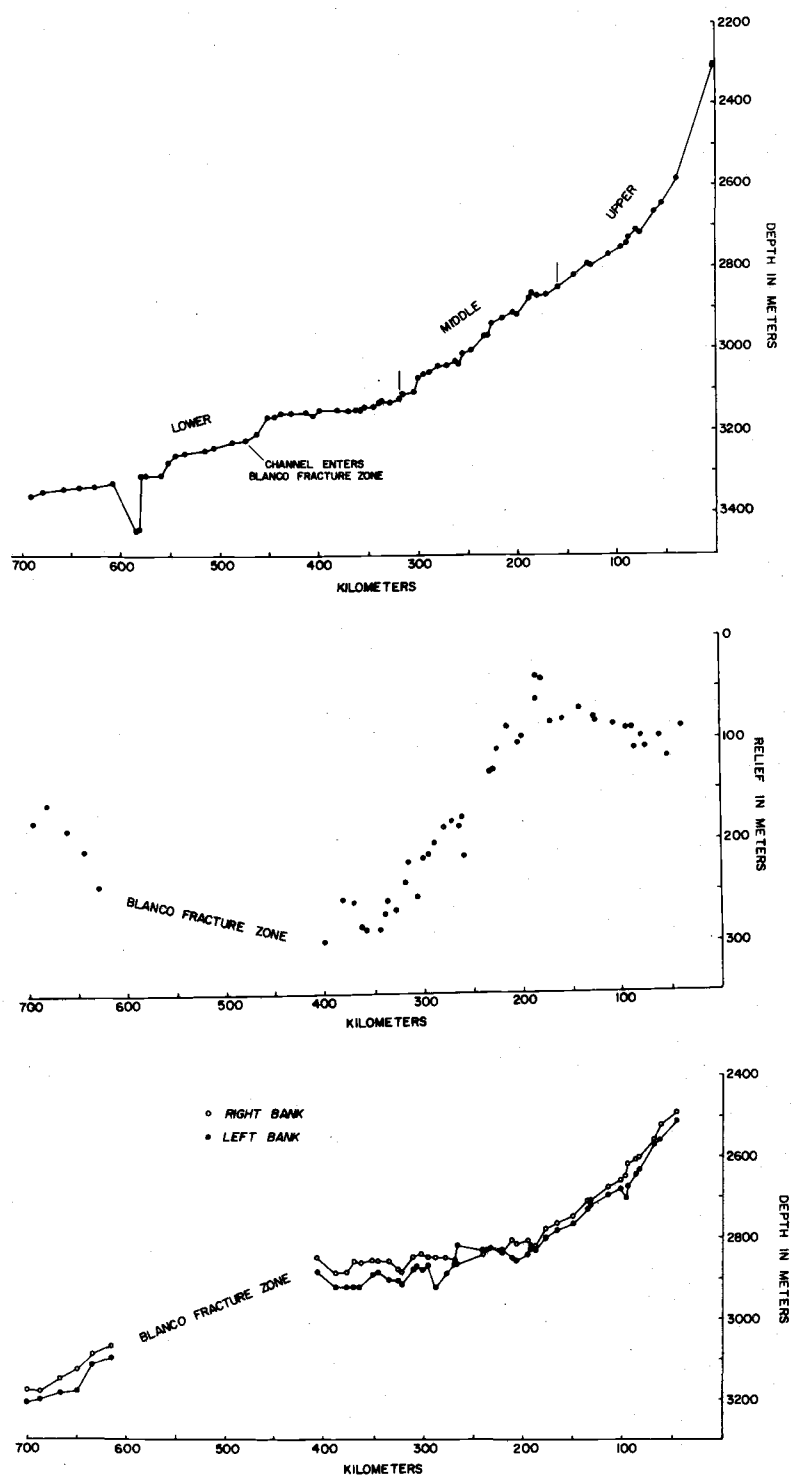


Figure 3. (Top) Longitudinal gradient of Cascadia Channel  
 (Middle) Longitudinal variation in channel relief  
 (Bottom) Longitudinal variation in depth to channel banks








top). The relatively smooth gradient of the channel floor is interrupted at least seven times by sections of reversed slope with maximum relief of two to eight meters. Slumping of sediment from the channel walls may be the cause of these humps or high areas along the channel axis. Near the western end of Blanco fracture zone the channel plunges 130 m into a very wide, recently depressed basin (Duncan, 1968). Vancouver Sea Valley has a fairly uniform gradient of about 1:1100, but it enters Cascadia Channel as a hanging valley, with a floor depth about 60 m above that of the main channel. This difference in depth suggests that either erosion has occurred in Cascadia Channel sometime after the formation of Vancouver Sea Valley, or that Vancouver Sea Valley is a fairly young feature and has never developed a continual gradient with Cascadia Channel.

#### Development of Channel Morphology

Cascadia Channel shows definite morphologic changes along its course across Cascadia Abyssal Plain, through Blanco fracture zone, and onto Tufts Abyssal Plain. The channel can be divided into distinct segments based upon its morphology in cross-section (Table 2).

Proceeding down the upper channel, the relief (depth from floor to highest bank) gradually decreases to the point at the base of the fans where the channel turns to the south (Figure 3, middle).

Table 2. Summary of Cascadia Channel morphology

Section number and length	Typical cross section (20X vertical exaggeration)	Average width (m)		Average channel relief (m)	Average bank relief (m)	Remarks
		Floor	Top			
UPPER CHANNEL						
1) 136 km		1050	2450	91	27	Levees common on right side; right side higher and steeper
MIDDLE CHANNEL						
2) 35 km		1910	3720	68	26	Channel widens and shallows; right side higher
3) 43 km		1390	3400	115		Seamounts on east; tributary channels enter here
LOWER CHANNEL						
4) 50 km		1430 floor 2890 terrace	6560	196	30	Terrace present; right bank steep and higher
5) 104 km		1040	5400	265	36	Channel narrows and deepens; right bank steeper and higher
6) 191 km		760	11300	583	238	Channel passes through fracture zone
7) 95 km		2550	6700	205	34	Channel on Tufts Abyssal Plain; right bank higher



Along the southward trending segment the relief increases to a maximum of 300 m before entering Blanco fracture zone. The channel relief in the fracture zone reaches a maximum of 1100 m, but is generally very irregular due to the seamounts which form the walls. As the channel emerges onto Tufts Abyssal Plain the relief begins to decrease regularly. The decrease in channel relief near the base of the fans and on Tufts Abyssal Plain is a result of changes in the height of its banks (i. e. from the presence of levees, fans, etc.), since the floor is a curve of almost continuously decreasing slope (Figure 3, top).

The right (west and north) bank of Cascadia Channel is consistently about 30 m higher (range 6 to 70 m) than the left (east and south) bank, if the seamounts of Blanco fracture zone and those along the east side of the channel at  $44^{\circ}50'N$ . are disregarded (Figure 3, bottom). This difference in relief has been noted in other channels by earlier investigators (Table 1). In upper Cascadia Channel levees are commonly developed on the right side of the channel which explain the difference in bank height on many crossings in this area. They rise as high as 28 m above the abyssal plain and extend up to 7.5 km away from the edge of the channel. The maximum relief from the levees to the channel floor is 117 m. Several upper channel crossings also show levees on the left bank, but these occur only on the outside of a large bend in the channel course. These levees rise as high

as 18 m and extend laterally for about 3 km. The middle and lower portions of Cascadia Channel which cross Cascadia and Tufts Abyssal Plain are devoid of levees. The consistently greater height of the right bank therefore must have some other origin, possibly structural.

The exact width of Cascadia Channel, both across the floor and the top, is often difficult to measure, because of the lack of a flat channel bottom on some crossings and because of a smooth transition from a steep wall to the horizontal abyssal plain in others. Most of the profiles display a smooth flat floor, but some are irregular, and, in others, the floor may slope gradually upward, merging with the walls. Each profile was made perpendicular to the channel trend using the existing bathymetry. The width of the channel floor varies along its course but in no consistent manner. It widens as one proceeds down the upper and middle channel from 650 to 3500 m where the channel turns to the south at  $45^{\circ}20'$  (Table 2, Section 2). This wide area, which is also very flat, occurs where the channel is also the shallowest, or at the point where the submarine fans merge with the abyssal plain. The channel gradient also decreases here and shows a section of reversed slope (Figure 3, top). This wide, flat portion of the channel with its decreased gradient is probably due to the deposition and ponding of large amounts of sediment in the channel axis. Along the remainder of the middle channel the bottom

width fluctuates between 600 and 2500 m. Below the union with Vancouver Sea Valley, the cross-sectional shape of the channel is distinct for about 50 km. A terrace occurs on the east side of the channel, 35 to 50 m above the floor (Table 2, Section 4). The terrace has the appearance of a pre-existing channel bottom which has undergone subsequent downcutting. In the Blanco fracture zone the channel bottom becomes constrained and the width decreases from 1850 to only a few meters as a V-shaped profile develops due to the impinging seamounts. Near the western end of the fracture zone the channel plunges into the wide depressed basin. After emerging from the basin, the channel increases in width and begins its course across Tufts Abyssal Plain. The channel floor is twice as wide (2550 m) on Tufts Abyssal Plain, on the average, as on Cascadia Abyssal Plain (1250 m).

The width of the top of the channel varies between 1250 and 9350 m on the abyssal plain, usually increasing or decreasing along with the channel bottom. The width across the top gradually increases where the channel crosses the southern part of Cascadia Abyssal Plain until it enters the fracture zone. Within this area it is greatly increased by the occurrence of seamounts and ridges which form the channel walls. On the abyssal plain the steepness of the walls varies from less than one to more than 21 degrees, being steepest on southern Cascadia and Tufts Abyssal Plains.

With the exception of Vancouver Sea Valley, too few crossings were made over the tributary channels to make any morphologic comparisons. Vancouver Sea Valley is very shallow and broad, and quite different from Cascadia Channel. The well defined portion of the channel, south of  $45^{\circ}20'N.$ , varies in width from 4000 to 5000 m. Above this point the valley is only a broad depression on the abyssal plain. The maximum channel relief is about 70 m, with the eastern bank invariably higher. This is the opposite of Cascadia and other deep-sea channels studied to date, and is probably due to the presence of the broad base of Nitinat Fan to the east. The floor of Vancouver Sea Valley frequently has a terrace on the western side. The terrace and valley floor are both flat with a difference in relief of from 10 to 20 m.

## COLLECTION AND ANALYSIS OF DATA

### Sample Collection

The sediment samples used in this study were collected on cruises of the R/V Yaquina from 1965 to 1967 (Figure 4). The sampling locations were planned to give a three dimensional picture of the sediment facies and sedimentary processes instrumental in the development of Cascadia Channel and its tributaries. Stations were carefully selected on cross-channel profiles as well as along the length of the channel. All samples were collected with a modified Ewing piston corer using a multiple corer (Fowler and Kulm, 1966) as a trip weight. The cores were collected in clear plastic liners and cut into 3 m sections on board ship. Each section was sealed, placed in galvanized downspout, and kept in cold storage (4° C.) until processed.

### Core Processing

The core processing procedure consisted of cutting the plastic liner open with a circular saw and sectioning the core lengthwise with a thin wire (Figure 5). The core was photographed, color coded (Geological Society of America Rock Color Chart, 1963), and logged using a binocular microscope. Selected core sections were also X-rayed (Faxitron model--Field Emissions Corp., McMinnville,

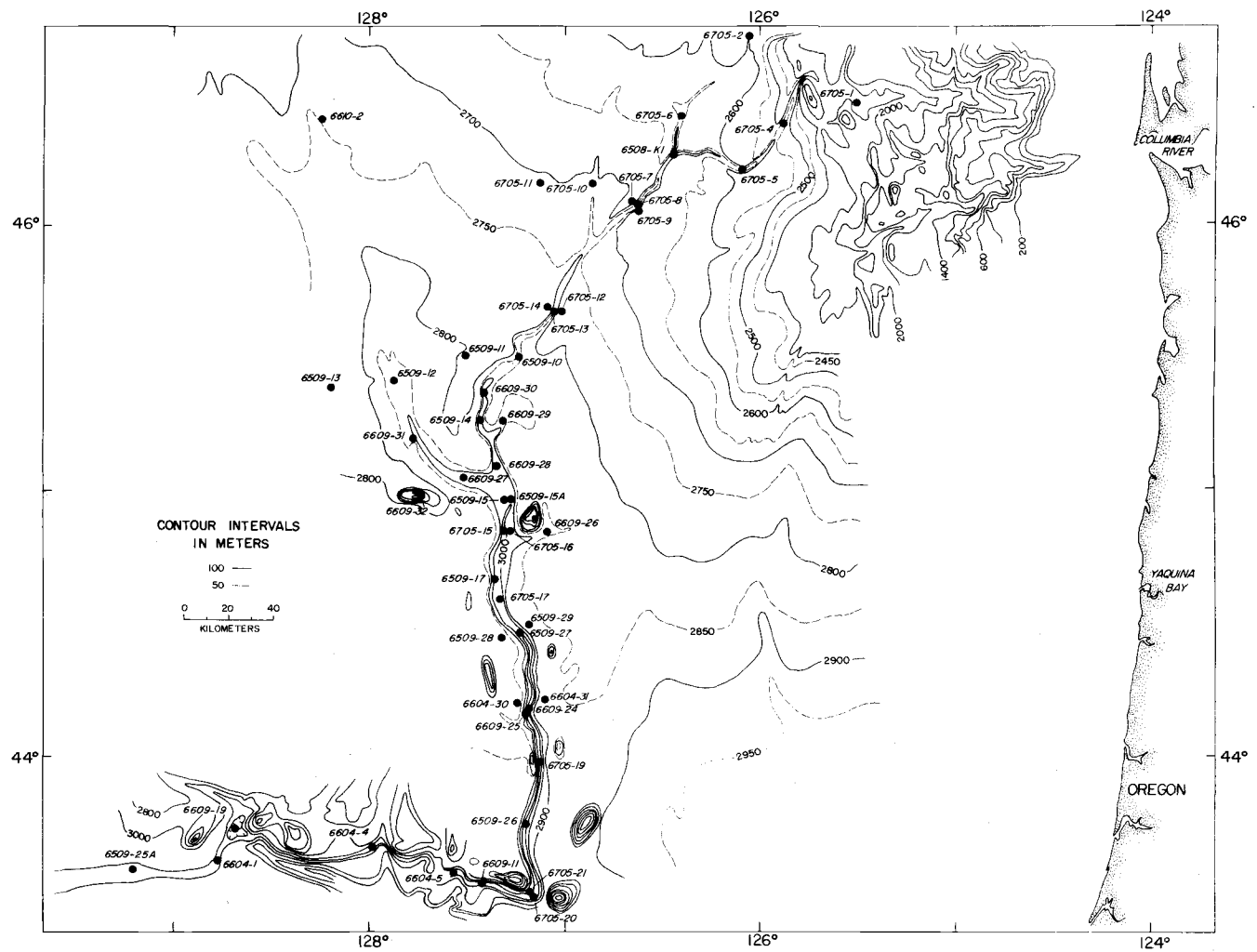


Figure 4. Piston core location map for Cascadia Channel and tributaries

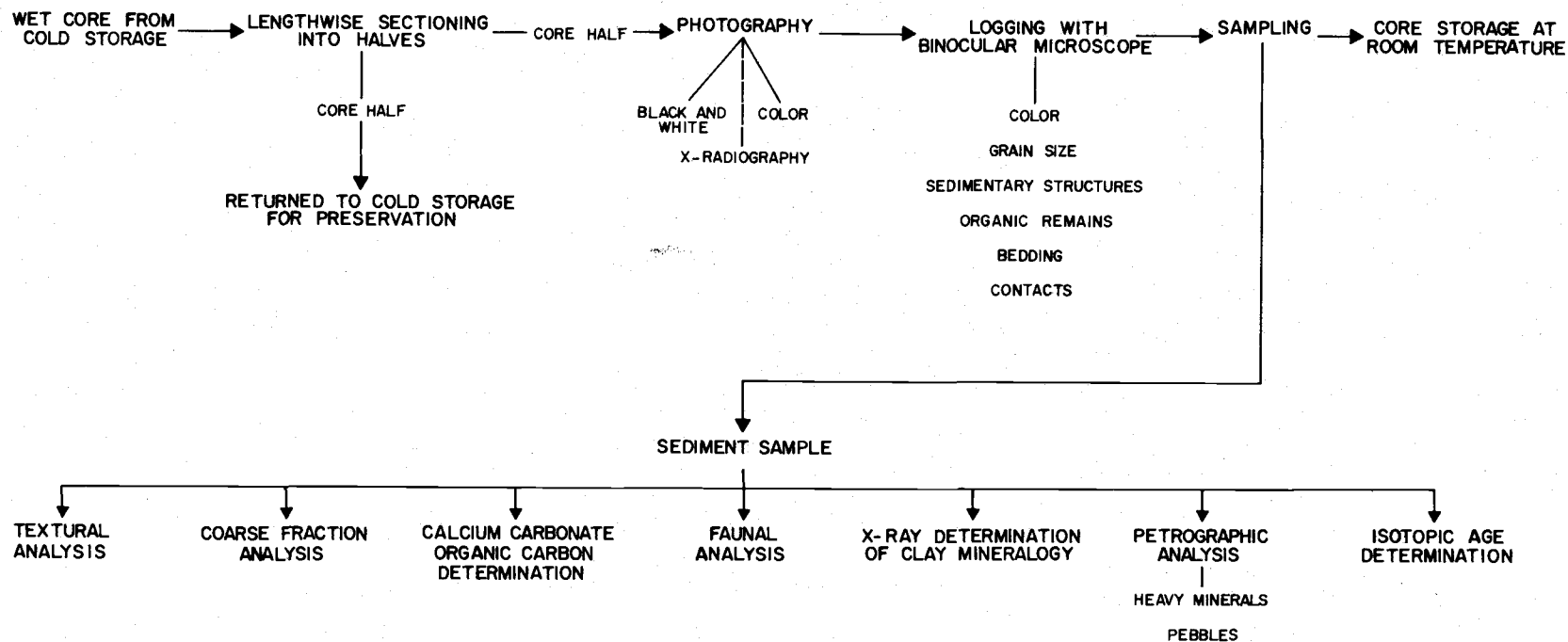


Figure 5. Flow sheet for core processing and sample analysis

Oregon) to reveal any internal structures. The cores were then sampled, with care taken not to contaminate samples or mix sediment types. Due to distortion of the upper portion of the piston cores, a short gravity core was opened from each station to supplement the study of the surface sediment.

### Sample Analysis

Complete and simplified textural analyses were made on 320 samples to determine the grain size distribution of the various sediment types, the variation in grain size within individual sedimentary units, and the spatial and temporal variation in the sediment size. The complete analysis involved standard hydrometer and sieve techniques (Krumbein and Pettijohn, 1938). Due to the fine-grained nature of the sediments and the small amount of material often available, the pipette method (Krumbein and Pettijohn, 1938) was also employed. The settling times were selected so that only the percents of sand ( $> 62$  microns), silt (62 to 4 microns), and clay ( $< 4$  microns) were determined. Prior to analyses all samples were dispersed in a 0.2% solution of sodium hexametaphosphate and rinsed of sea water using millipore filters. The silt and clay contents were then determined by the pipette method and the sand was determined by weighing all material remaining on a 0.062 mm screen after washing and drying.



A complete coarse fraction count was made on 300 samples to determine the composition of the various sediment types. A split of the material greater than 0.062 mm was spread on a grided slide and at least 300 grains were counted using a binocular microscope. The coarse fraction components were divided into three main groups, detrital grains, platy or current sensitive grains (mica, plant fibers, volcanic glass) and biological remains (Foraminifera, Radiolaria, diatoms, etc.) which are important in distinguishing sediment types. A count of Radiolaria and planktonic Foraminifera was also made on 530 samples for stratigraphic control which will be discussed later. These samples were only taken from pelagic or hemipelagic clays, and were selected at 10 cm intervals or wherever the clay occurred. A total of at least 100 tests were identified and counted in each sample.

Organic carbon and calcium carbonate contents were determined in selected samples of the various sediment types using a Leco induction furnace coupled with a Leco gasometric carbon analyzer, according to the method described by Curl (1962). The samples were oven dried, ground to a fine powder, and then redried before analysis. Two or three samples were run for agreement and the results were averaged and calculated in terms of percent organic carbon and calcium carbonate by weight of the total sample.

The clay mineralogy of 32 samples was determined using X-ray

diffraction techniques. The samples were processed according to the techniques outlined by Russell (1967) for the recognition of montmorillonite, illite, chlorite, and kaolinite in marine sediments. All X-ray work was done on a Norelco diffractometer with a Geiger-Muller counting tube. Data were recorded on a linear scale, strip chart recorder at  $1^\circ$  per inch per minute. Machine settings were as follows: time constant four seconds, current 25 ma, voltage 50 KVP,  $1^\circ$  scattering and receiving slits, 0.006 inch divergence slit; nickel filtered Cu radiation ( $\lambda = 1.54 \text{ \AA}$ ) was used for all samples. Samples were scanned from 3 to 14 degrees  $2\theta$  with the rate meter at 200 cps as full scale, and from 24 to 26 degrees  $2\theta$  with the rate meter at 100 cps. Following these procedures, montmorillonite is identified on the traces by a  $16.8 \text{ \AA}$  peak, and illite by a  $9.95 \text{ \AA}$  peak. Using the criteria of Biscaye (1964), it was concluded that no kaolinite occurs in the sediments and the peak at  $7.08 \text{ \AA}$  is the 002 peak of chlorite. The semi-quantitative technique for the determination of the composition of the clays suggested by Biscaye (1956) and used with success by Duncan (1968) was employed to differentiate sediment types. The percentages of illite, chlorite, and montmorillonite were calculated from the areas under their principal peaks, multiplied by scale factors to compensate for differences in diffraction intensities.

In order to determine the source areas of the coarser sediments

and their temporal variations, the heavy mineralogy of the sands and the petrography of the gravels was studied. Material finer than 0.062 mm was removed by wet sieving and the heavy mineral fraction was concentrated using tetrabromoethane (sp. grav. = 2.96). This fraction was mounted in Aroclor (R.I. = 1.65-1.66) and 200 or more grains were identified using a polarizing microscope and a mechanical stage. Almost all of the heavy minerals were between 0.062 and 0.125 mm in size, although some grains were as large as 0.250 mm. Thin sections of 22 pebbles found in several sediment types were also examined with a polarizing microscope and their lithology determined.

## STRATIGRAPHY

The sedimentary history of an area can be determined if the ages of the sediment units, or their time of deposition, are known. Depositional rates can then be calculated for various time intervals, correlations can be made and comparisons drawn between areas close together or far removed.

Duncan (1968) developed a paleoclimatic curve which enabled him to date and correlate sediments in the Cascadia Basin and Blanco fracture zone. The climatic curve for this area is based primarily on the relative abundances of planktonic Foraminifera and Radiolaria. The presence of volcanic ash from the Mt. Mazama eruption 6600 years ago, changes in the color of the lutites, and the presence of certain microfossils have also been used as stratigraphic indicators (Carlson, 1967; Nelson, 1968; Duncan, 1968).

### Mt. Mazama Volcanic Ash

A distinct sedimentary horizon which represents a short interval of time and is widespread geographically is invaluable in the correlation of unconsolidated sediments and sedimentary rocks. The catastrophic eruption of Mt. Mazama in the Oregon Cascades 6600 years ago was of great significance in the marine environment. The ash from this eruption blanketed a large area of the Pacific

northwest (Figure 6) and was transported with other detrital material to the oceans through the river systems. The ash has been found in the sediments of Cascadia Channel, Willapa Canyon, Astoria Canyon, Fan, and Channel, and Blanco Valley (Figure 6) and has been correlated with the Mt. Mazama eruption by refractive index and by radiocarbon dating of the adjacent sediments (Nelson et al., 1968). The presence of the ash in Cascadia Channel and its absence from the immediately adjacent environments indicates that the ash was not deposited as a blanket covering, but instead was transported along the ocean bottom, primarily within channels, as turbidity currents (Nelson et al., 1968). The first appearance of Mt. Mazama ash in a core can be used as an approximate time line in the sediments of Cascadia Basin. Although some time probably elapsed before the ash entered the marine environment, the lowermost occurrence approximates 6600 years B. P.

#### Planktonic Foraminifera-Radiolaria Abundance

The last several million years have been characterized by world wide climatic changes. They have persisted to the present time and are probably still occurring, although at a rate too slow to be observed. These periodic changes from warm to cool have greatly altered the earth's surface; during cooler periods sea level was lowered due to the transfer of water from the oceans to the

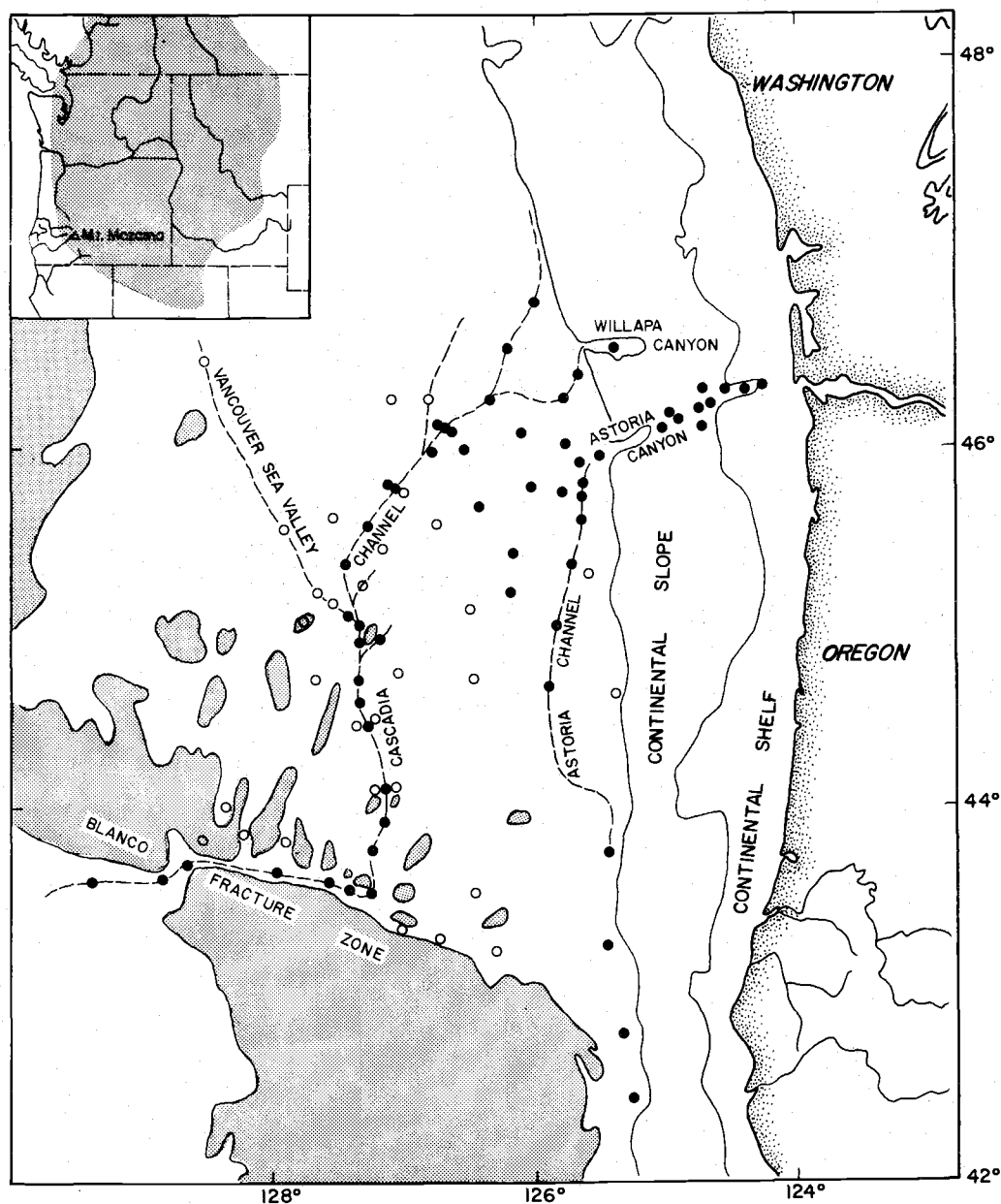


Figure 6. Distribution of volcanic ash from Mt. Mazama on the continent (inset) and in the marine environment (● cores containing ash; ○ cores without ash) (modified after Nelson et al., 1968)

continents, where it took the form of ice caps and glaciers. These changes in sea level were accompanied by changes in oceanic water temperatures and circulation patterns, which in turn affected the planktonic marine organisms such as Radiolaria and Foraminifera. Species variation and changes in coiling directions of planktonic Foraminifera, as well as differences in the relative abundances of planktonic Foraminifera and Radiolaria have been recognized as indicators of climatic changes (Ericson, 1959; Emiliani, 1966; Bandy, 1960; Nayudu, 1964; Duncan, 1968). Paleoclimatic curves can be developed using these faunal variations; they can be related to sediment types and also used for correlation. Duncan (1968) established a paleoclimatic curve for the last 35,000 years in Cascadia Basin using the relative abundance of planktonic Foraminifera and Radiolaria (Figure 7). The pelagic and hemipelagic sediments high in planktonic Foraminifera (primarily Globigerina pachyderma and G. bulloides) characterize the cooler or glacial periods, while Radiolaria-rich sediments are common in warmer or interglacial periods. This variation has been attributed by Arrhenius (1952) and Nayudu (1964) to intensified atmospheric and oceanic circulation during glacial periods resulting in a greater mixing of the nutrient rich subsurface water with the surface water. Present day oceanographic observations off Oregon (Smith, 1966) indicate that the coastal upwelling, which brings the nutrient rich bottom water to

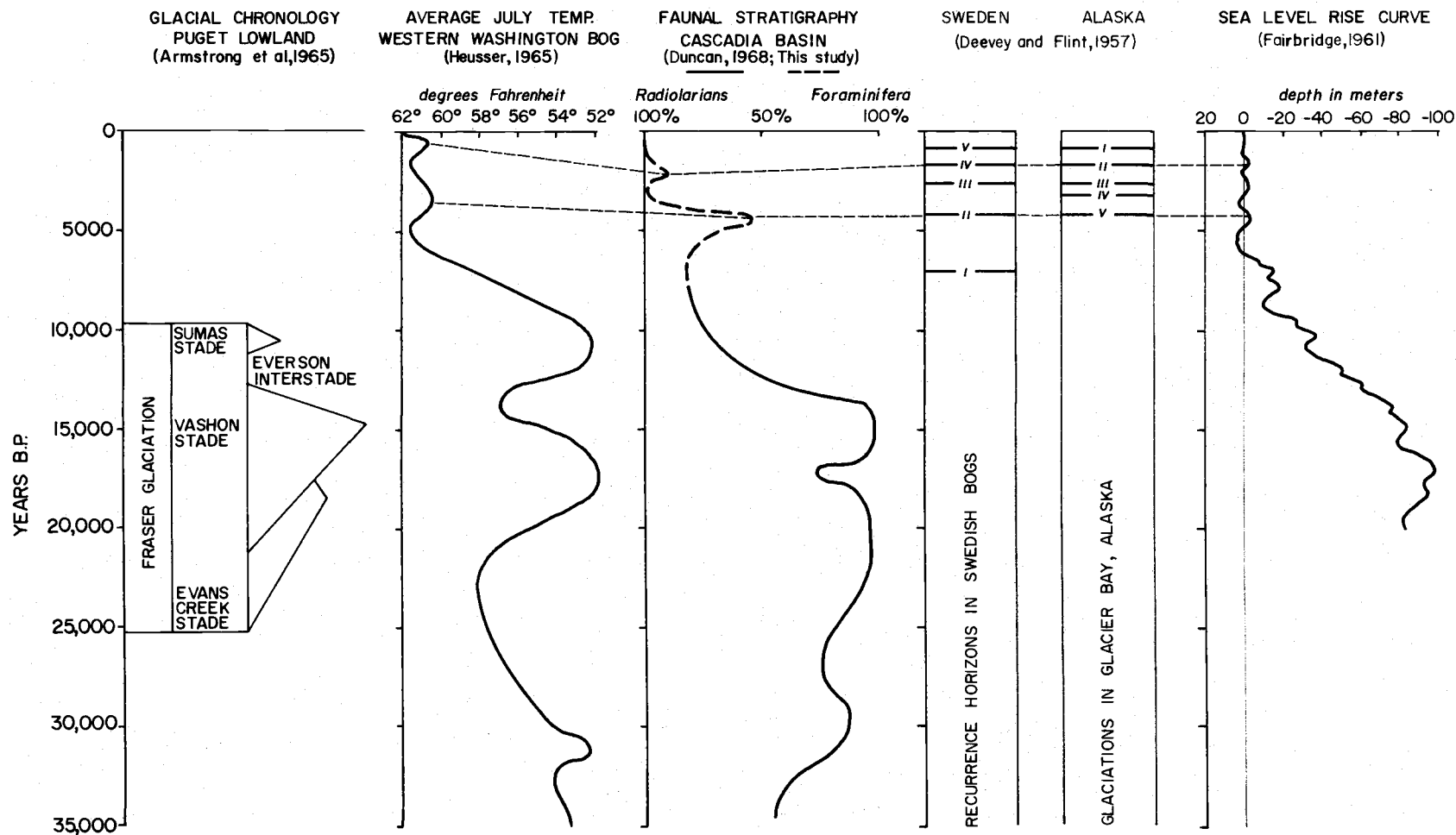


Figure 7. Summary and correlation of late Pleistocene and Holocene glacial chronology, floral and faunal stratigraphy, and sea level rise



the surface, is limited to within about 100 km of the shoreline. Even with a lower Pleistocene sea level, it seems doubtful that upwelling could have been effective much farther from shore. This mechanism, therefore, seems inadequate to explain the faunal stratigraphy of western Cascadia Basin and Blanco fracture zone. Changes in oceanic water temperature between glacial and interglacial periods may have been even more important in controlling the abundance of these planktonic organisms. A series of recent plankton tows in the western north Atlantic from 41° 00' to 13° 00' N. latitude (Cifelli and Sachs, 1966) shows that, in general, planktonic Foraminifera are relatively more abundant in the cooler northern water, while Radiolaria are more abundant in the warm southern water.

### Paleoclimatology

The paleoclimatic curve developed for Cascadia Basin (Figure 7) shows a rather abrupt transition from present day interglacial conditions to glacial conditions which existed prior to 12,500 years ago (Duncan, 1968). Several older warming periods, or intervals richer in Radiolaria, have been recognized within the Pleistocene section; the first extends from about 18,000 to 16,000 years B.P., the second occurs from 28,000 to 25,000 years B.P., and a third begins about 34,000 years B.P. In cores taken in basins of the continental borderland off southern California, Bandy (1967) found that

large numbers of Radiolaria (per gram of sediment) were deposited from 28,000 to 26,000 years B.P. and from 19,000 to 16,000 years B.P. These two intervals correspond very closely to the two radiolarian-rich intervals noted off Oregon.

With the exception of Blanco Valley and eastern Cascadia Basin, most of the areas sampled by Duncan (1968) were characterized by low sedimentation rates. Consequently the paleoclimatic curve was compressed, especially in the period from 12,500 years B.P. to the present (designated Holocene in this area). The high sedimentation rates in Cascadia Channel and its tributaries present a greatly expanded stratigraphic section where this Holocene sequence can be analyzed more closely. A detailed paleoclimatic curve for the last 12,500 years in Cascadia Basin has been developed by the writer from cores taken in Cascadia Channel and the immediate vicinity. Several Globigerina-rich intervals interrupt the Holocene section (Figure 7). These zones seem to indicate cooler periods, and also may reflect slight glacial advances on the continents. The lower interval extends from about 5000 to 4000 years B.P., and can be recognized in the sediments from those areas in Cascadia Basin which have relatively high Holocene sedimentation rates (Cascadia Channel and its tributaries, and eastern Cascadia Abyssal Plain). The interval can be dated rather precisely because it occurs just above the lowest horizon containing Mt. Mazama ash.

The second interval is less distinct and not as widespread geographically. It occurred sometime around 2000 years ago, assuming uniform Holocene sedimentation rates.

The relationship between the continental and marine expression of late Pleistocene and Holocene climatic events is not completely clear. Continental events have been recorded in glacial drifts and tills, pollen sequences in bogs and lakes, and sea level rise curves from the continental margins. Some similarities are evident in the climatic events recorded in the deep-sea faunal stratigraphy and in the late Wisconsin glacial advances and retreats of the adjacent Puget Lowland as defined by Armstrong et al. (1965) (Figure 7). The Fraser glaciation correlates closely with the cool period represented in the deep-sea sediments which extended from about 25,000 to 12,500 years B.P. Both the deep-sea and continent have also recorded warming or interglacial conditions about 18,000 to 16,000 years B.P. within this cool period (Armstrong et al., 1965; Duncan, 1968). A marked recession of the glaciers occurred between 13,000 and 11,000 years ago which corresponds well with the period of decreasing production of planktonic Foraminifera relative to radiolarians. The most abrupt change in the faunal stratigraphy occurred about 12,500 years B.P. in Cascadia Basin and is considered as the start of Holocene time (postglacial time by Duncan, 1968) and sedimentation in the deep-sea environment.

The slight glacial advance on land at the end of Fraser glaciation (Sumas Stade) is not noticeably evident in the marine sediments, and the Globigerina-rich intervals higher in the Holocene deep-sea section have not been detected in the Puget Lowland glacial deposits. If the cool intervals at 5000 to 4000 years B.P. and 2000 years B.P. are areally significant, some expression of the climatic change should appear in the continental deposits. As mentioned previously, however, the marine and continental records may express similar climatic changes but they may not be perfectly synchronous in time.

The oldest cooling period in the Holocene section may correspond to the Bahama Emergence of Fairbridge (1961) which occurred between 4600 and 4000 years ago (Figure 7). Lower sea level stands (average of -4 m below present sea level) during this time have been recorded in the Bahamas, New Zealand and Australia, the Netherlands, Venezuela, and the east and Gulf coasts of the United States (summarized by Fairbridge, 1961). The time about 4300 years ago is often marked as a phase of renewed glacial activity and has been designated the "Little Ice Ages" by Matthes (1939). The more recent cooling interval (2000 years B.P.) noted in the deep-sea sediments may correspond to the Florida Emergence of Fairbridge (1961) which extended from about 2100 to 1600 years B.P. and lowered sea level an average of two meters (Figure 7). This emergence has been recorded in many of the same locations as the Bahama

Emergence (summarized by Fairbridge, 1961). The remains of a drowned forest several meters below sea level were found off the southern Oregon coast and dated at 1730 years B.P. (Rubin and Alexander, 1958). This may be a result of a sea level lowering, corresponding to this cooling period.

Based on pollen profiles from a bog in western Washington, Heusser (1965) developed a paleoclimatic curve for the last 35,000 years (Figure 7). Two cool intervals are indicated in the last 5000 years which correspond closely to the Globigerina-rich zones in the deep-sea sediments. Pollen profiles from subarctic central Canada show a cool period about 5000 years ago and also one extending from about 2600 to 1500 years B.P. (Nichols, 1967). Glacial episodes at Glacier Bay, Alaska, and recurrence horizons in Swedish bogs have been recorded at about 4300 and 1700 years B.P. (Deevey and Flint, 1957) (Figure 7).

The only known marine correlation with the Holocene cooling periods occurs in the previously mentioned work of Bandy (1967) in the continental borderland off southern California. Relatively high Holocene sedimentation rates in the basins have resulted in an expanded stratigraphic column. Almost all of the cores pictured contain faunal intervals suggestive of cooling just above the midpoint of the Holocene (11,000 years B.P.) section. The analyses indicate zones lower in Radiolaria (numbers/gram) and higher in planktonic

Foraminifera (Globigerina pachyderma) within this interval, similar to the cores from eastern Cascadia Basin. It seems evident that some major climatic change occurred around 5000 to 4000 years B.P., and perhaps again around 2000 B.P., which was recorded in the marine sediments and continental deposits of the Pacific coast of the United States.

It is important here to recognize that the general world climatic picture since the close of the Pleistocene (last 18,000 to 20,000 years on the continent; last 11,000 to 12,500 years in the deep-sea environment) has been one of warming or amelioration. However, wherever complete and detailed records of climatic changes have been analyzed, there are indications of climatic reversals, or cooling intervals, represented within this period. These reversals seem to be of regional significance and appear to be useful in correlation. The regional significance of the paleoclimatic curve in the Holocene section is illustrated in Figures 8 and 9, which show the stratigraphy of most of the cores from Cascadia Channel and adjacent areas grouped according to physiographic environments. Nearly all of the cores which penetrate the 5000 to 4000 years B.P. Globigerina interval show some indication of this cooling period. In the remaining cores which do not show the interval, the Holocene section is too thin to investigate in detail.

Paleoclimatic curves also give an indication of the effect of the

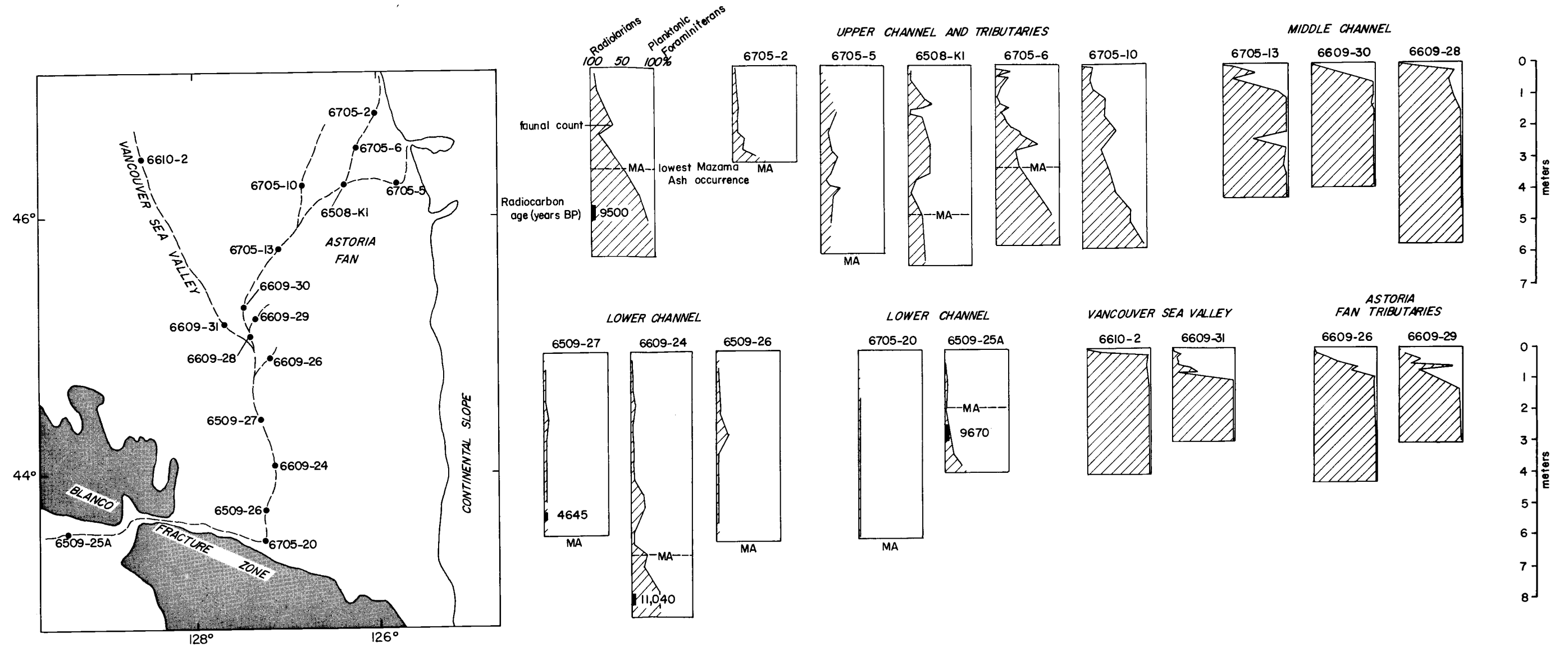


Figure 8. Faunal stratigraphy of selected cores from the axis of Cascadia Channel and its tributaries

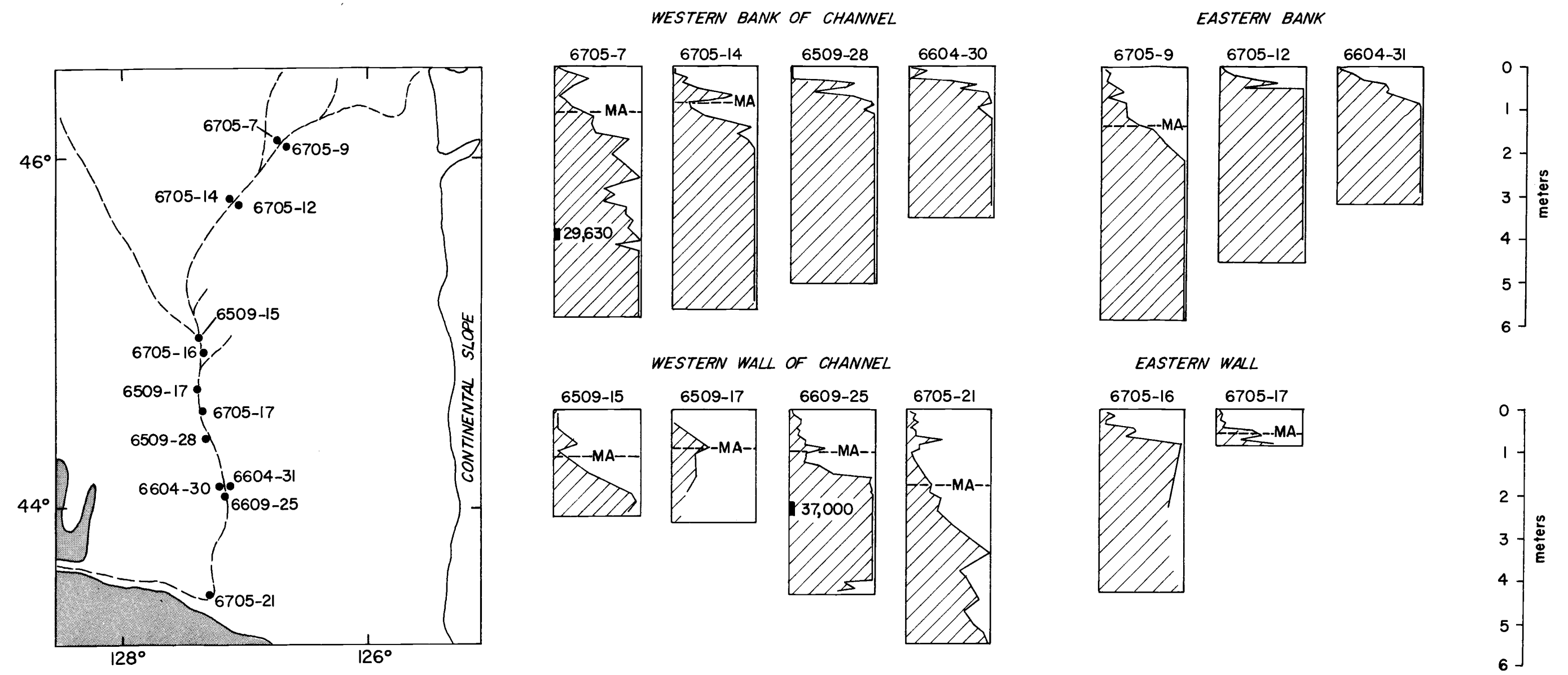


Figure 9. Faunal stratigraphy of selected cores from walls and banks (including levees) of Cascadia Channel. See Figure 8 for core legend.



channel on circulation patterns and abundances of the planktonic organisms. All the cores from the west wall and bank of Cascadia Channel show the well defined lower Globigerina interval above the Mazama ash, as well as a zone of increased Radiolaria just below the Holocene-Pleistocene break. In cores from the eastern bank, the upper Globigerina interval is less distinct and the Radiolaria interval is completely absent. The channel may actually have some effects on the hydrography and surface productivity, or perhaps variations in sedimentation on either side of the channel produced these apparent faunal differences.

#### Stratigraphic Variations

The thickness of the Holocene sediments in Cascadia Channel and the adjacent environments (Figures 8 and 9) ranges from several centimeters on the western plain to over 840 cm within the channel. With the exception of the middle channel, all of the sediments cored from the floor of Cascadia Channel are Holocene in age, and represent rapid rates of deposition. The middle channel has a thin Holocene covering (5 to 35 cm) which overlies Pleistocene sediment.




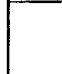




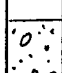
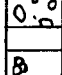


The east and west banks of the channel generally consist of thick Pleistocene sections overlain by 50 to 215 cm of Holocene sediment which is thickest along the upper channel. The channel

walls generally have a thicker sequence of Holocene sediment than the banks but this depends upon the height of the banks above the floor and the distance down channel. Vancouver Sea Valley and the tributary channels from Astoria Fan are characterized by thin layers of Holocene sediment which overlie Pleistocene sections.

## SEDIMENT TYPES

Six distinct sediment types can be recognized within Cascadia Channel and the adjoining areas on the basis of color, lithology, and composition (Table 3). Their textural variations are best represented on a triangular diagram with sand, silt, and clay as the end members. Coarse fraction constituents are grouped according to origin and hydrodynamic characteristics and are also plotted on a triangular diagram. Mineral grains and rock fragments (with the exception of mica), which require relatively strong currents for transportation, are included in the detrital group. The second group includes mica, plant fragments and volcanic glass, which are more sensitive to currents due to their platy shape or low density. Biogenic and authigenic material which accumulates in situ, such as Radiolaria, diatoms, benthic and planktonic Foraminifera, fecal pellets, and pyrite, make up the third. The close tie between the end members of the texture and composition triangles (sand-detrital grains; silt-platy grains; clay-biogenic material), illustrated by the similar position occupied by each sediment type in the two triangles, is indicative of the similarity in hydrodynamic characteristics of the associated materials during processes of transportation and deposition. Each sediment type will be briefly described and subsequent chapters will describe the stratigraphic and physiographic

Table 3. Sediment types and characteristics

Sediment Type	Symbol	Color	Texture	Composition	Ave. organic carbon content		Ave. calcium carbonate content	Microfauna	Age	Depositional Process		
Olive green silt	tail		5Y3/2	silty-clay	mica, volcanic ash, plant fibers		2.3%	0.5%	Displaced benthic Foraminifera, diatoms, Radiolaria	Holocene	Turbidity current	
	base		5Y3/2	fine sand-silt	mica, detrital grains, volcanic ash		0.5%	1.0%				
Gray clay			5Y4/1	silty clay	Radiolaria, diatoms, Foraminifera, fecal pellets		1.0%	Holocene	1.2%	Abyssal benthic Foraminifera, diatoms, radiolaria, planktonic Foraminifera	Pleistocene and Holocene	Pelagic and hemipelagic deposition
			5GY4/1				0.3%	Pleistocene	4.0%			
			5Y4/2									
Terrigenous sand-silt			N-3	clayey silt to coarse sand	Detrital grains, mica					Displaced benthic Foraminifera	Pleistocene	Primarily turbidity current
			5Y4/1									
Pebbly clay			5Y4/1	sand-silt-clay	Detrital grains, pebbles		0.4%		0.7%	Scarce	Pleistocene	Ice rafting
												
Foraminiferal ooze			5Y7/2	sand-silt-clay	Planktonic Foraminifera				35%	Planktonic Foraminifera	Pleistocene	Pelagic deposition
			5GY4/1									
Gravel			N-3	sand to pebbles	Detrital grains, shell debris				Displaced benthic Foraminifera	Pleistocene	Turbidity current (?)	

distribution of the sediments and will elaborate on the depositional processes.

### Olive Green Silt

The Holocene sediments in Cascadia Channel and its northern tributaries consist predominantly of olive green silt (Table 3). This silt also occurs on the walls of the channel, and on the banks where levees are present. It has a wide range of textural, compositional and structural properties depending upon the depositional environment (Figure 10). Thicknesses of the silt layers range from 3 to over 400 cm and are fairly uniform within individual environments. The olive green silt layers consist of two distinct parts (Figures 11 and 12). The basal zone is coarse-grained, consisting of sand or silt, and is usually laminated and graded; detrital grains and mica constitute the coarse fraction. The basal contact is sharp, and commonly shows grooves cut into the underlying gray clay, which may be filled with fine- to medium-grained sand.

Above this basal zone, and sharply separated from it, is an apparently homogeneous section. It is usually much thicker and consists of silty clay which becomes finer grained upward. Mica and plant fibers compose the coarse fraction; they increase in abundance upward, often reaching 70 to 80% of the coarse fraction. The organic carbon content of this homogeneous tail is very high (2.0-2.6%) and

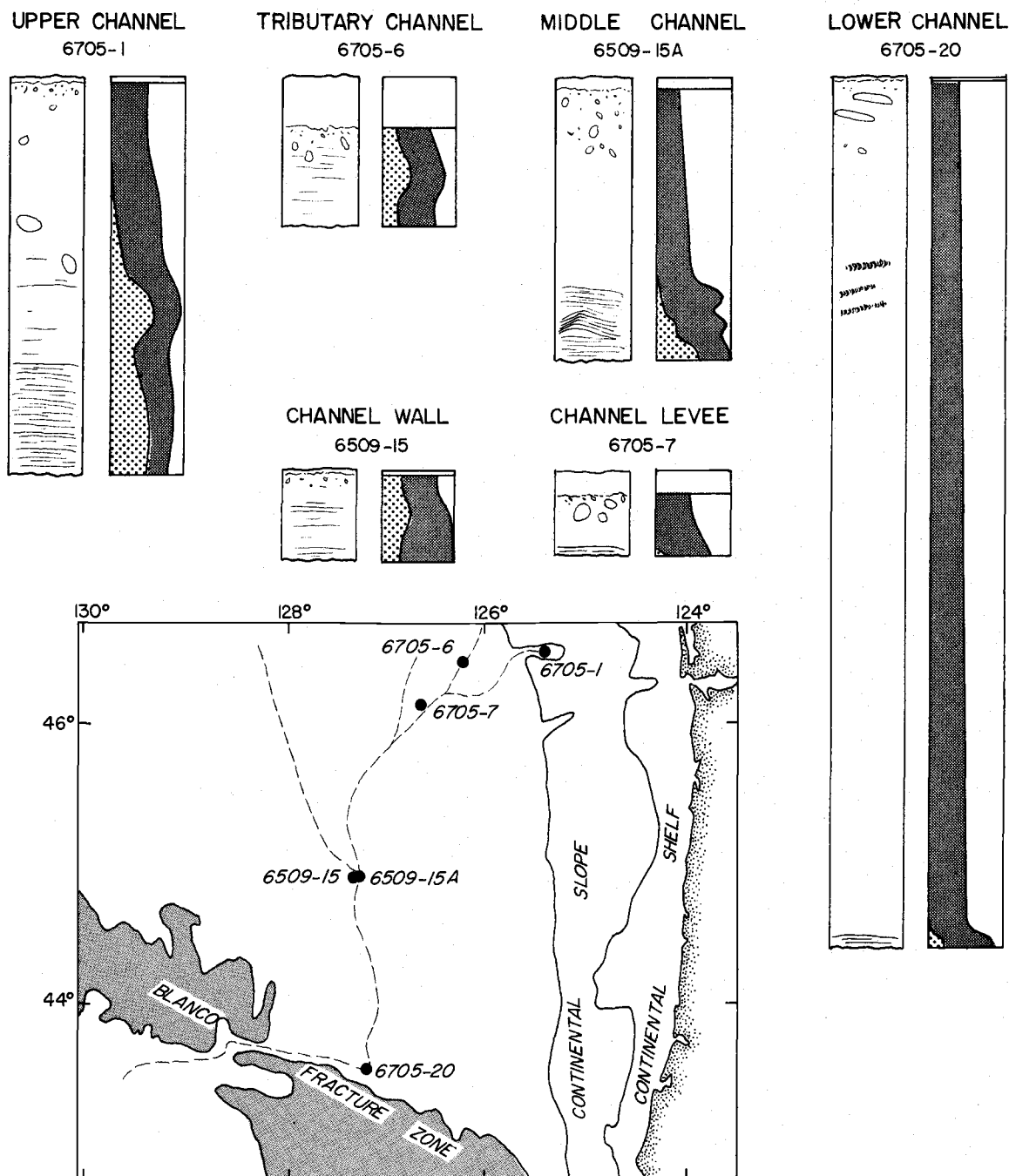


Figure 10. Lithology of olive green silt sequence in various channel environments. Left-hand profile represents core log; right-hand profile indicates sand-silt-clay composition of sequence. Note hemipelagic layer at top of sequence and presence of burrows.

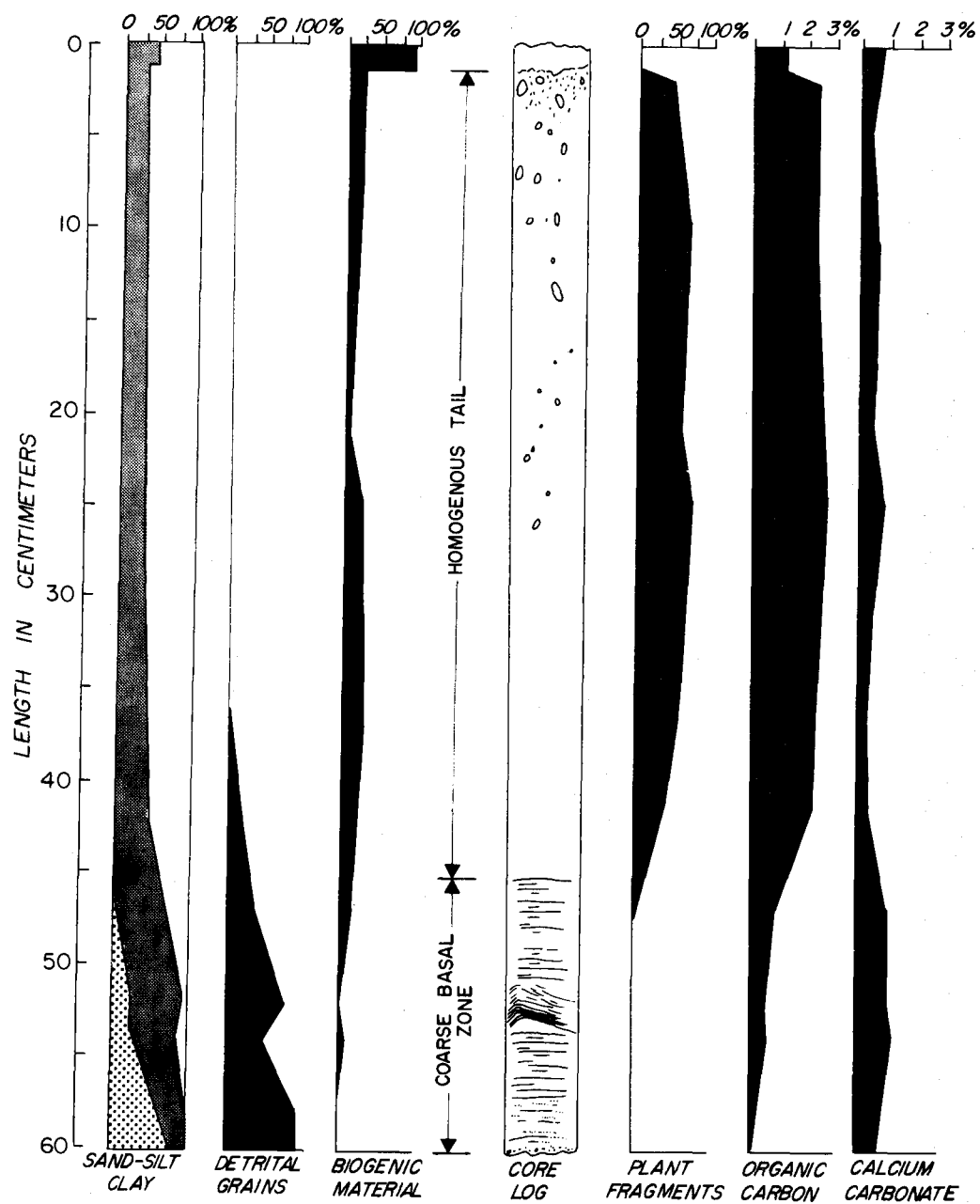


Figure 11. Vertical variation in texture and composition of typical olive green silt sequence from axis of Cascadia Channel

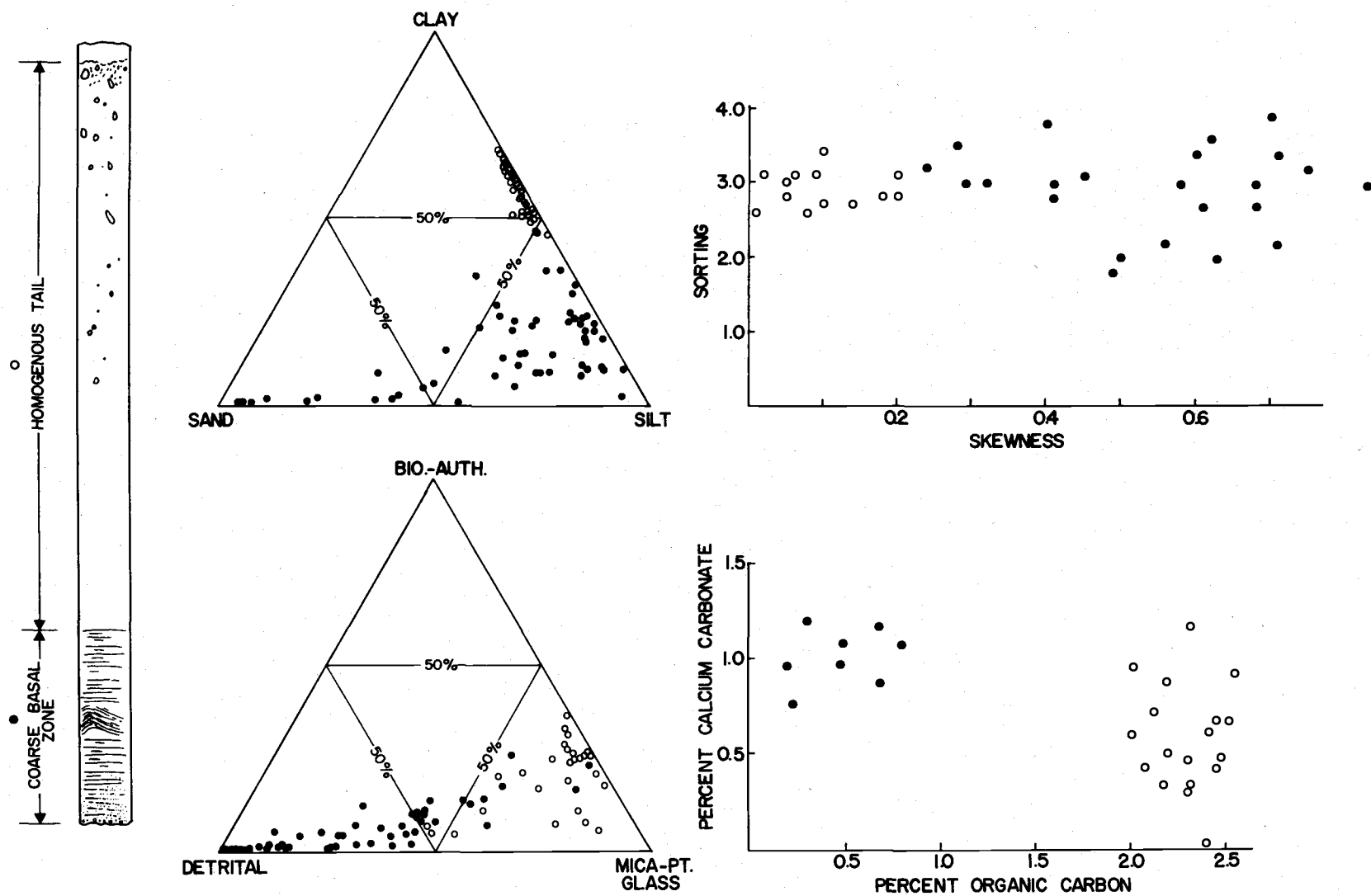


Figure 12. Textural and compositional characteristics of olive green silt sequences. Note difference between coarse basal zone (●) and homogeneous tail (○)



closely parallels the amount of plant fibers (Figure 11). The calcium carbonate content is usually low, around 0.5%. In contrast, the calcium carbonate content of the basal layer is about 1.0% while the organic carbon amounts to only 0.5%. Gray burrows of various sizes and shapes are commonly found in the upper interval, and may penetrate as far as 50 cm downward from the upper surface of the layer. Benthic Foraminifera displaced from continental shelf and slope depths are common constituents (Griggs, 1966; Duncan, 1966).

The described characteristics of these sediments and their physiographic distribution indicate deposition by turbidity currents. Textural, structural, and compositional differences between the coarse basal zone and the finer-grained, homogeneous "tail" of the olive green silt layers are striking (Figure 12) and are important in determining the nature of the depositional medium which will be discussed in a later chapter.

### Gray Clay

Gray clay (5Y4/1) with gradations to dark greenish gray (5GY4/1) and olive gray (5Y4/2) occurs in all cores from Cascadia Channel and the adjoining environments (Table 3). The clay is interbedded with the olive green silts and the terrigenous sand-silt layers of the channel system and the abyssal plain. It constitutes the uppermost sediment section in the abyssal environments outside the

channel. Due to oxidation at the sediment-water interface (Duncan, 1968), the upper several cm of the gray clay are commonly brown in color (10YR2/2).

Most of the gray clays are silty clays while some are clayey silts or clays (Figure 13). Those which are finer-grained occur far from the continent whereas the coarser ones are found throughout the area. Clay content, which varies from 52 to 84 percent, shows a general increase with distance from the mouth of the Columbia River. The coarse fraction of the clays is mainly biogenous. Radiolaria predominate in the surface sediments and those of interglacial periods, while planktonic Foraminifera are more abundant in the Pleistocene sediments of glacial periods. Burrowing by organisms has added significant amounts of detrital material to some of the clay.

The calcium carbonate content of the gray clays ranges from 0.2 to 7.4 percent; it increases as the abundance of planktonic Foraminifera increases passing from Holocene into Pleistocene sediments (Figure 13). The organic carbon content is low in the Pleistocene clays (0.3-0.4 percent) and somewhat higher in those of Holocene age (0.6-1.8 percent) (Figure 13).

The thickness of the gray clay layers ranges from laminae of less than a centimeter to structureless sections as thick as 90 cm. Upper contacts are usually sharp and contain grooves, presumably

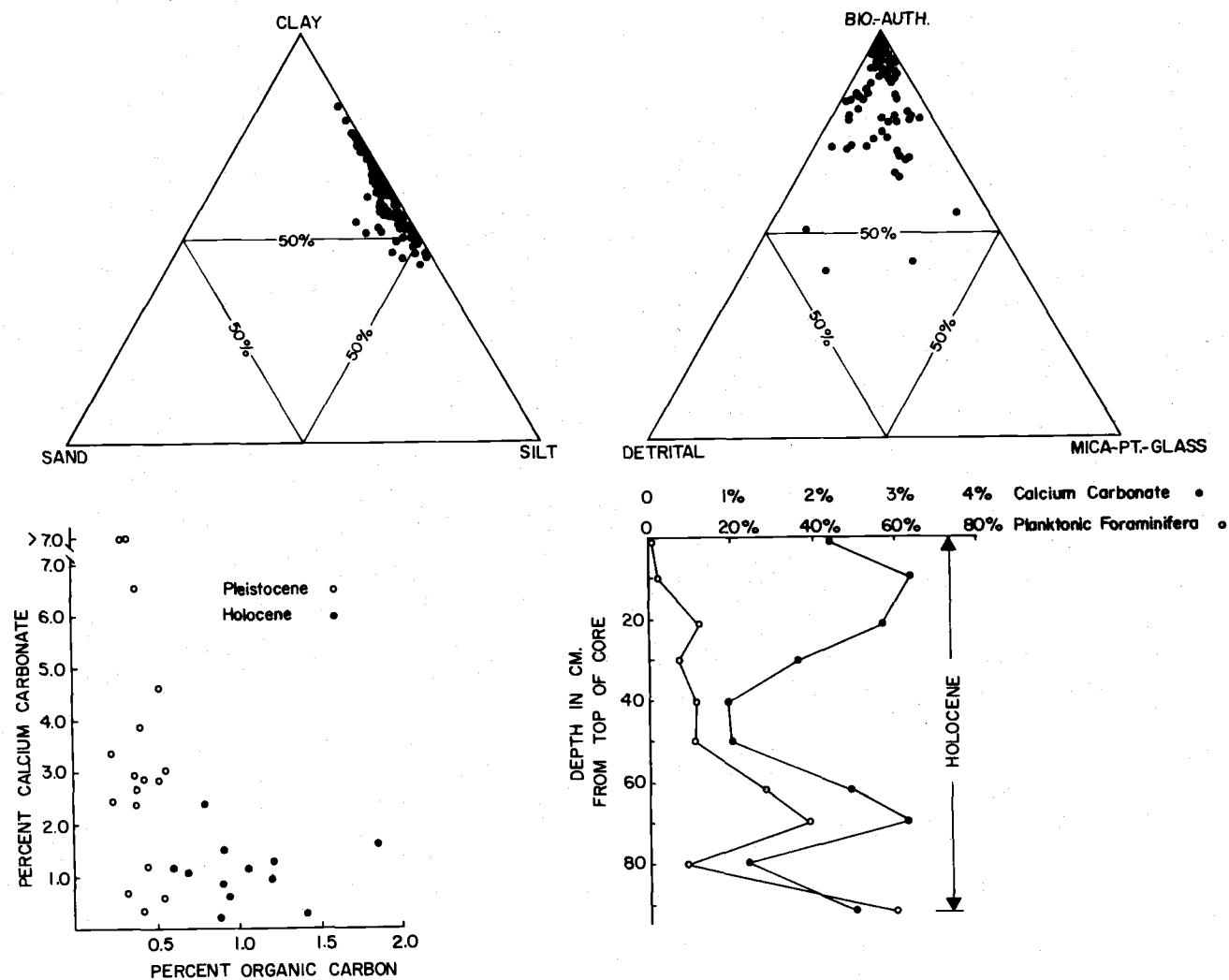


Figure 13. (Top) Texture and composition of gray clays. (Bottom) Calcium carbonate and organic carbon contents of Holocene and Pleistocene gray clays. Compositional variation in gray clay with depth shown in core 6609-31

from the emplacement of the overlying coarse material which is usually present. The lower contact is irregular and mottled where organisms have reworked the sediment. The biogenic coarse fraction and fine grain size of these clays, which decrease away from shore, indicate that this material represents the pelagic or hemipelagic deposition in this area.

#### Terrigenous Sand-Silt

Pleistocene sections of Cascadia Abyssal Plain and the Cascadia Channel system are characterized by terrigenous sands and silts. These are coarser (Figures 14 and 15) and better sorted than the Holocene olive green silts and also lack their green color. They can be separated into thin (1-10 mm) laminae or thick (1-150 cm) layers.

The laminated sediments consist of gray clay interrupted by regularly or randomly spaced laminae of silt or very fine sand (Figure 14). They may consist of a single clean laminae or several clean laminae separated by a clayey one. Lower contacts are sharp whereas the upper ones are more gradational. The coarse fraction of the interbedded clay is often high in mica and plant fibers.

The thick sand-silt layers also have sharp, often irregular basal contacts and may be laminated. Laminations consist of clayey layers high in mica and plant fibers which alternate with better sorted

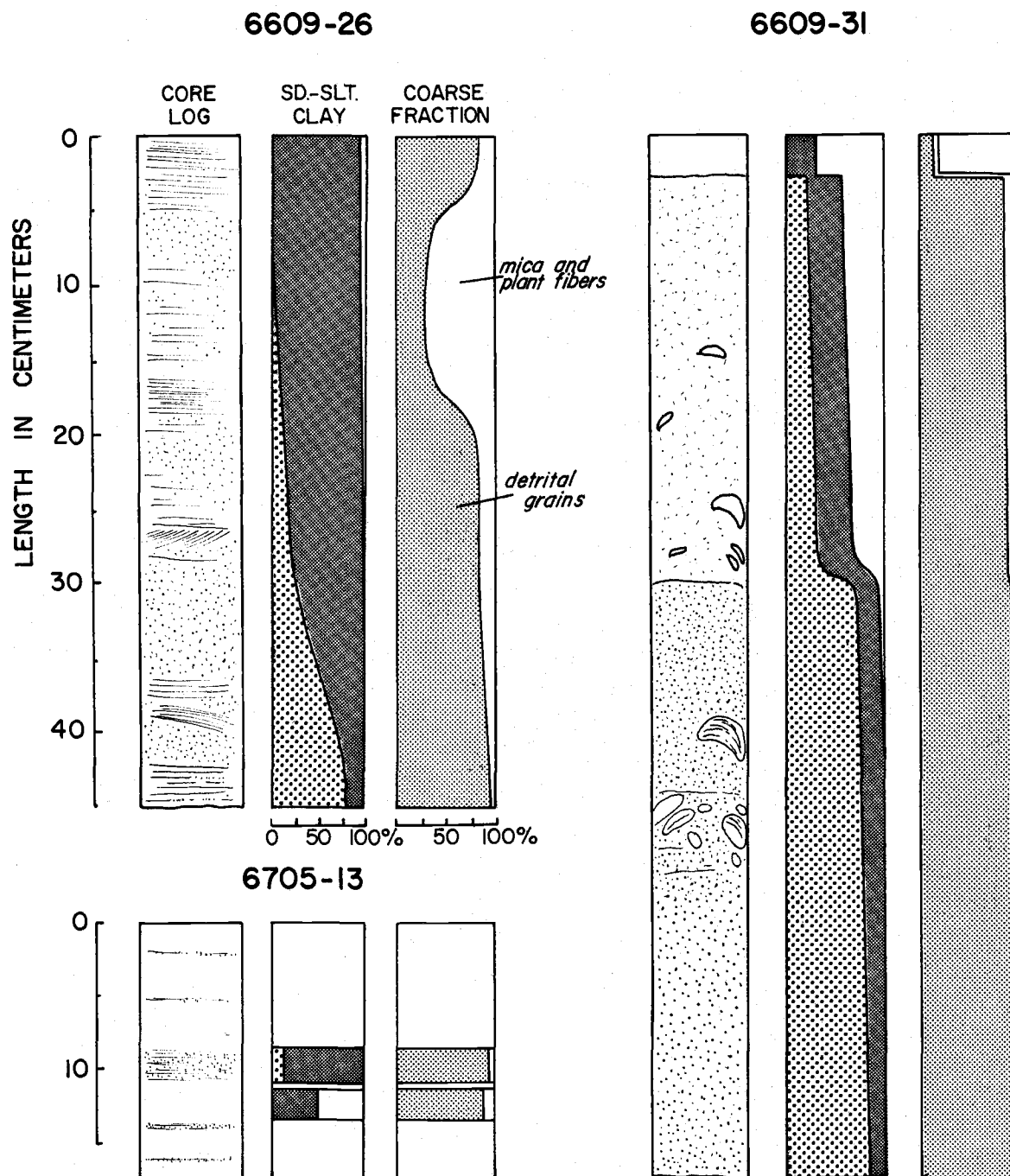
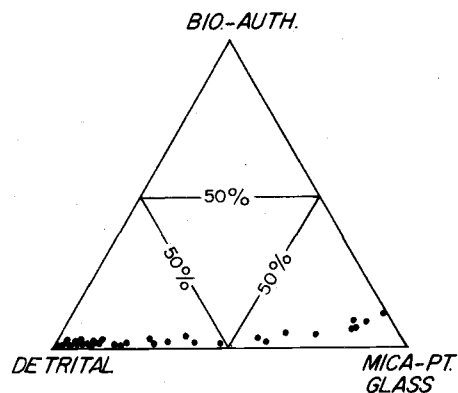
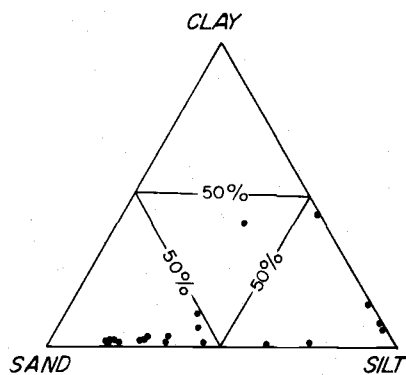
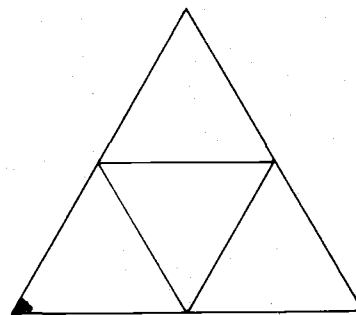
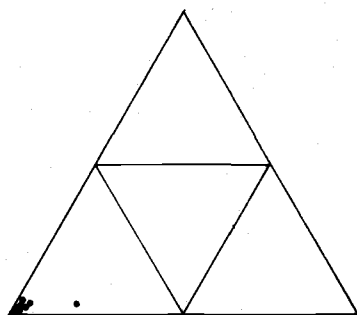


Figure 14. Textural and compositional variations in selected terrigenous sand-silt sequences. (Upper left) Thick sand unit which is graded and contains parallel and cross laminations. (Right) Thick graded unit with finer-grained tail. (Lower left) Thinly laminated clay layers.

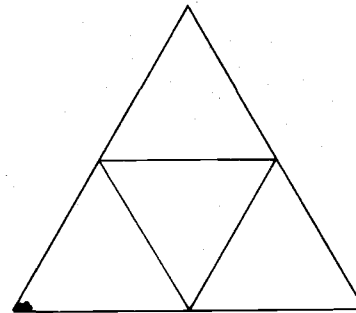
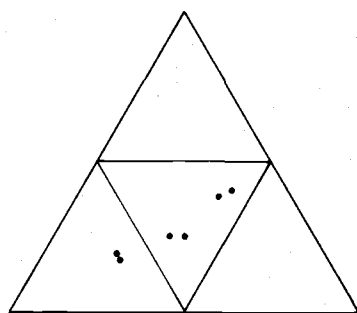
## TERRIGENOUS SAND-SILT



## GRAVEL



## PEBBLY CLAY



## FORAMINIFERAL OOZE

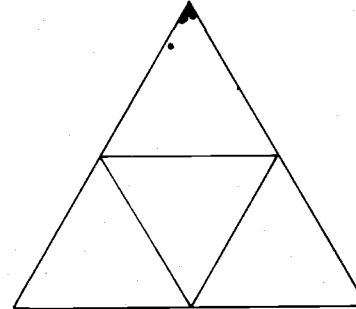
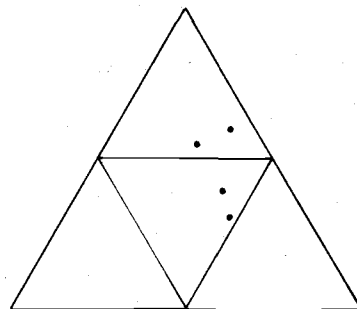


Figure 15. Texture and coarse fraction composition of terrigenous sand-silts, gravels, pebbly clays, and foraminiferal oozes

layers dominated by detrital grains. Cross-bedding, graded bedding, reverse grading, as well as massive structureless sections are present (Figure 14). An overall compositional gradation from detritals at the base to platy grains at the top also is common. A clayey tail, sharply separated from the sand-silt layer, may occur above it. Distorted clay clasts or galls, and displaced Foraminifera are commonly found in this fine tail as well as in the coarse lower interval.

The graded nature of most of these layers, the displaced benthic Foraminifera, and the incorporated clay clasts which are distorted, suggest that turbidity currents were the depositional mechanism for the thicker layers (Figure 14).

### Gravels

Coarse granular material consisting of sand and gravel has been found up to 750 km from shore along the axis of Cascadia Channel. The gravels have a very low silt and clay content (< 5 percent, see Figure 15) but are moderately to poorly sorted. Individual pebbles are primarily equidimensional in shape and are rounded to well rounded, while the finer material is more angular. Sedimentary, igneous, and metamorphic rocks are represented; basalt is the most common lithology. Thick walled molluscan shell material and wood fragments also occur in the gravel. Small numbers of

benthic Foraminifera are present, and 80 percent of the fauna is displaced from shallower water; 25 percent of the fauna originated on the inner shelf, or in water depths less than 50 m (Fowler, 1967, personal communication).

### Pebbly Clays

Gray pebbly clays of Pleistocene age up to 5 m thick occur in the axis and on the wall of Cascadia Channel. These poorly sorted sediments have an abrupt lower contact and a gradational or abrupt upper contact. They are massive and structureless, but may contain zones without pebbles and thin sand or silt layers. The pebbles are commonly more concentrated within certain intervals where they are actually in contact with each other. Using X-radiography, layers with high concentrations of sand and coarser material several cm in thickness were detected and are interbedded with thinly laminated clay layers (Figure 16). The grain size within these sediments ranges from fine clay to clasts up to 7 cm in length (Figure 15). Most of the pebbles are equant or rod shaped, generally rounded, and commonly have their long axis oriented in a vertical or oblique direction in the core (Figure 16). They may also be faceted and striated. Semi-consolidated clays and siltstones, graywackes, igneous and metamorphic rock types are present.

The depositional mechanisms usually considered in regard to



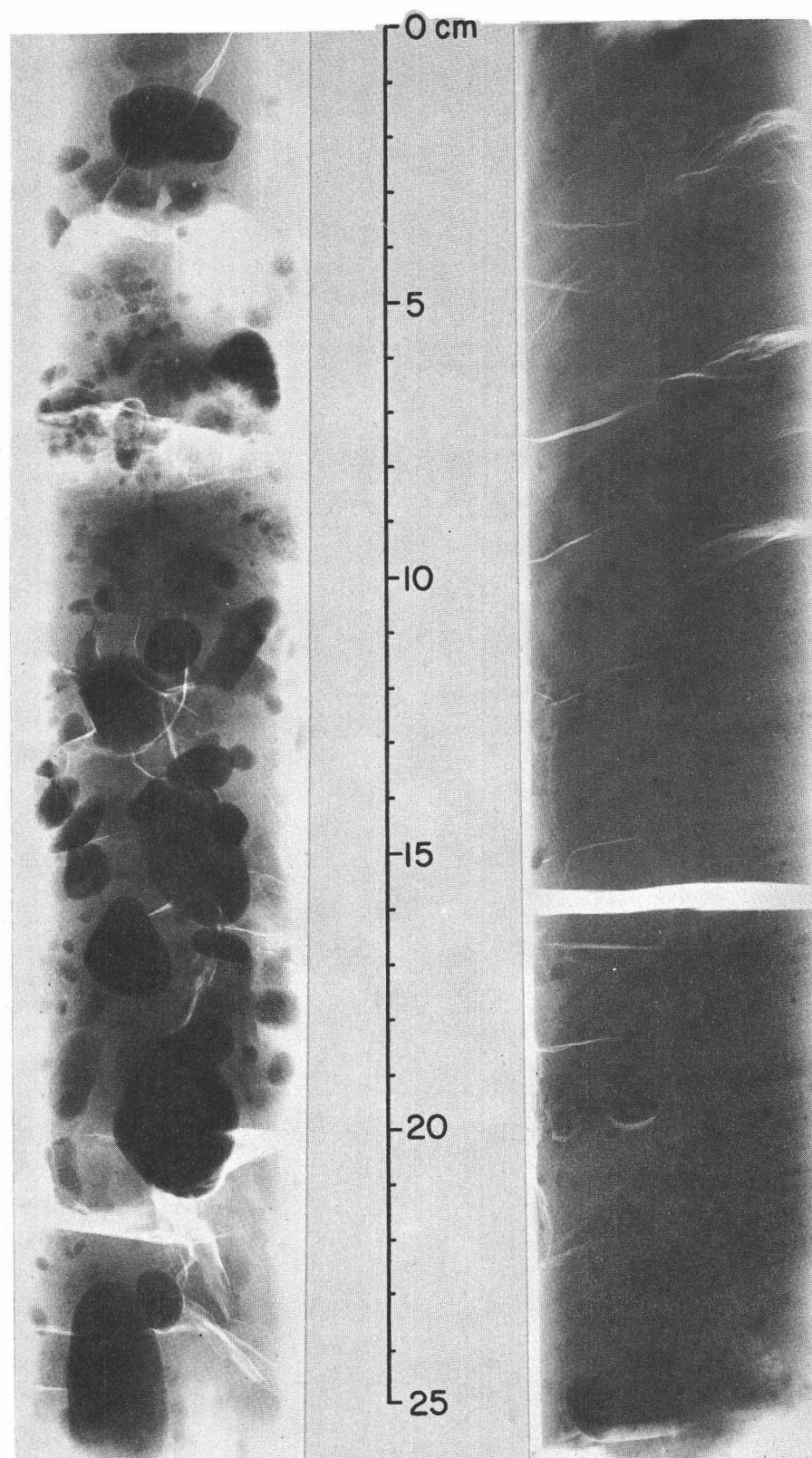


Figure 16. X-Radiographs of Pleistocene pebbly clays

pebbly clays or mudstones are viscous mudflows or rafting of some type. The interbedding of laminated and gravelly clays, the silt and sand layers, the great distance required for transportation, and the proximity to a glaciated region, seem to indicate ice rafting as a depositional mechanism.

### Foraminiferal Ooze

Fine-grained sediments with high concentrations of planktonic Foraminifera are often characteristic of Pleistocene sections in areas of low depositional rates in Cascadia Basin.(Duncan, 1968). A 2 meter thick section of greenish gray (5GY5/1) foraminiferal ooze occurs below a sequence of gray pebbly clay in the wall of Cascadia Channel. The lutite is interrupted by several dark yellowish brown (10YR3/2) silty layers. The ooze is very poorly sorted due to the abundance of sand sized foraminiferal tests (Figure 15) which compose 95-100 percent of the coarse fraction and result in a calcium carbonate content of 25 to 30 percent.

A seamount adjacent to Vancouver Sea Valley is capped by a foraminiferal ooze, yellowish gray (5Y7/2) in color. Very little sediment has collected on this seamount as it has an irregular surface and only about 20 cm of the ooze overlies a dark yellowish brown basaltic rubble. The rubble contains dark volcanic glass, and basalt fragments up to 3 cm in diameter. The basalt is partially altered to

a soft yellowish colored material, probably palagonite. The ooze consists of mineral grains and rock fragments, volcanic glass, Radiolaria, and Foraminifera. The calcium carbonate content is 42 percent. Both of these oozes are believed to represent normal pelagic deposition in their respective areas.

## PHYSIOGRAPHIC DISTRIBUTION OF SEDIMENTS

Seven distinct sedimentary environments are recognized within the Cascadia Channel system. Each distinct environment is treated separately and the physiographic location, lithology, and sediment ages for the cores from each environment are discussed (Figure 17).

### Upper Channel

Alternating sequences of olive green silt of turbidity current origin and gray hemipelagic clay characterize the Holocene sediments of upper Cascadia Channel and its northern tributaries. Graded silt layers and the interbedded gray clays are uniform in thickness and in grain size within individual cores (Figure 18, 6705-1, 6705-2, 6705-10). Deeper in the cores, approaching the Pleistocene, the silt layers thicken and coarsen to fine-grained sand. The absence of the interbedded gray clays closer to the continent suggests that turbidity currents have either occurred too rapidly for hemipelagic sediment to accumulate, or erosion has occurred, resulting in a repetitious sequence of olive green silts (6705-1, 6705-4). Overall Holocene sedimentation rates are high in the upper channel, reaching 45 cm/1000 yrs in one of the tributaries, and 71 cm/1000 yrs in Cascadia Channel. Rates of hemipelagic deposition vary from 4 to

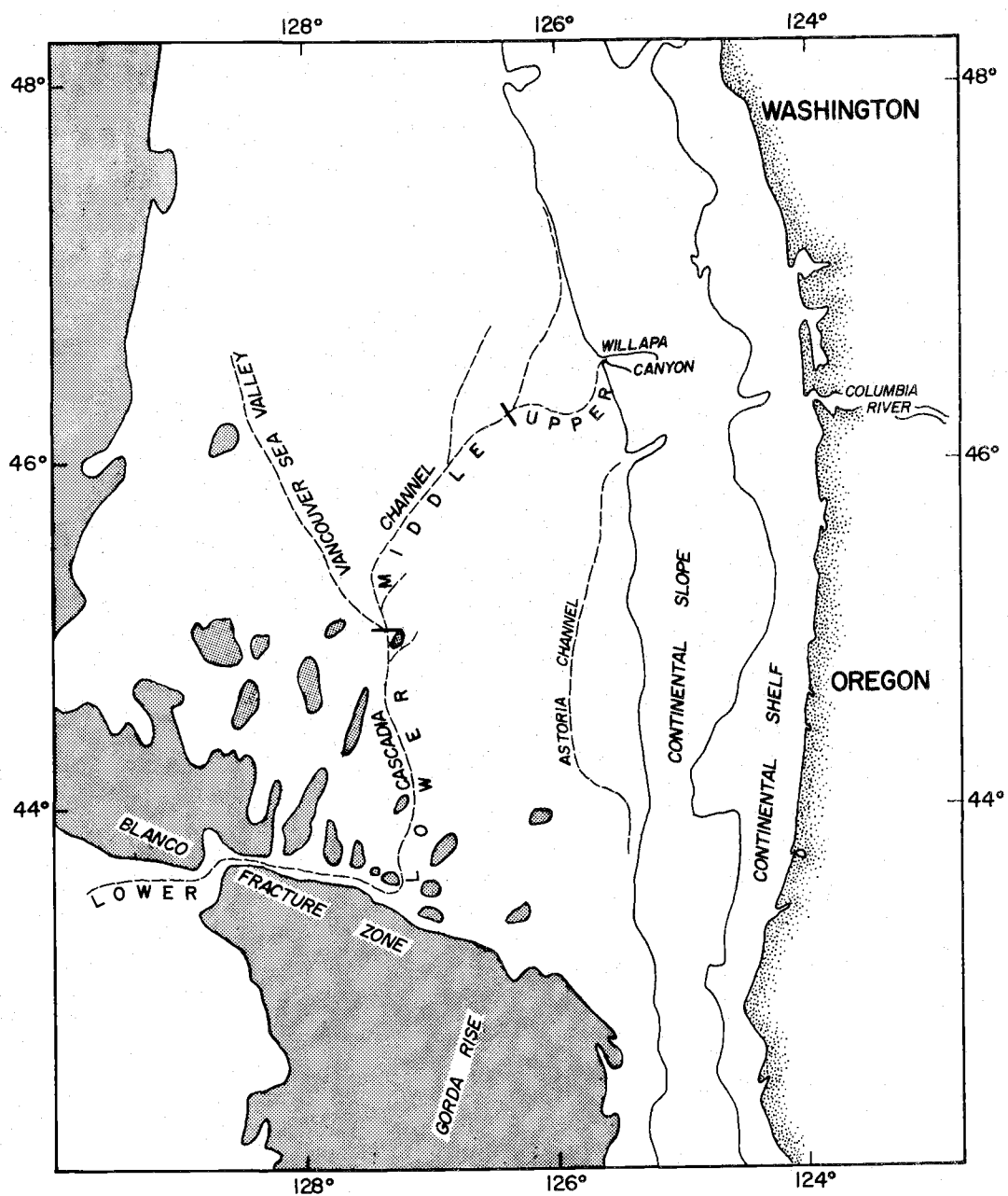


Figure 17. Physiographic divisions of Cascadia Channel

# UPPER CASCADIA CHANNEL

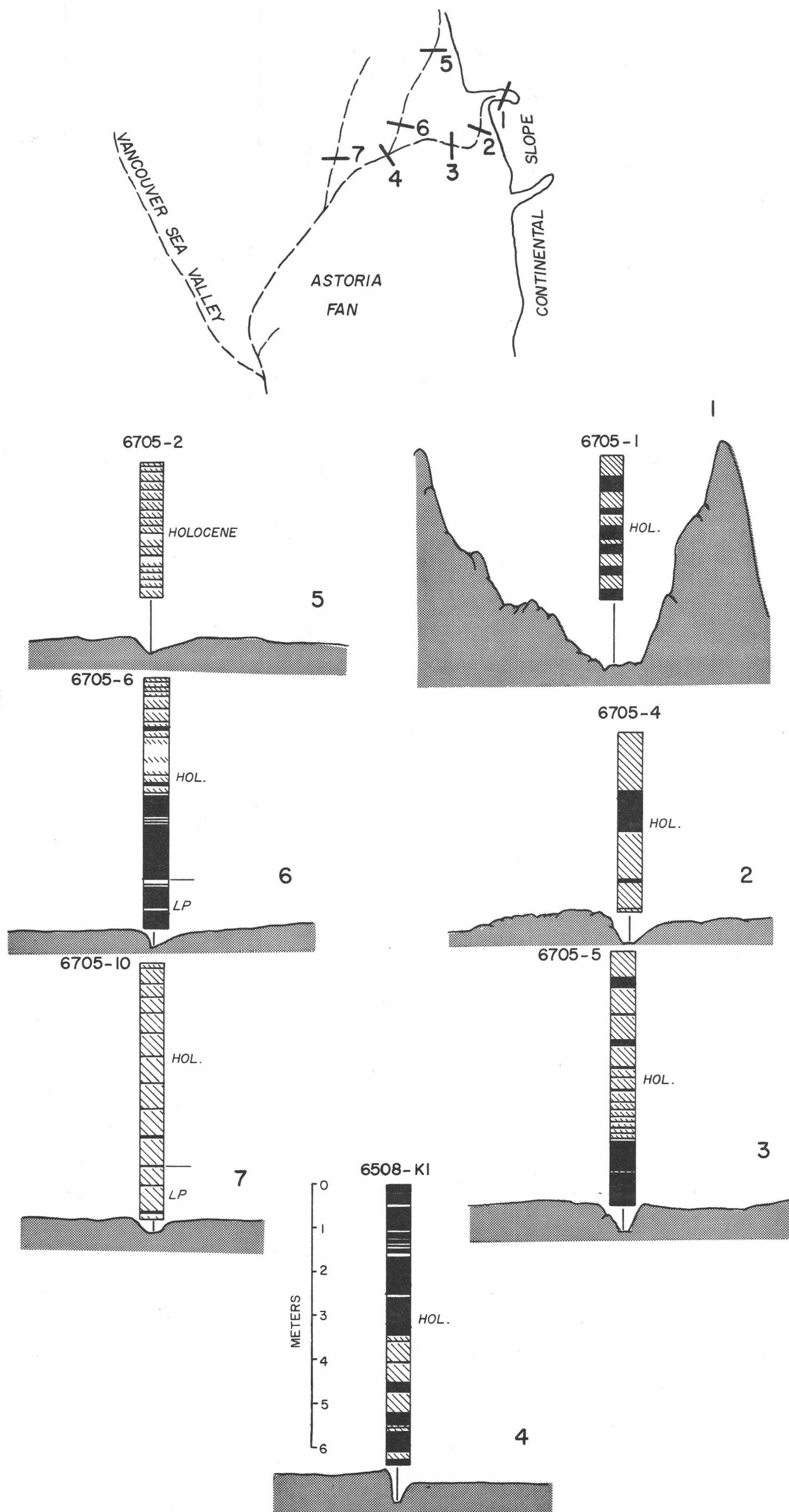


Figure 18. Lithology of cores from upper Cascadia Channel. Vertical exaggeration of profiles 20X; Core lithologies explained in Table 3. HOL= Holocene LP= Late Pleistocene.

over 14 cm/1000 yrs.

### Middle Channel

Sedimentation within the middle channel is anomalous in relation to the remainder of the channel. At least five periods of distinctly different sedimentation have been recorded (Figures 19 and 20). The lowest and oldest unit is a gray clay containing many thin, clean silt laminations (6705-13). Above it and separated by a sharp contact, is a pebbly clay horizon which extends for at least 75 km along the middle channel. It grades upward into another clay sequence with silt laminations (6609-30). Still higher is a section of gravel and coarse sand (6509-14, 6609-30, 6705-8) which contains shallow water benthic Foraminifera, coarse molluscan debris, and wood fragments. The most recent sediments are the rhythmic alternations of olive green silt and gray clay, found along the remainder of the channel. With the exception of core 6509-10, Holocene sedimentation in this area has been negligible. The presence of extensive Holocene deposits both to the north and south, and the unconformities and incomplete stratigraphic sequences in the cores (Figure 20), indicate that the turbidity currents passing through the area, have not deposited any material. The turbidity currents apparently retain their erosional or non-depositional character until they reach the location of core 6509-10 (Figure 19). The wide and flat nature

## MIDDLE CASCADIA CHANNEL

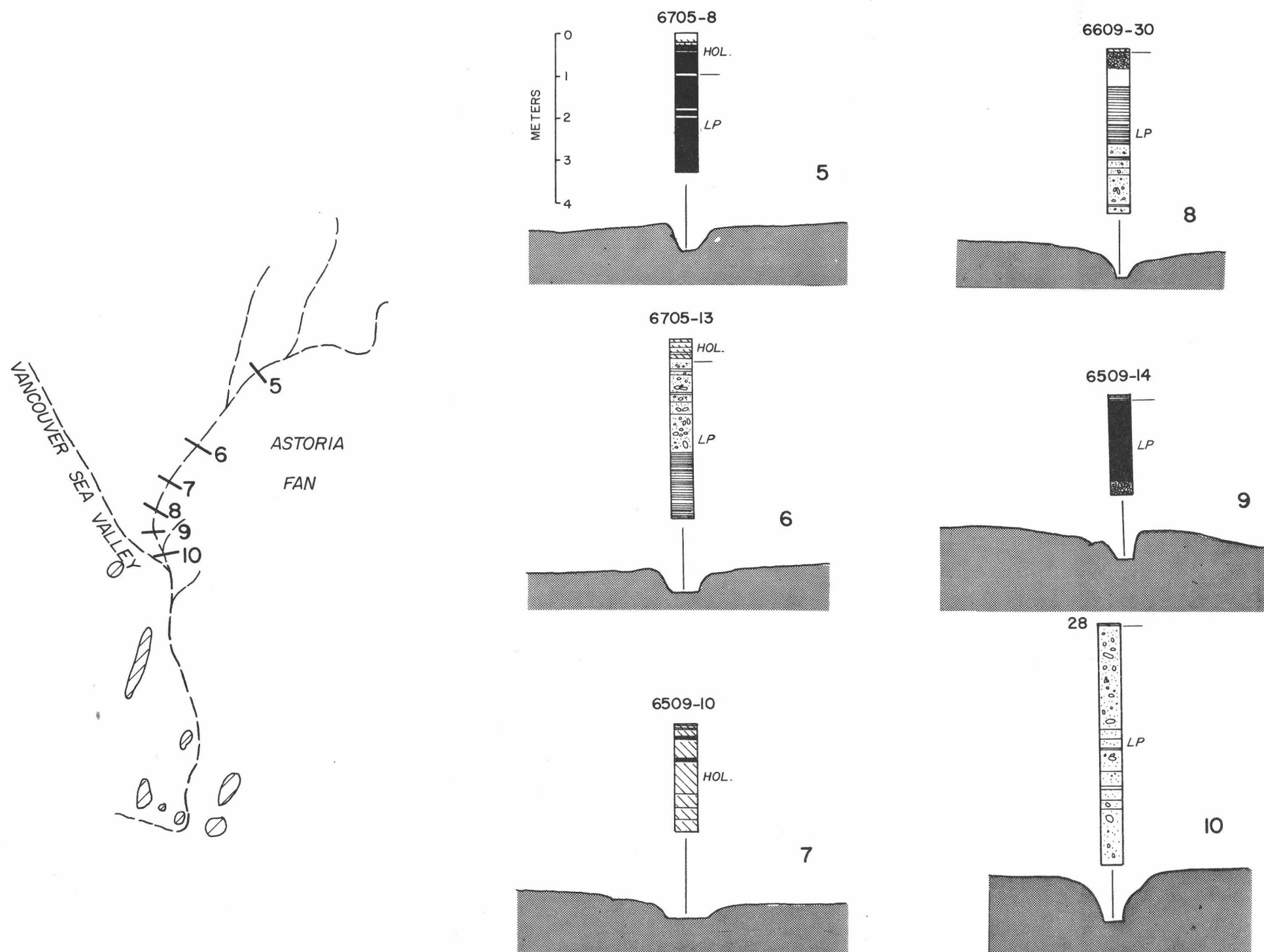


Figure 19. Lithology of cores from middle Cascadia Channel. See caption of Figure 18 for core explanation.



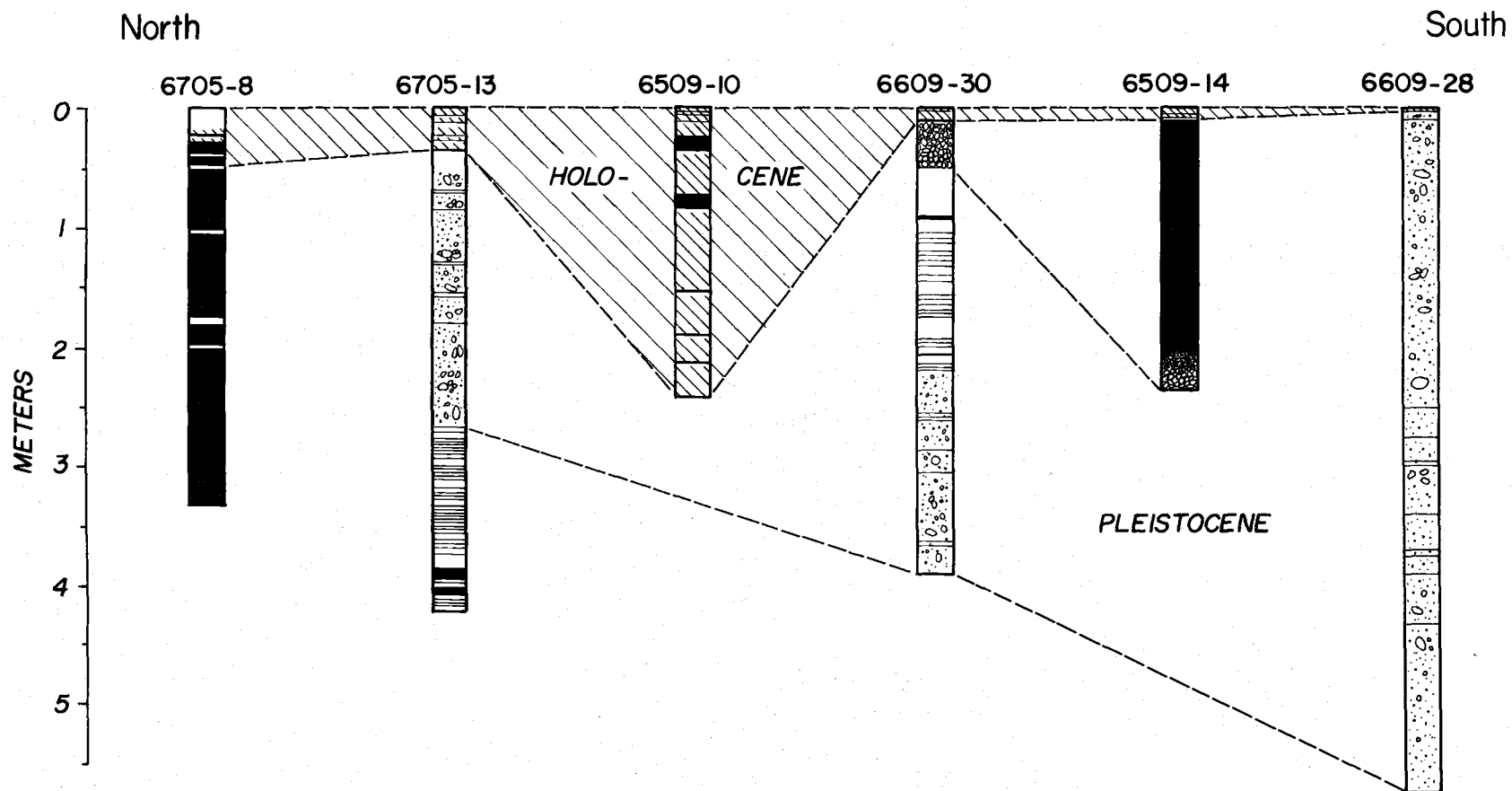


Figure 20. Longitudinal stratigraphic correlation of cores from axis of middle Cascadia Channel. See caption of Figure 18 for core explanation

of the channel floor, the decreased gradient, and the typical graded cycles in the core from this area, indicate extensive turbidity current deposition. Below this point, the channel narrows and Holocene sedimentation is again almost lacking, until Vancouver Sea Valley is reached. The channel floor is very smooth or irregular, as well as level or sloping where cores show erosion or non-deposition.

#### Lower Channel

Holocene sedimentation in the lower channel is exceedingly uniform and thick (Figure 21) and consists of the typical rhythmically interbedded olive green silts and gray hemipelagic clays. The uniform thickness of both the graded beds and the clay layers within each core shows the similarity of the turbidity current flow conditions. The coarse basal layers of the silts show a general thinning down channel. A lack of recognizable hemipelagic sediment at the surface of these cores, and the absence of extensive burrowing in the surficial layer compared to the extensive reworking in lower layers, indicate that the last flow was recent. The presence of Mazama Ash in the sediment and a C-14 date of 4645 years B.P. (6509-27) at depth (Figure 21) also suggest recent turbidity current activity. Holocene depositional rates here are very high if the turbidity current deposits are included (up to 125 cm/1000 yrs), and much lower for the hemipelagic clays (4-9 cm/1000 yrs). The longest

# LOWER CASCADIA CHANNEL

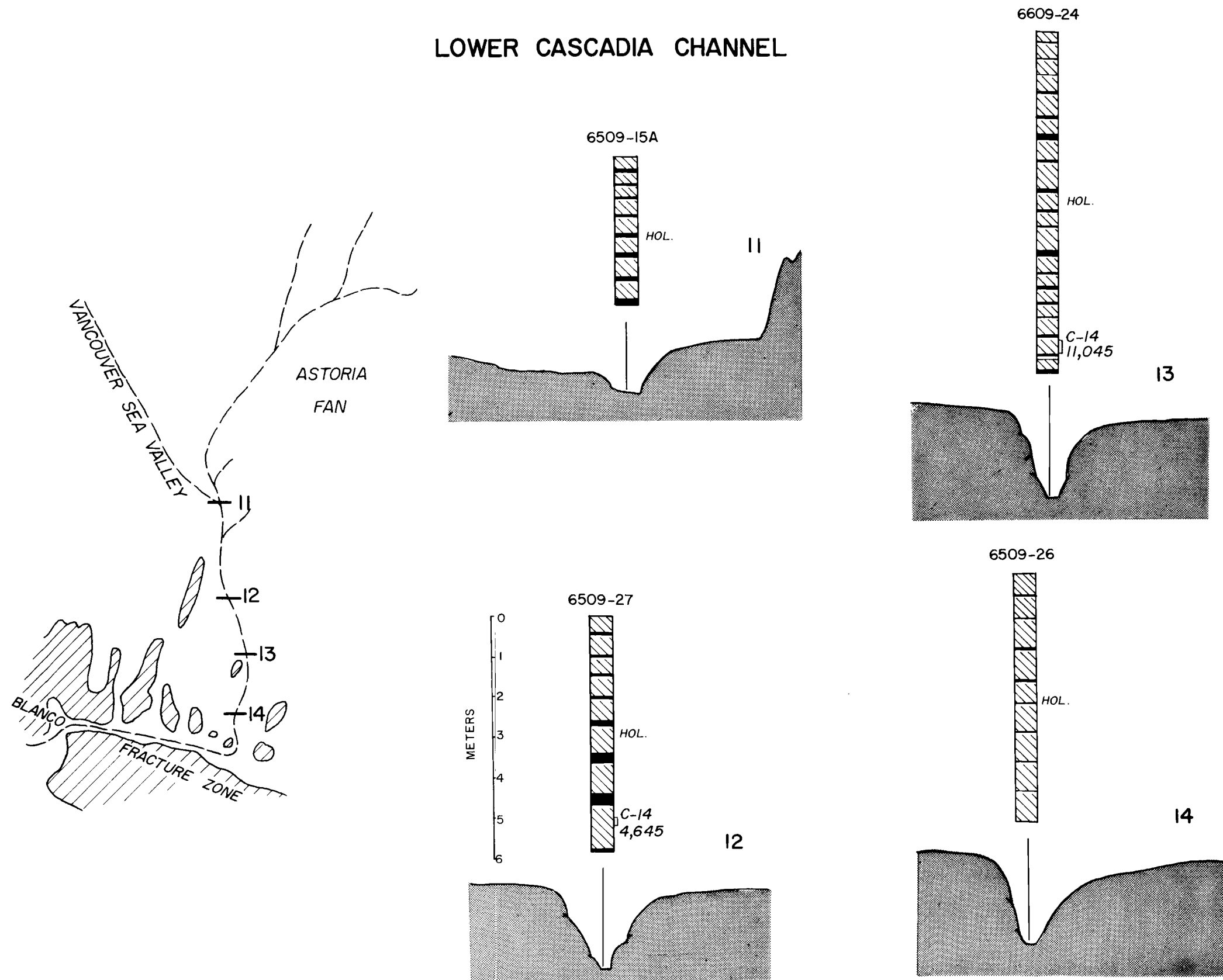


Figure 21. Lithology of cores from lower Cascadia Channel. See caption of Figure 18 for core explanation.

stratigraphic section is over 8 m and contains 17 repetitious cycles which extend back over 11,000 years, almost into the Pleistocene.

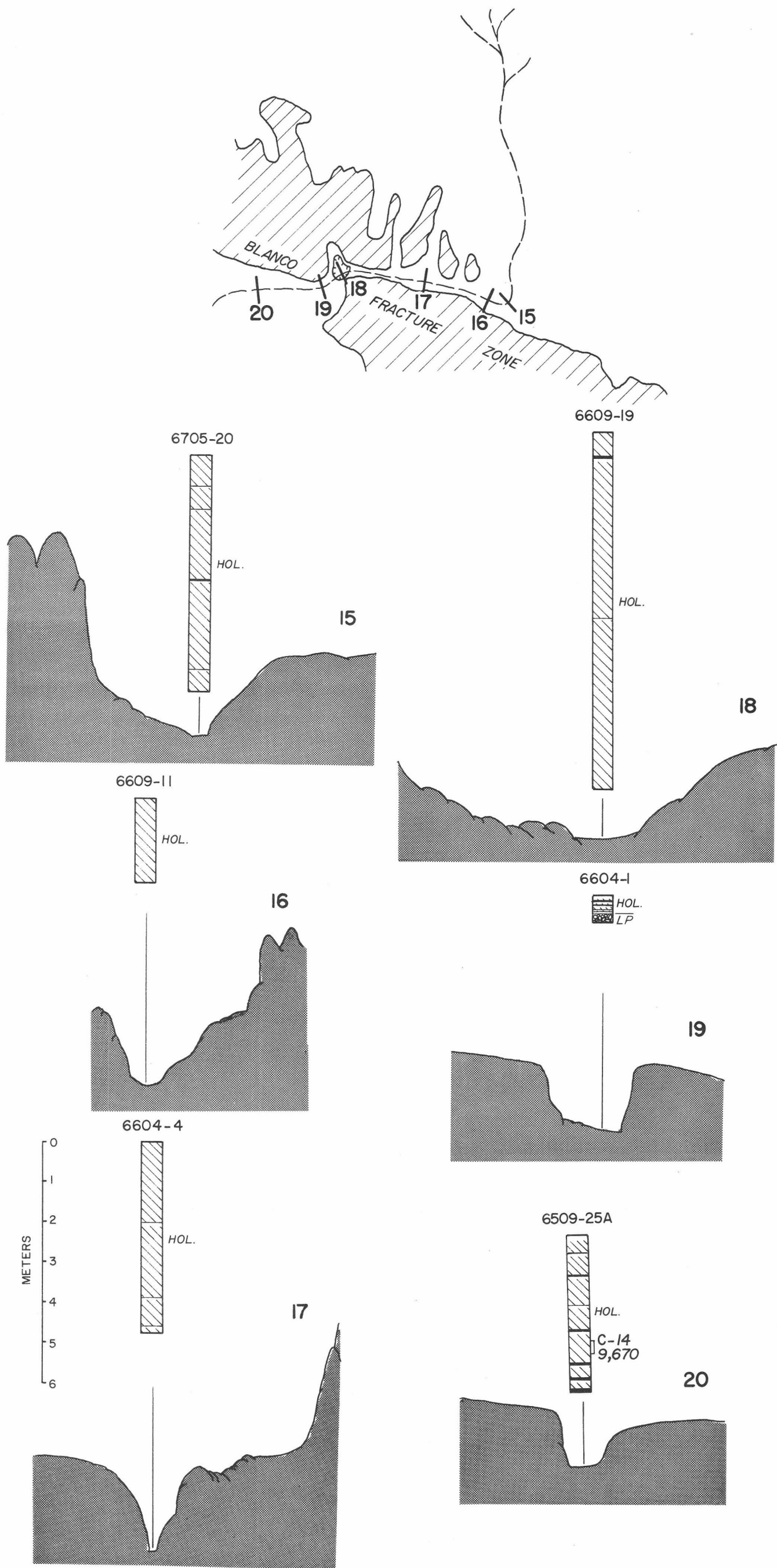
Although the channel is narrow and tightly confined within Blanco fracture zone, Holocene deposition has been very high. Cores 8 m long have only penetrated several olive green silt-gray clay cycles (Figure 22). The silts sequences are very thick, averaging 192 cm. Coarse basal layers are only 1 to 2 cm thick, and the remainder of each unit consists of the fine-grained tail (Figure 10). A recent structural depression along the channel axis at the western end of the fracture zone contains the thickest cycles, and appears to be acting as a sediment trap (Duncan, 1968). The presence of Mt. Mazama ash both up and down channel of the depression dates its formation at some time during the last 6600 years. Depositional rates here probably exceed 400 cm/1000 yrs. The absence of recent turbidity activity in the channel on Tufts Abyssal Plain is indicated by the hemipelagic clay covering (7 to 10 cm) on the cores from that area (6509-25A, 6604-1).

#### Channel Walls

The sedimentary sequence on the walls of Cascadia Channel demonstrates that Holocene turbidity currents have risen above the channel floor to deposit the olive green silts. Two cores from the west wall of the lower channel, 4 m above the bottom, contain up to

LOWER CASCADIA CHANNEL

Figure 22. Lithology of cores from lower Cascadia Channel (Blanco fracture zone). See caption of Figure 18 for core explanation.



21 cycles of alternating silts and clays (6509-15, 6509-17, Figure 23). The silt sequences are much thinner here than on the channel floor (Figure 10) and range from 3 to 15 cm. Sediments cored on the lower portion of the east wall contain none of the typical channel turbidity current deposits in the Holocene section (6705-16, 6705-17). This time interval is represented only by 75 to 150 cm of hemipelagic clay in the two cores taken 8 and 37 m above the channel bottom (6705-16 and 6705-17, respectively). The Pleistocene section of core 6705-16 consists of thick terrigenous sand layers, probably representing turbidity current deposition, which imply a greater thickness and competence for the Pleistocene flows. These sediments were probably deposited by turbidity currents which flowed down Astoria Fan during the Pleistocene.

Higher on the western wall of the channel, only hemipelagic clay has been deposited in Holocene time (6609-25, 127 m above the channel bottom). The lowest and oldest sediment in the Pleistocene section is a foraminiferal ooze; the upper portion has been dated at 37,000 years B.P. Above it lies a thin pebbly clay sequence, identical to that found along the middle channel (Figure 23). The pebbly clay contains large semi-consolidated silt and claystone clasts as well as granules and pebbles. It grades upward into a clay with thin sandy interbeds, which is transitional between the Pleistocene and Holocene. The sharp contact between the ooze and the pebbly

## CASCADIA CHANNEL WALLS

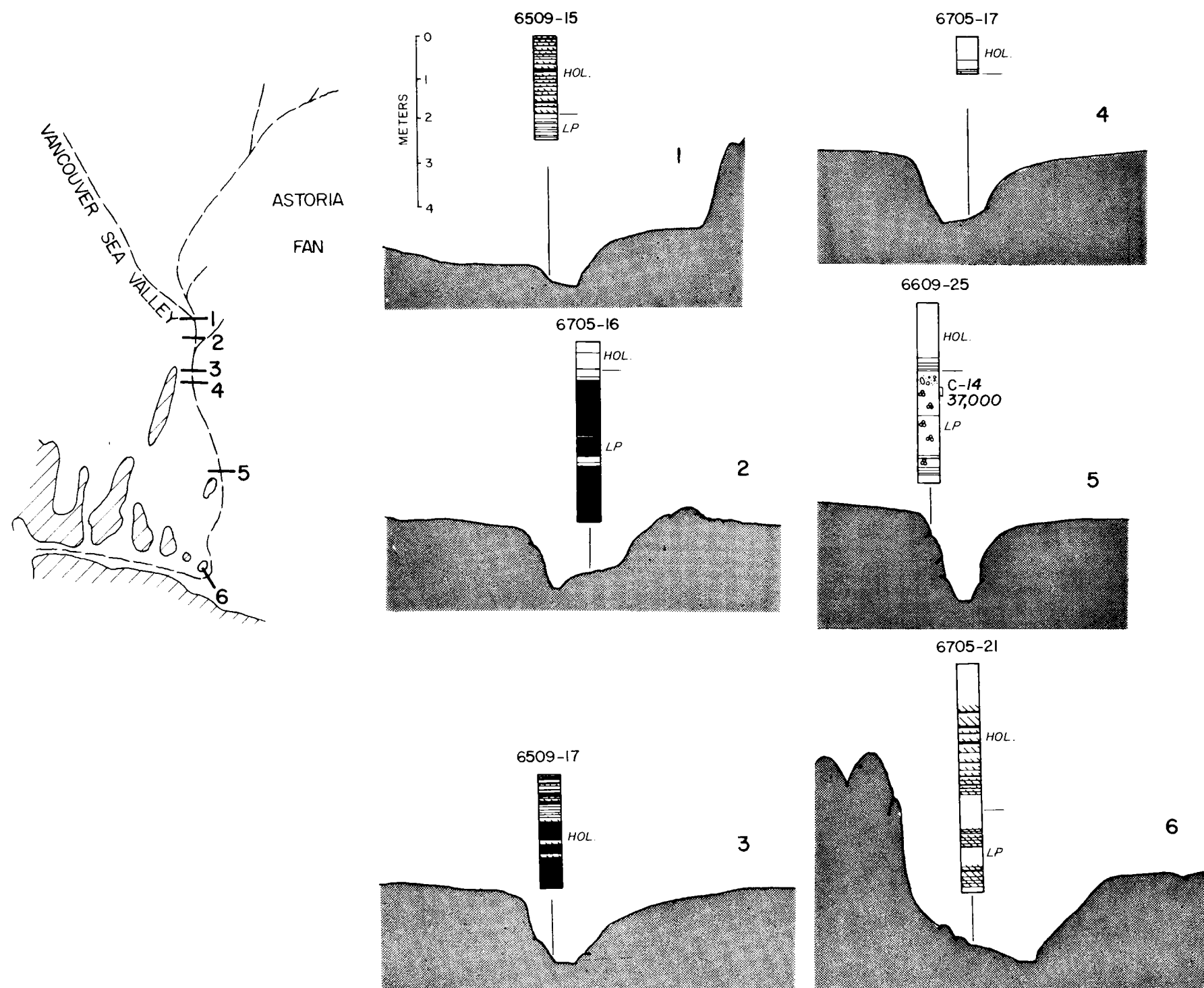


Figure 23. Lithology of cores from walls of Cascadia Channel. See caption of Figure 18 for core explanation.

clay suggests a hiatus of some duration. The presence of only 50 cm of Pleistocene sediment above the dated interval suggests that extensive erosion or non-deposition has occurred. Farther to the south, where the channel enters Blanco fracture zone, sediment on the western wall shows that turbidity currents have risen 54 m above the floor to deposit the typical olive green silt cycles (6705-21, Figure 23). The thicker units here, in contrast to other wall cores, are probably due to the welling up of the large amounts of material funneled into this opening during the passage of a turbidity current. The flow must make a right angle turn here where the channel floor is relatively narrow.

#### Channel Banks and Levees

In order to study cross channel sediment variation and to determine if turbidity current spillover has occurred, four coring profiles were taken across the channel along its length (Figure 24). The northern most profile (1) shows a well developed levee to the west, rising 28 m above the plain and extending 6.5 km laterally. Cores from the west and the east (6705-7, 6705-9), 86 and 77 m above the channel bottom respectively, contain the characteristic alternating sequences of olive green silt and gray clay, and illustrate Holocene turbidity current overflow. The graded olive green silts are only 5 to 10 cm thick; they frequently have very thin (1 to 2 cm) coarser



# CASCADIA CHANNEL BANKS AND LEVEES

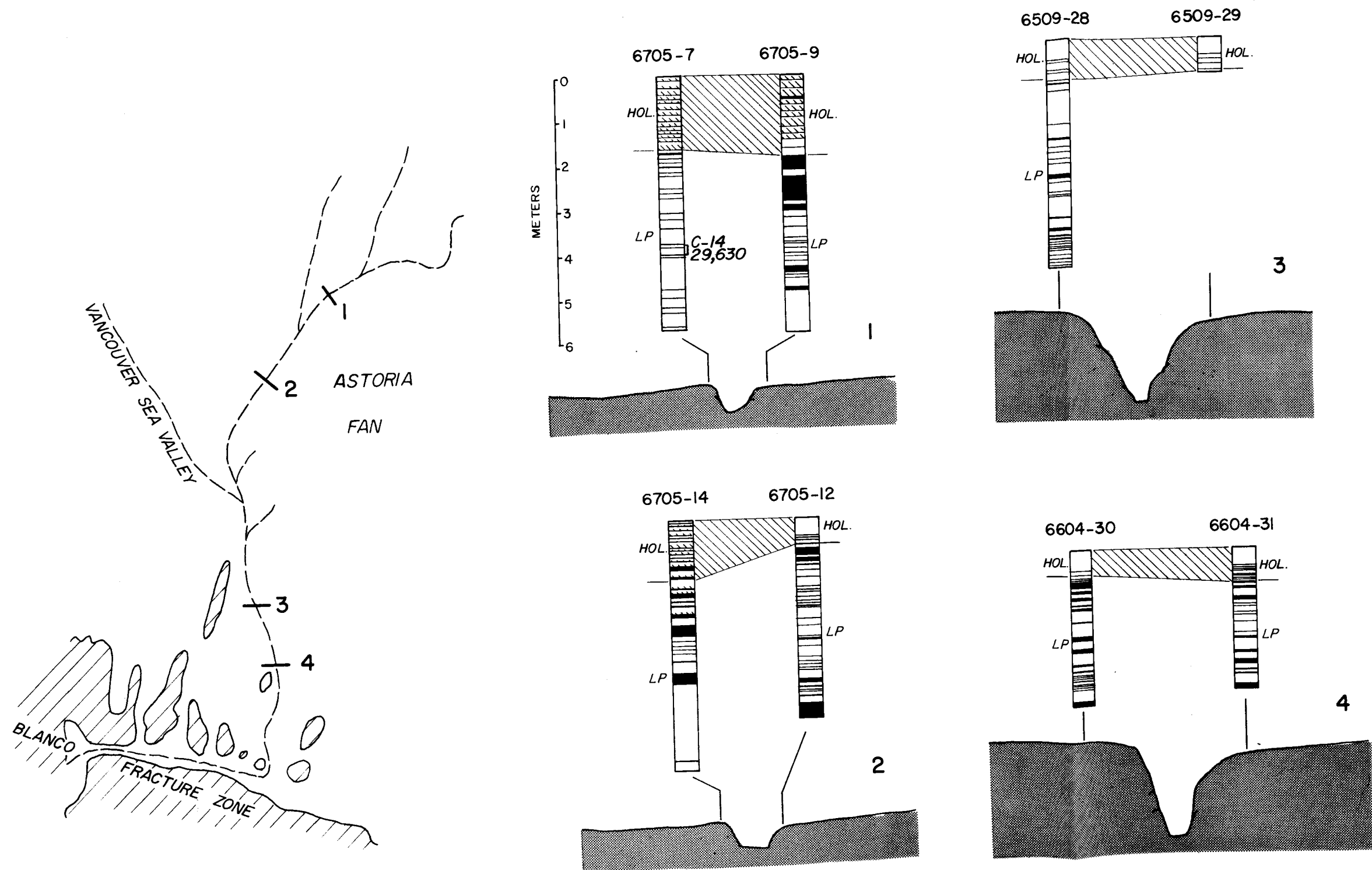


Figure 24. Lithology of cores from banks and levees of Cascadia Channel. See caption of Figure 18 for core explanation.

layers at the base and contain Mazama ash.

The next profile to the south (2) again shows a well developed levee to the west which extends laterally for 4 km and rises 13 m above the plain. Turbidity currents have overflowed onto the western plain (6705-14) but have not been recorded in the hemipelagic Holocene sediments on the eastern bank. The asymmetry, or tilt of a turbidity current, first suggested by Menard (1955), is verified at this location. The core on the levee to the west (6705-14), showing overflow, is 68 m above the channel floor; the core to the east is lower (6705-12), only 59 m above the channel floor and shows no overflow.

Coring profiles were also made across the lower channel where no levees are apparent and the relief of the channel floor ranges from 238 to 286 m (Figure 24). Holocene sediment of all four cores (6509-28, 6509-29, 6604-30, 6604-31) consists of hemipelagic clay, which illustrates that none of the turbidity currents which passed through this part of the channel topped the banks.

The Pleistocene sections in all of the levee and bank cores consist of gray clay interbedded with terrigenous sand-silt layers. The cores landward of the channel contain a greater proportion of coarse material than those to the west. A C-14 date (29,630 years B.P.) in the Pleistocene section of core 6705-7 indicates a late Pleistocene depositional rate of 13 cm/1000 yrs, identical to the Holocene rate for the overlying levee sedimentation.

Only six to 11 percent of the levee heights can be accounted for by Holocene turbidity current deposits, which indicates that these features were formed mainly by Pleistocene sedimentation. The underlying sediment, which probably represents Pleistocene overflow, ranges from thin silty laminae to 60 cm thick beds of medium grained sand, and generally is coarser and cleaner than the Holocene olive green silts. The range in grain size and thickness of the Pleistocene coarse layers, in comparison with the uniformity of the Holocene olive green silt sequences, suggests that the competency and load of the Pleistocene turbidity currents must have been quite variable.

#### Vancouver Sea Valley and Astoria Fan Tributaries

During the Pleistocene large amounts of sand moved through Vancouver Sea Valley and the channels on outer Astoria Fan (Figure 25). The Pleistocene sedimentary deposits consist of beds of fine sand, up to 150 cm thick, which contain laminations, commonly display graded bedding and are interbedded with thin hemipelagic gray clays (Figure 14). Turbidity currents have been inactive in these channels since Pleistocene time, and deposition of Holocene hemipelagic clay has continued without interruption. Depositional rates range from  $< 2$  cm/1000 yrs, farthest from shore (6610-2), to 8 cm/1000 yrs in southern Vancouver Sea Valley. The

# VANCOUVER SEA VALLEY AND ASTORIA FAN TRIBUTARIES

74

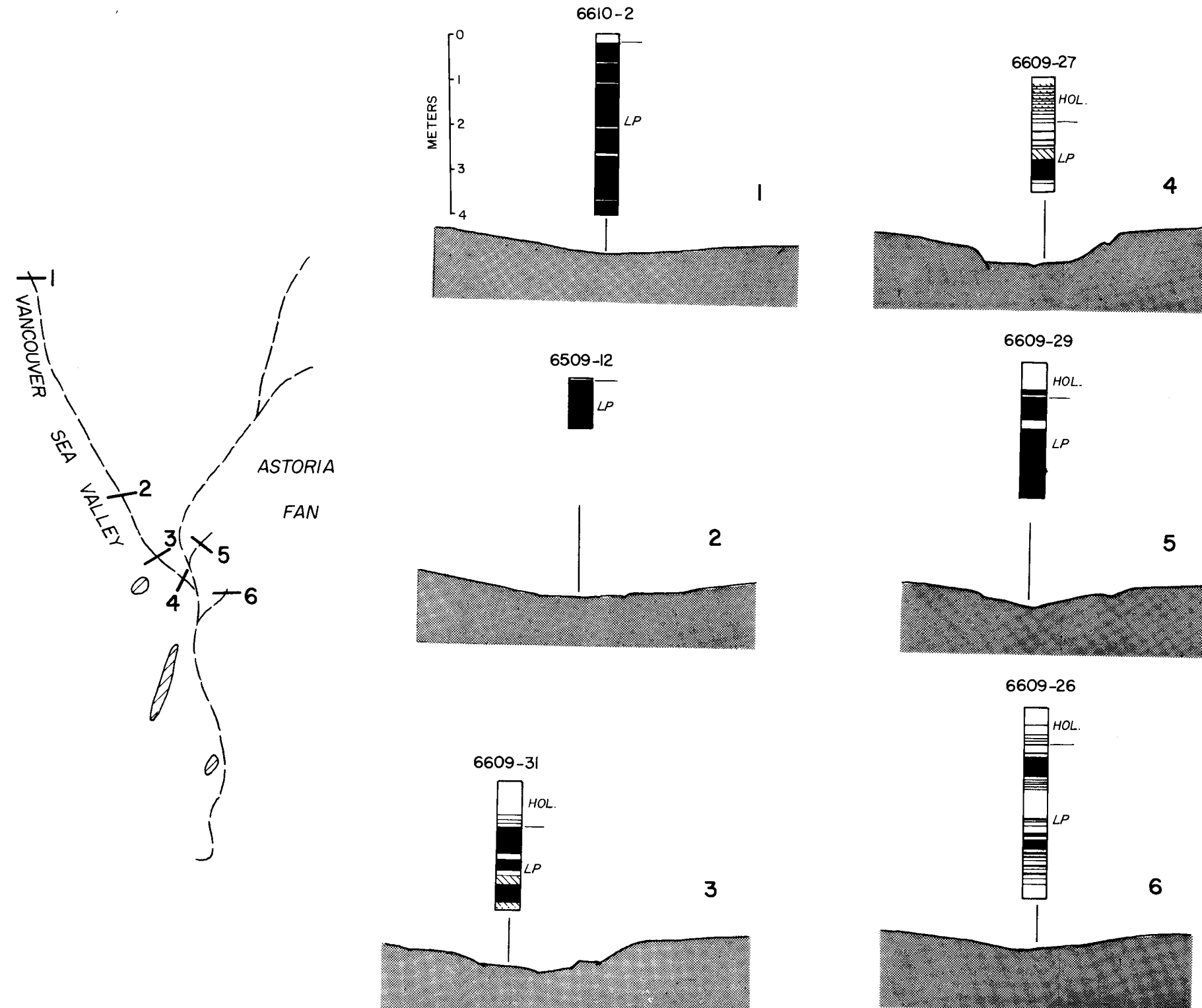


Figure 25. Lithology of cores from Vancouver Sea Valley and Astoria Fan tributaries. See caption of Figure 18 for core explanation.

southern-most core from Vancouver Valley (6609-27, Figure 25) contains eight thin sequences of olive green silt which have spilled over from Cascadia Channel during Holocene time. The flows must have been at least 80 m high and spread laterally 15 km to reach this point from the floor of Cascadia Channel.

### Cascadia Abyssal Plain

Sedimentation on the abyssal plain during Pleistocene and Holocene time has been similar to that in Vancouver Sea Valley and on the banks of lower Cascadia Channel. Turbidity currents have been largely inactive and hemipelagic clays compose the Holocene sections. The Pleistocene is characterized by the appearance of many terrigenous sand-silt layers interbedded with gray clay.

A core from a seamount adjacent to Vancouver Sea Valley (6609-32) revealed only a very thin (20 cm) covering of foraminiferal ooze overlying a basaltic rubble. The seamount either has slopes too steep for the sediment to accumulate on, has been swept free of sediments by currents, or is a recent tectonic feature in the area.

### Summary of Sediment Distribution

Turbidity currents have been actively depositing thick, olive green silt sequences throughout upper and lower Cascadia Channel during Holocene time. These deposits alternate cyclically with thin

layers of hemipelagic gray clay which settles out of suspension during periods of non-turbidity current deposition. This rhythmic sedimentation occurs in the northern tributaries and extends for at least 650 km along the axis of Cascadia Channel. The Holocene sediment sequence on the walls of the channel indicates that the turbidity currents commonly rose above the floor to deposit the characteristic olive green silts. Levees which flank the western side of the upper and middle channel also contain the same sediment sequence, which indicates turbidity current overflow in this area. South of  $45^{\circ}30'N$ , where the channel turns to the south, no levees are present, and only hemipelagic clay has been deposited on the channel banks in Holocene time.

Erosion and/or non-deposition has characterized the middle channel during the Holocene. The turbidity currents which deposited the characteristic sequences to the north and south left for the most part, only a thin surficial covering along the middle channel. Pleistocene sections of diverse lithology, including pebbly clays, laminated clay-silt sequences, gravels, and terrigenous sand-silt units, are capped by several centimeters of olive green silt or gray clay (Figure 26). The coarse, clean gravels have also been cored beyond Blanco fracture zone along the axis of the lower channel. Pebbly clays extend for over 75 km along the axis of the middle channel (Figure 26) and have also been cored in the channel wall 100 km

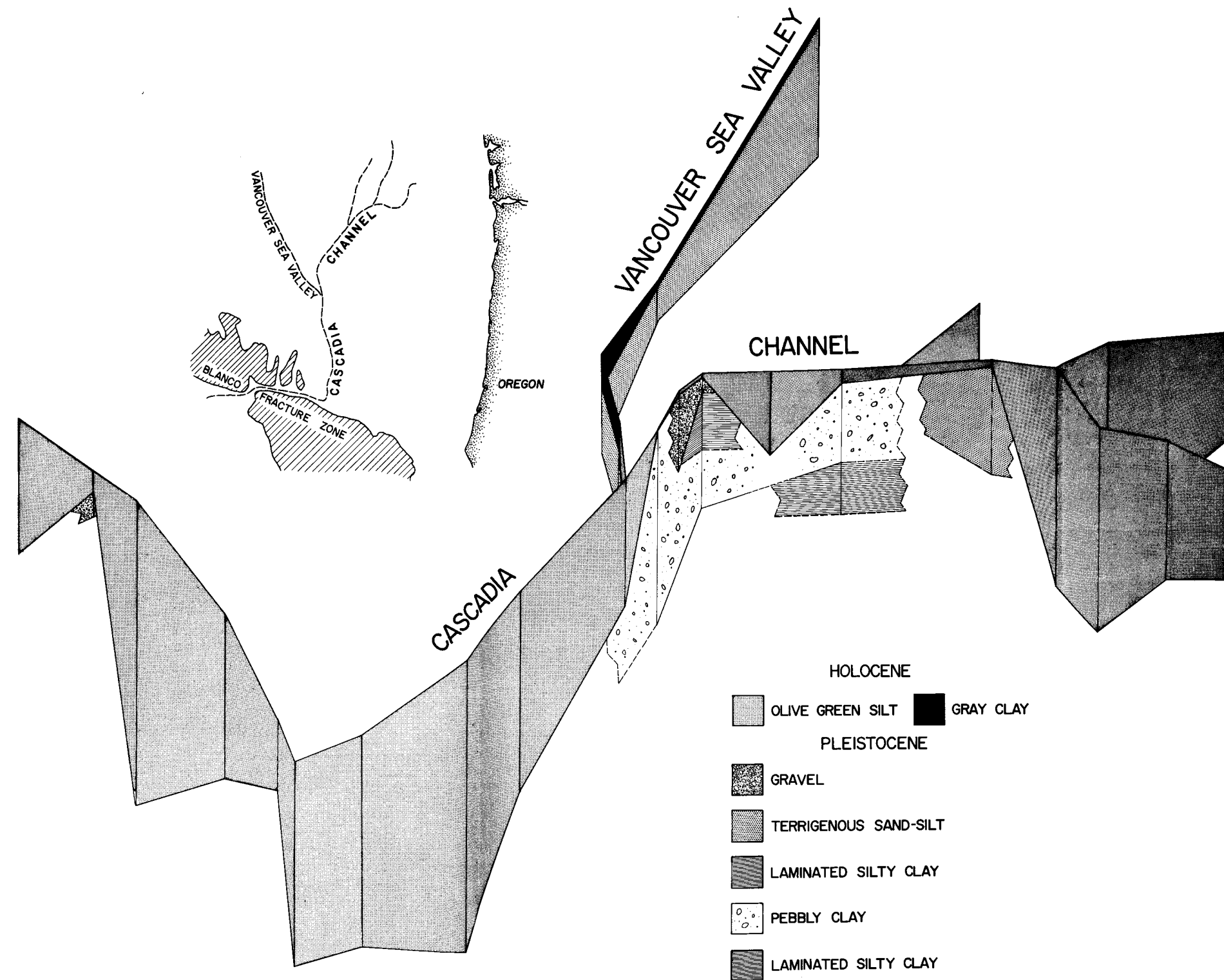


Figure 26. Holocene and Pleistocene sediment facies along the axis of Cascadia Channel

further south. The Pleistocene sections of the channel levees, banks, and walls consist predominantly of terrigenous sand or silt layers of varying thickness, interbedded with gray clays.

Large amounts of sand moved through Vancouver Sea Valley and the channels on lower Astoria Fan during the Pleistocene. These channels have, however, been inactive since that time and only hemipelagic clay has been deposited during the Holocene.



## DEPOSITIONAL PROCESSES

### Holocene Turbidity Currents--Empirical Data

Turbidity currents have been recognized for years under such names as density and suspension currents, but not until Kuenen and Migliorini (1950) demonstrated that graded bedding was a natural result of these currents was their importance in the marine environment recognized. In recent years many studies have been made of marine sedimentary rocks, sea floor sediments, and deposits in experimental tanks, which emphasize the importance of this sedimentation mechanism.

A turbidity current has greater density than the surrounding fluid due to its load of suspended sediment. A slump or failure in unconsolidated sediment on a slope is the most common mechanism cited as giving rise to a turbidity current. Due to its excess density, the turbid mixture can move downslope, following the low areas in the bottom topography. The erosive ability of these currents is still poorly known, whereas deposition occurs when the flow no longer has the competence to transport the sediment. This may be due to a decrease in slope or velocity, or to an overloading of the current.

Several individuals have investigated the properties of turbidity currents and their relationship to the deposits, either by the use of

laboratory models (Kuenen, 1965, 1966; Middleton, 1966a, b; 1967), or by detailed field studies (Bouma, 1962; Walker, 1967). The need for an accurate picture of modern turbidity current characteristics and properties in the marine environment is obvious. Most studies to date have been concerned with submarine canyons and fans or abyssal plains where sediments are discontinuous and where correlation is virtually impossible. Cascadia Channel is an extensive and confined route for turbidity currents. Its location relatively close to shore, and its origin, near the site where large volumes of sediment from the Columbia River are deposited, make it a perfect location for modern turbidity current analysis.

Previously mentioned evidence for turbidity current origin of the Holocene olive green silts in the channel system includes grading of grain size and composition, erosional basal contacts, interbedding with hemipelagic clays, and most important, the physiographic distribution of the sediments. This evidence and other data are elaborated upon in order to determine the nature of this medium of transportation and deposition. The above mentioned and subsequently described characteristics rule out deposition by normal currents (Kuenen, 1967). The extremely poor sorting and high clay content of these sediments also indicate they have not been reworked by normal currents.

### Foraminiferal Distribution

Displaced Foraminifera from three intervals in a single graded unit (255 to 310 cm deep in core 6509-15A) ranged from 66 to 88 percent of the total fauna (Figure 27). Only in the lowermost sample were many forms present which seem restricted to abyssal depths greater than 2400 m (Uvigerina senticosta, Nonion pompilioides, Bulimina rostrata, Gyroidina gemma, and G. soldenii) and even here they only comprise eight percent of the fauna. A significant number of species restricted to very shallow water are found in all three samples (Eggerella advena, Buliminella elegantissima, Elphidium incertum, Bucella frigida, and B. tenerima). These forms vary from ten to 41 percent suggesting that the origin of the coarse sediment was in very shallow water, probably less than 100 m in depth.

In addition to these species, a high percentage of forms have depth ranges restricted between 200 to 2000 m. This group is dominated by Bolivina argentea, B. pacifica, B. spissa, Epistominella pacifica pacifica, Uvigerina peregrina, Buliminella exilis, and Loxostoma pseudobeyrichi. The presence of a fauna restricted to shallow water and its mixture with a fauna from intermediate depths, indicate that the transporting turbidity current originated in shallow water, but accumulated and mixed sediment as it flowed to its abyssal depositional site. Phleger (1951) found a similar mixed fauna in

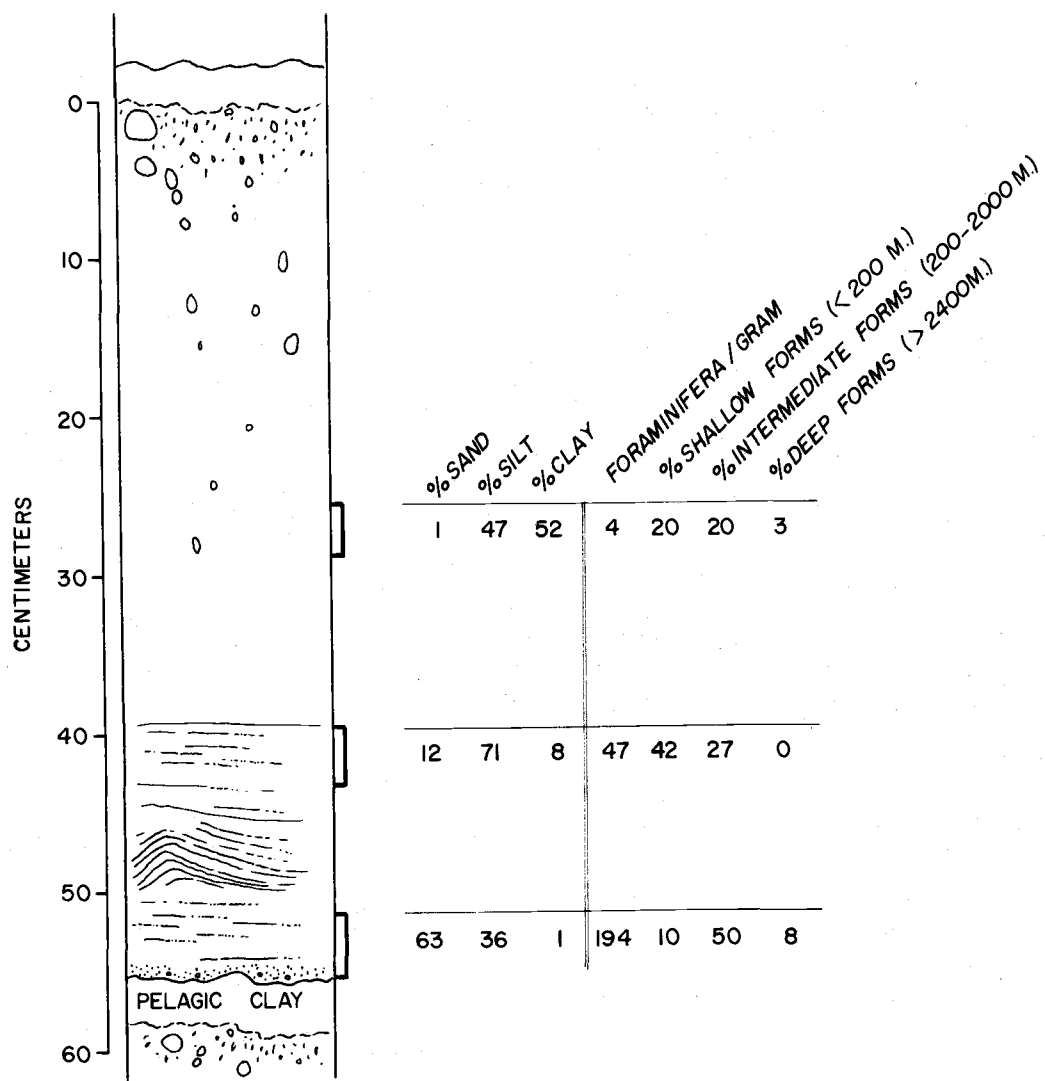


Figure 27. Olive green silt sequence from lower Cascadia Channel axis (6590-15A) illustrating textural and microfaunal variations

Coronado Canyon at a depth of 1200 m.

A sorting of the fauna has also been recognized in addition to the mixing described. The numbers of Foraminifera per gram are high in the coarse basal layer, and low in the fine-grained tail (Figure 27). The tests behave hydraulically as the silt and sand grains, and tend to be separated from the finer clays during the differential settling of a turbidity current. To illustrate the distinct size gradation in the graded unit, the percentage of two small species were calculated (Eggerella advena, Epistominella exigua). Only four percent of the fauna in the lowest sample consisted of these forms. In the overlying finer-grained samples, 52 and 37 percent of the fauna consisted of these two species. Sorting is also illustrated by the size variation of Univerina peregrina. The average length of this species in three samples from the base of the sequence upward was 0.32 mm, 0.16 mm, and 0.09 mm. The average size of this species in each sample is about half that of the interval below it. It is apparent that a size sorting of the Foraminifera as well as a faunal mixing results from the action of a turbidity current in this area.

#### Mt. Mazama Ash Distribution

The distribution of volcanic ash in the marine environment from the eruption of Mt. Mazama has recently been summarized (Nelson et al., 1968) (Figure 6). The presence of the ash in coarse layers

from submarine canyon and channel environments, and its absence from the remainder of the abyssal plain indicate that deposition was from turbidity currents and not from aerial fallout. Volcanic ash occurs in the olive green silts along the entire length of Cascadia Channel sampled (650 km) and in the upper channel levees and the western walls.

### Textural and Structural Variations

The internal sequence of structures in turbidites has been described in detail and related to flow regimes and depositional environments (Kuenen, 1953; Bouma, 1962; Walker, 1965, 1967).

The great majority of the graded sequences from Cascadia Channel are different than those described by Bouma and Walker (Figure 28).

The channel deposits are finer-grained (silty) and the lower four intervals usually constitute only ten to 20 percent of the bed, while the fine-grained tail (pelitic interval) is very thick. In contrast to studies of lithified units, the pelagic sediment can be easily distinguished from the pelitic interval, or fine-grained tail, by difference in color.

Four structural sequences characterize about 90 percent of the turbidity current deposits examined (Figure 28). Approximately one-half of the sequences consist of a basal laminated interval (d of Bouma, upper interval of parallel lamination) and a thick homogeneous tail,

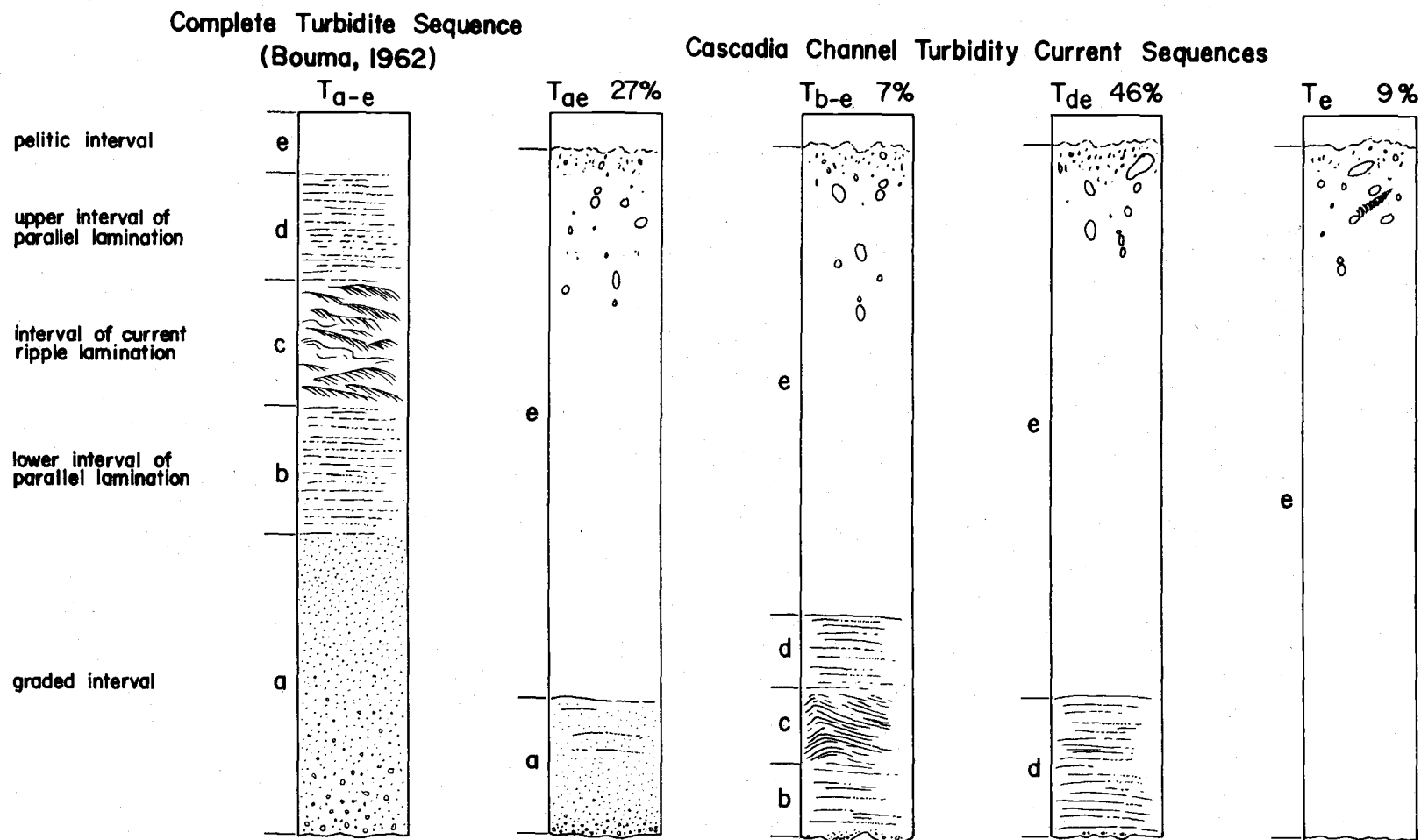


Figure 28. Complete turbidite sequence (Bouma, 1962) and turbidity current sequences from Cascadia Channel. Percentage occurrence of Cascadia Channel sequences are indicated.

or pelitic interval (e). The laminae are 2 to 10 mm thick and grade from silt or very fine sand to clayey silt. The second most common sequence has a thin basal graded interval (a) and a thick pelitic interval (e). A number of layers consist only of the homogeneous pelitic interval ( $T_e$ ), while others contain almost the complete sequence of structures ( $T_{b-e}$ ).

Several cores from the upper and middle channel (6509-10, 6705-6, Figures 18 and 19) display thin olive green clayey layers below the coarser-grained silt sequences. The coarse fraction of these layers is high in mica and plant fibers, in contrast to the greater abundance of detritals in the overlying coarse layer. A similar interval has been found in calcareous turbidites from Germany and was designated a "pre-phase" (Meischner, 1964). In the channel sediments this interval is easily distinguished from the hemipelagic clay by its color. The author believes that it represents deposition from the faster moving body of a turbidity current, which at this point was moving more rapidly than the head with its concentration of coarse material.

Another structure not previously discussed are the clasts of gray clay found within the deposits. These are much more abundant in the Pleistocene sands of the adjoining environments (Vancouver Sea Valley) but do occur in the Holocene sediments of Cascadia Channel. The clasts and the irregular, grooved basal contacts of the graded



beds are the only sedimentological evidence for erosion by the turbidity currents presently active in the channel.

The relationship between the sedimentary structures present in a sequence and the proximity to turbidity current source areas has been studied by Walker (1967). However, all previous work has been done on lithified units in which source areas and dispersal patterns had to be interpreted from sole markings and other criteria. Cascadia Channel offers an excellent location to study the sequence of structures and their development along a known route for turbidity currents in which the transport direction and source area are known. The clear cut relationship between turbidite structures and proximal and distal environments found by Walker is not apparent in this study. One difficulty lies in the designation of intervals, such as those which are both graded and laminated. A complete sequence ( $T_{a-e}$ ) has never been encountered in the channel. The sequence  $T_{a,e}$ , occurs most commonly in the proximal environments (6705-1, 6705-2, 6705-5, 6705-6), but also occurs far from shore (6609-24). The most complete development of structures ( $T_{b-e}$ ) occurs midway along the channel (6509-15A, Figure 28) where more than 50 percent of the cycles in the core contain this sequence. The most commonly occurring sequence ( $T_{d-e}$ ) is found throughout the 650 km of the channel which has been studied.

The finer-grain size and the undeveloped lower intervals (a-d)

in Cascadia Channel sequences, compared to turbidite sequences exposed on land, is probably related to the location of the unconsolidated sediments being studied. They occur in channels from 50 to over 650 km from shore, with gradients of 1:250 to over 1:4000. The great distances from shore and the reduced gradients of the channel environments, contrast to the ancient restricted basins with their steeper gradients, coarser material, and proximity to shorelines (Kuenen, 1964). As a result, lower flow velocities, finer-grained sediment, and a lack of the extensive development of structures of the upper flow regimes (a-d, Walker, 1965) characterize the turbidity currents within Cascadia Channel.

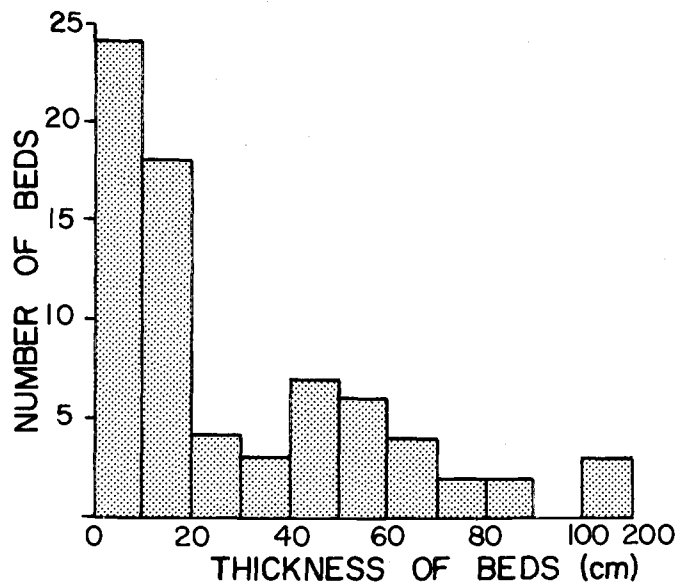
Some hydraulic properties of the turbidity currents can be interpreted from the textural and compositional characteristics of the sedimentary sequences. The differences between the coarse basal zone (a-d) and the fine homogeneous tail (e) of a typical graded unit have been discussed (Figure 12), and a change in the properties of the depositing turbidity current is indicated. The coarser-grained, more positively skewed, basal portion (a-d) of each bed represents deposition from the traction carpet which contains a high concentration of coarse material. The structures present (graded bedding, parallel lamination, convolute lamination) are the result of velocity changes and perhaps some simultaneous current reworking. In contrast, the finer-grained, organic-rich upper portion (e) of each

bed represents deposition from the suspension load or sediment cloud. The gradual, but regular, increase in clay content upward in the tail seems to substantiate the slow settlement of this material from suspension. Both the base and the tail of each graded unit are very poorly sorted as a result of the high clay content throughout (Average: base--15 percent clay, tail--58 percent clay).

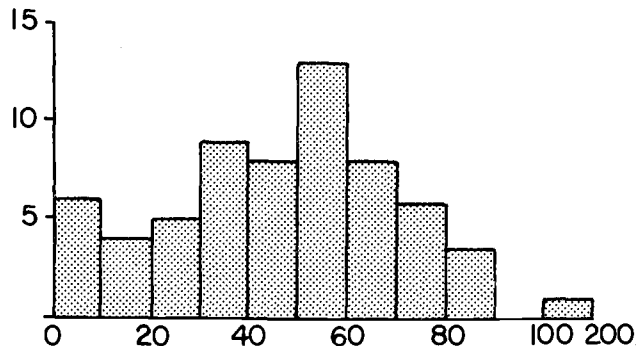
The generalization that turbidites in proximal environments are thick and those in distal environments thin (Walker, 1967), is reversed along the axis of Cascadia Channel (Figures 29 and 30). The thickest sequences have been deposited along the lower portion of the channel, and thinner units closer to shore. On the other hand, the coarse basal layer is thickest close to shore and thinnest farther away (Figure 30). The deposition of most of the coarser material from the traction load probably occurs in the upper channel, resulting in a thicker basal zone. Farther down channel, there is an increased amount of deposition from suspension, resulting in a thicker tail. The maximum grain size present, with few exceptions, in the proximal and distal areas is fine sand. However, the amount of sand in the coarse basal zone (a-d) decreases with distance from shore (Figure 30). The uniformity of flow conditions in the lower channel is illustrated by the consistent variation in the thickness of the layers proceeding from one core to another down the axis (Figure 31). The successive cycles gradually increase in thickness with

# TRIBUTARY CHANNELS

90



## CASCADIA CHANNEL HEAD TO BLANCO FRACTURE ZONE



## CASCADIA CHANNEL BLANCO FRACTURE ZONE TO TUFTS ABYSSAL PLAIN

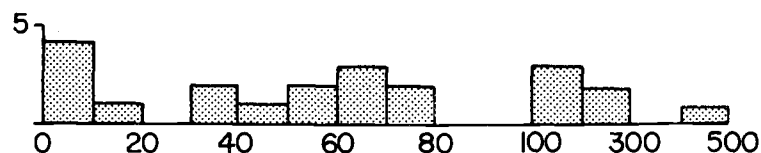


Figure 29. Histograms of thicknesses of individual Holocene turbidity current sequences along Cascadia Channel axis.

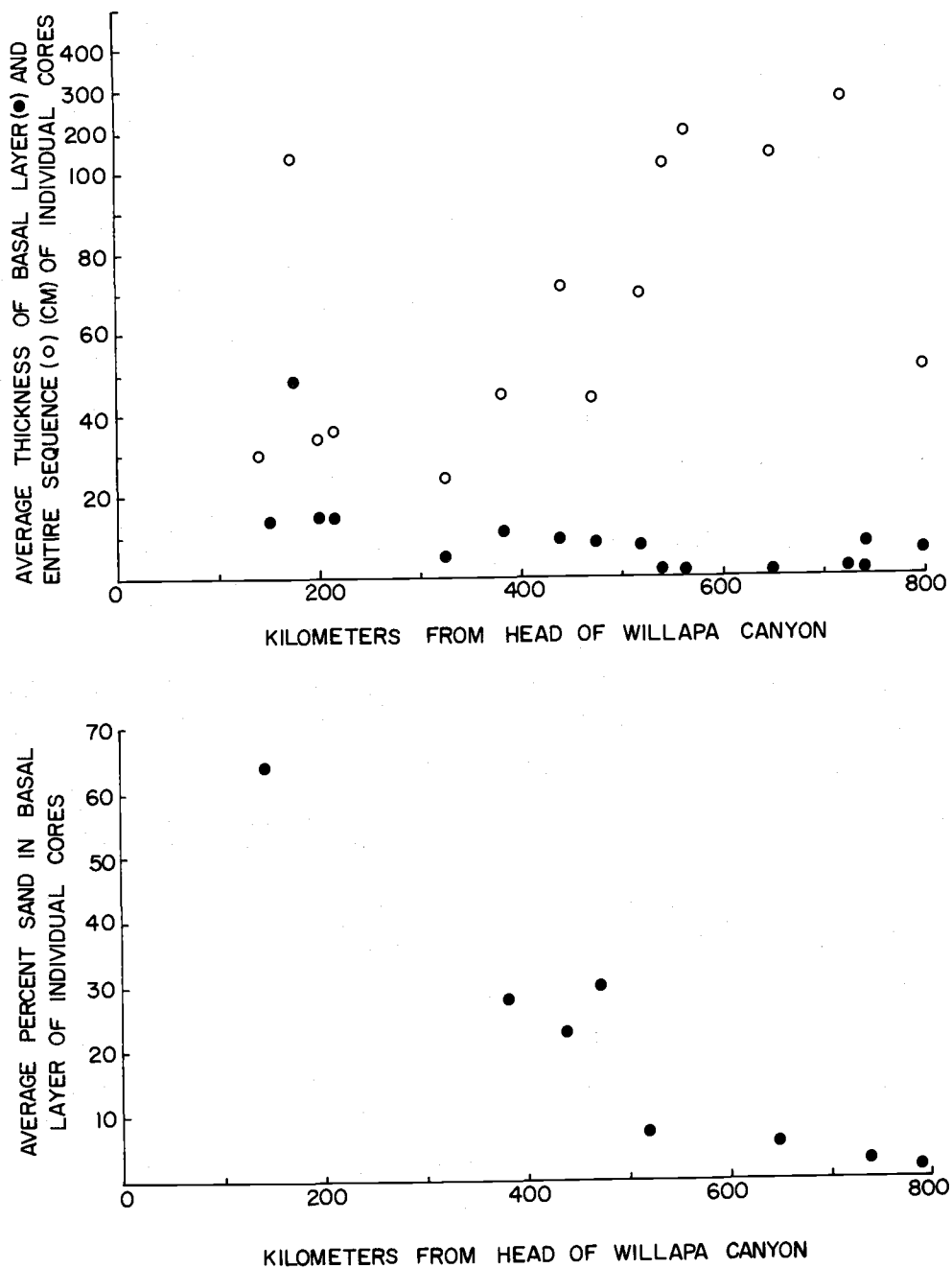


Figure 30. (Top) Average thickness of entire turbidity current sequence and coarse basal zone in individual cores along axis of Cascadia Channel  
(Bottom) Average sand content of coarse basal zone of turbidity current sequence in individual cores along axis of Cascadia Channel

depth as the Pleistocene is approached.

### Correlation of Flows

The confined nature of Cascadia Channel and the uniformity of the deposits over long distances suggests that individual turbidity currents are continuous and that their deposits can be correlated. Four cores along 140 km of the lower channel (6509-15A, 6509-27, 6609-24, and 6509-26, Figure 31) were analyzed for possible correlation of individual cycles. Assuming that the uppermost graded unit in each of the cores represents the same turbidity current and the second unit represents another flow, etc., then the hemipelagic clay layers deposited between flows should show similar characteristics, since they would be synchronous in time. The ratio of Radiolaria to planktonic Foraminifera in the successive pelagic clay layers, used in developing the paleoclimatic curve for this area, correlates closely from core to core. Planktonic Foraminifera show a marked increase in the fourth pelagic clay layer from the surface in the three southern cores, whereas the Foraminifera are almost absent in the remaining layers.

Striking similarities are apparent in the depth of penetration and abundance of burrows within the three lower cores (Figure 32). The second, fifth, and seventh graded layers contain abundant and distinct burrows to depths of 25 cm or greater. In intervening flows

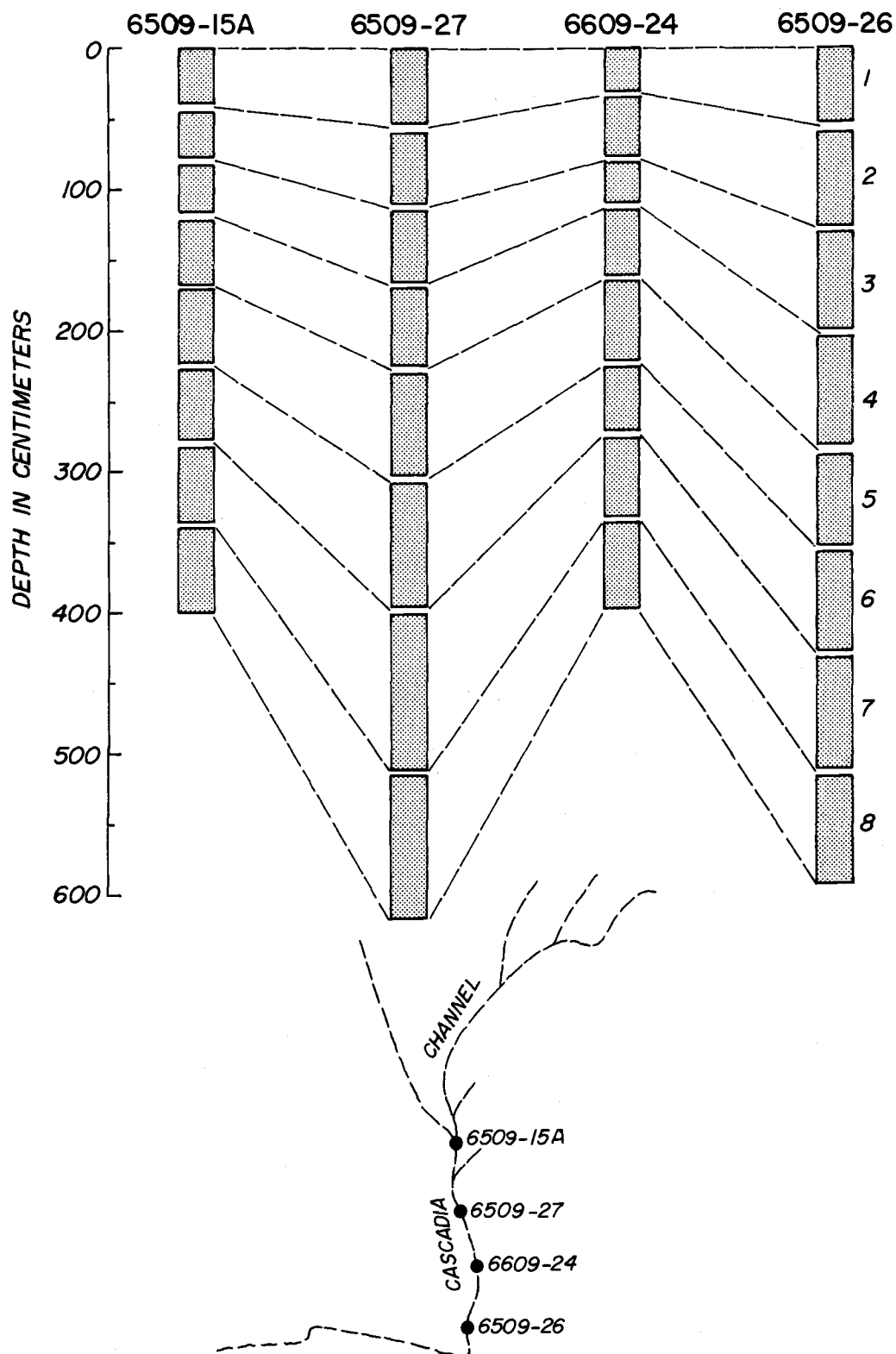


Figure 31. Thickness of successive turbidity current sequences along axis of lower Cascadia Channel

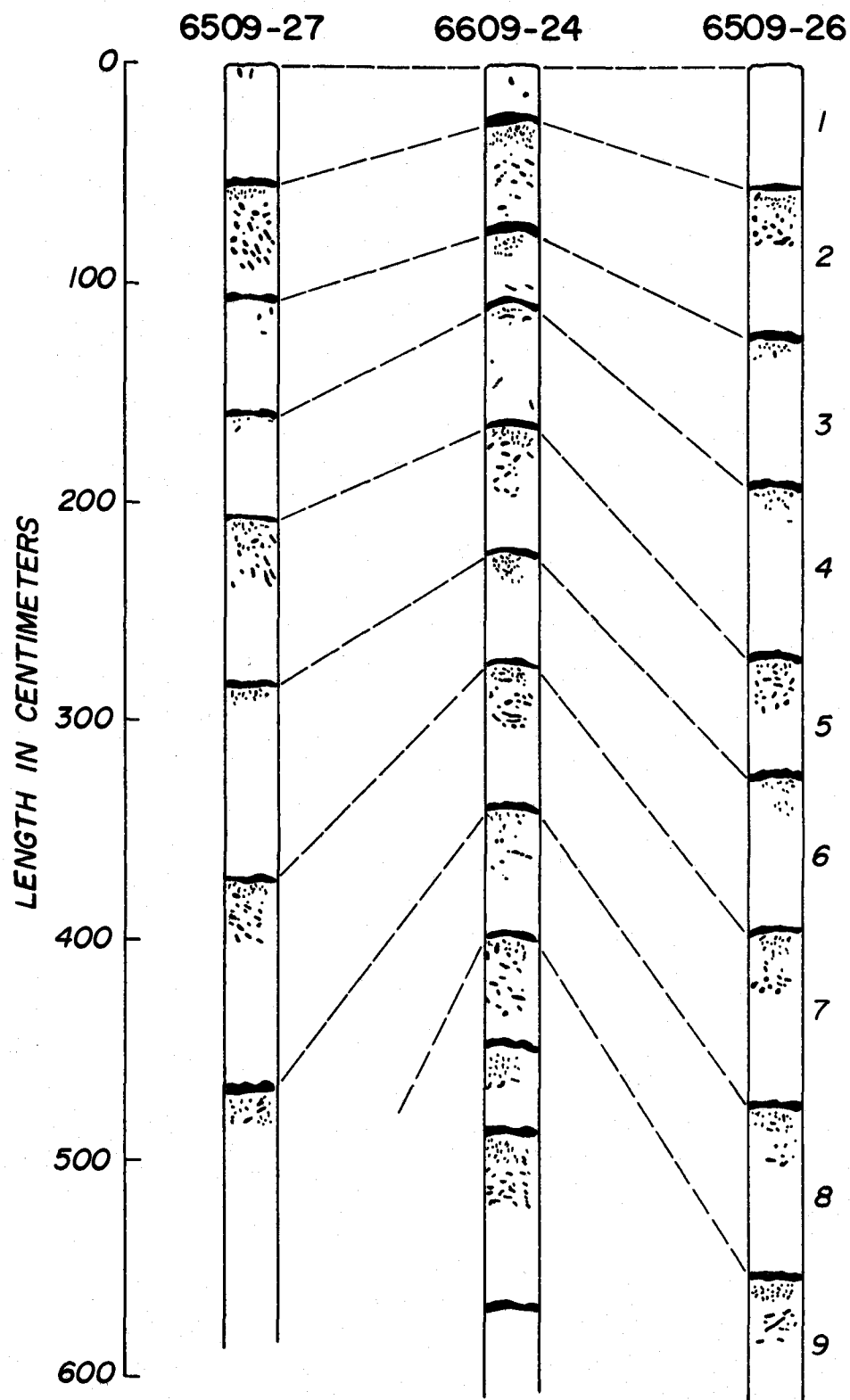


Figure 32. Correlation of burrowing in successive turbidity current sequences in cores from lower Cascadia Channel. Darkened layers are hemipelagic clays.



the burrowing is much less abundant and confined primarily to the upper 5 or 10 cm. Additional cores from the channel axis both north and south show similar patterns. The causes of this variation are unknown at the present time but the correlation is obvious (Griggs, Carey and Kulm, 1968).

The first occurrence of Mazama Ash in the longest channel core (6609-24) is in the 13th layer from the surface. One of the cores from the western wall of the channel (6509-15, about four meters above the floor) contains 21 cycles which include the entire Holocene section. The 13th flow in this core is also the lowest occurrence of Mazama ash. Farther up the channel, where cores showing overflow were taken on the east and west levees (6705-7, 6705-9, Figure 18), fewer flows are present, but the eighth layer from the surface in both cores contains the first occurrence of the ash. All the evidence presented shows that within sections of Cascadia Channel individual turbidity currents leave continuous deposits over an extensive area which can be correlated.

### Flow Periodicity

Average recurrence interval, or time period between turbidity currents, can be calculated if the age of some horizon in the core is known. Published data on flow periodicity is scarce (Table 4) and, with the exception of one estimate (McBride, 1960), only represent

Table 4. Recurrence intervals for Holocene turbidity currents (\* lithified turbidities of Ordovician Age)

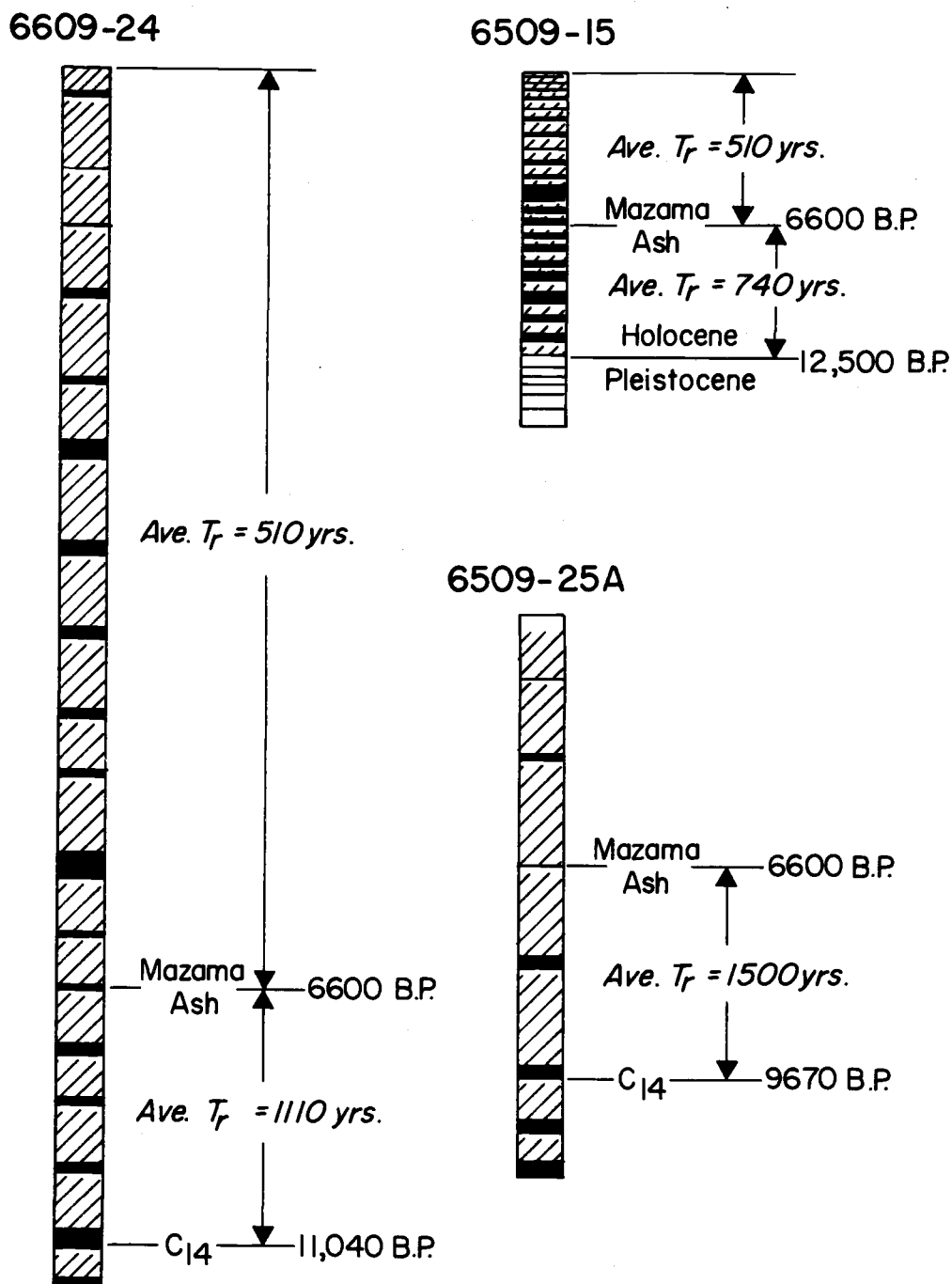
Location	Method or Evidence	Time Period	Reference
Colorado-River-Lake Mead	Visual observation	1 yr	Gould (1951)
Congo Submarine Canyon	Cable breaks	2 yrs	Heezen <i>et al.</i> (1964)
Magdalena River Delta	Cable breaks	2 yrs	Menard (1964)
Continental Borderland Basins			
Feeding Canyons	Estimate	1-10 yrs	Gorsline and Emery (1959)
Center of Basins	Carbon- 14	400 yrs	
Martinsburg Fm (Appalachians-Ordovician) *	Estimate	500 yrs	McBride (1960)
-----			
Cascadia Channel System			
Location	Core	Method or Evidence	Time Period
Tributary channel	6705-2	Mazama ash	410 yrs
Willapa channel	6705-5	Mazama ash	440
Tributary channel	6705-6	Mazama ash	470
Upper channel	6508-K1	Mazama ash	510
Lower channel	6609-24	Mazama ash	510
		Carbon-14	1110
Channel wall	6509-15	Mazama ash	510
		Pleistocene-Holocene boundary	740
Lower channel	6509-27	Carbon-14	580
Channel levee	6705-14	Mazama ash	660
Channel levee	6705-7	Mazama ash	825
Channel levee	6705-9	Mazama ash	825
Tributary channel	6705-10	Pleistocene-Holocene boundary	1040
Lower channel	6509-25A	Carbon-14	1500
		Mazama ash	

Holocene events. Values recorded for turbidity current deposits in near shore submarine canyons are on the order of several years, whereas in deeper basins the time interval between flows seems to be much longer (400 to 500 years). It is apparent that relatively few flows which pass through the submarine canyons have sufficient volume or velocity to reach the more distant basins or abyssal plains.

Stratigraphic markers previously discussed have been used to determine the average Holocene flow periodicity within Cascadia Channel. In the case of Mt. Mazama volcanic ash, it should be mentioned that the introduction of the ash into the marine environment occurred about 6600 years ago or shortly thereafter. Recurrence intervals calculated using this horizon may therefore be slightly high. The uniform thickness of the hemipelagic clay layers between each graded unit implies that time intervals between flows were of a similar duration. In addition, the uniform thickness of the cycles suggests turbidity currents of similar size and material. A certain amount of time would probably be necessary for the deposition of material in the source area of sufficient volume to cause instability resulting in a turbidity current capable of flowing the length of the channel. These factors suggest that the average recurrence interval in this area is probably quite representative.

As in the submarine canyons, the time interval between flows

is also somewhat shorter in the upper channel environments (6705-2, 6705-5, 6705-6, Table 4); all of the turbidity currents which passed through these areas apparently did not reach the middle and lower channel. From the middle channel to Blanco fracture zone the periodicity of the flows in post-Mazama time is very uniform, varying from 500 to 600 years (Table 4). The levees and the portion of the channel on Tufts Abyssal Plain have higher recurrence intervals (825 to 1500 years) as would be expected of environments which were not reached by every flow. Intervals between flows in the tributary channel from Nitinat Fan (6705-10) are about twice as large (1040 years) as those in Cascadia Channel. This may be due to the great distances from the sediment source. From 12,500 to 6600 years ago, turbidity currents were less frequent than in post-Mazama time, at least along the lower channel. Recurrence intervals of 740 to 1500 years are characteristic of this earlier time (Figure 33). One explanation might lie in the closer connection between the Columbia River and Astoria Canyon during late Pleistocene and early Holocene time (Carlson, 1967). Most of the Columbia River sediment load was probably transported through Astoria Canyon at this time. With the Holocene rise in sea level, the marine transport of the Columbia River sediment discharge probably began to approach its present path (Gross and Nelson, 1966; i.e., moving northwest towards the head of Willapa Canyon). More sediment would have



$T_r$  = Turbidity Current Recurrence Interval

Figure 33. Turbidity current recurrence intervals for dated sections of selected channel axis (6609-24 and 6509-25A) and wall (6509-15) cores. Core 6509-25A was taken west of Blanco fracture zone and has been isolated from late Holocene flows.

been supplied to Willapa Canyon, and subsequently, more turbidity currents would have passed through Cascadia Channel.

### Holocene Turbidity Currents -- Flow Reconstruction

#### Flow Dimensions

The physiographic distribution of known turbidity current deposits in Cascadia Channel and the occurrence of submarine levees can be used to determine the lateral, longitudinal, and vertical extent of these flows (Figure 34, Table 5). Bathymetric records of channel crossings taken 10 to 15 km apart combined with piston coring profiles were used in this analysis.

Turbidity currents at least 117 m high have passed through the upper channel in Holocene time (Figure 34, Profile A). Along the middle channel (Profiles B to E) the heights decreased to about 80 m. Levee development, indicating overflow, is characteristic of the upper 200 km of the channel. The width of the levees, which extend to the west and to the east in some cases, and their vertical sequence of Holocene turbidity current deposits demonstrate that individual flows extended laterally up to 13 km from the channel axis with an average width of about 7 km. A single core taken from Vancouver Sea Valley near its juncture with Cascadia Channel contains thin alternating layers of olive green silt and gray clay (6609-27, Figure

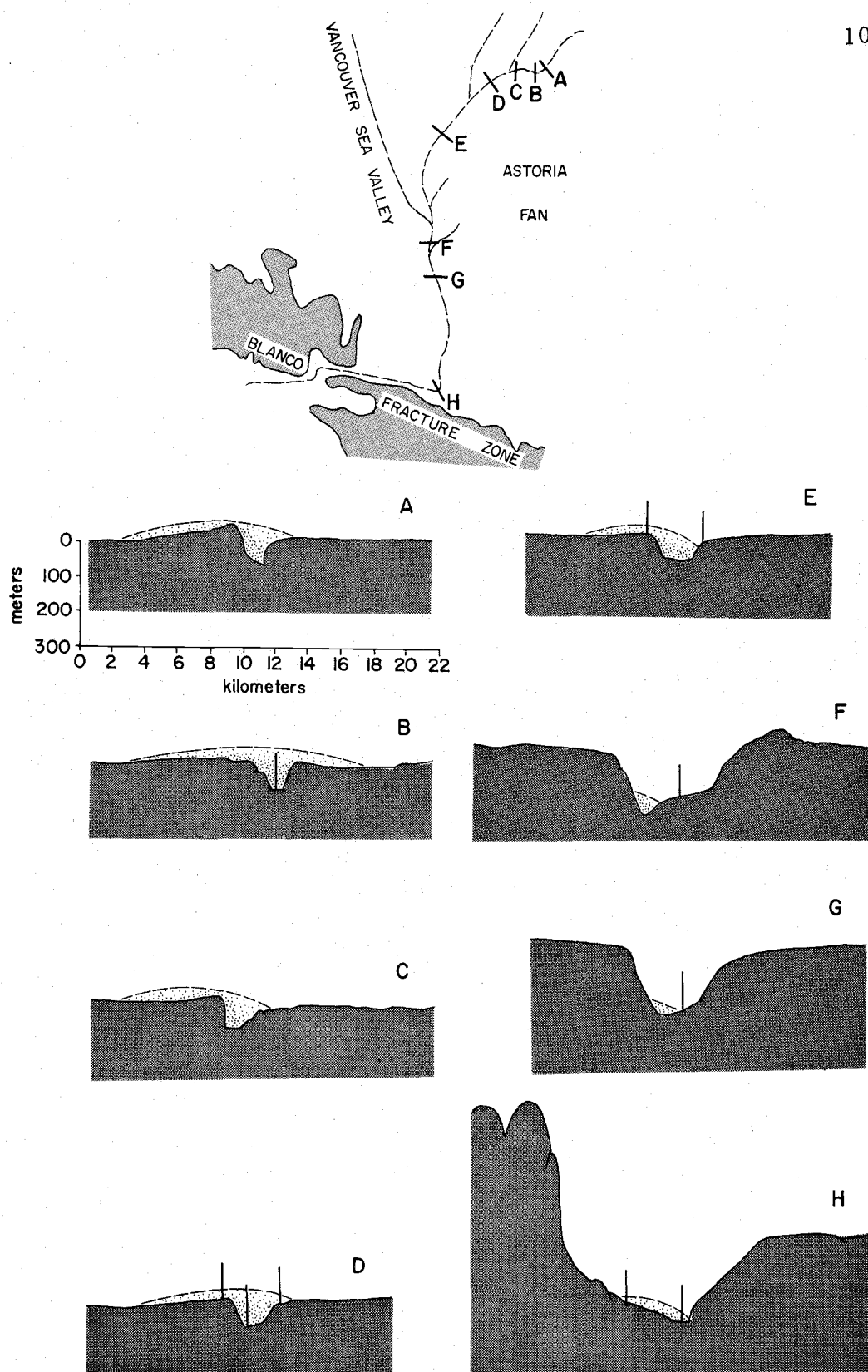


Figure 34. Reconstruction of a typical Holocene turbidity current in Cascadia Channel. Flow dimensions derived from levee and sediment distribution. Vertical lines indicate core locations. Vertical exaggeration of profiles 20X.

Table 5. Dimensions of turbidity currents in Cascadia Channel interpreted from sediment distribution and levee development

Distance from head of Willapa Canyon (km)	Flow height (m)	Lateral ex- tent to west (km)	Width of channel floor (km)	Lateral ex- tent to east (km)	Total width of flow (km)
131	117	6.0	2.0		8.0
138	99	7.5	2.5	3.0	13.0
153	108	3.0	2.5		5.5
185	86	6.5	2.5		9.0
201	82	1.5	2.0		3.5
237	80	4.0	2.0		6.0
248	82	1.5	2.0		3.5
324	80	15.0	2.0		17.0
337	< 37		0.6		0.6
357	> 4		1.5		1.5
367	< 8		2.5		2.5
381			1.0		1.0
415			1.1		1.1
460			1.2		1.2
483	54	5.5	2.5		8.0
735			2.7		2.7



25). The absence of these characteristic Holocene deposits up channel indicates the sediment represents overflow from Cascadia Channel and demonstrates that turbidity currents were at least 80 m high and spread 17 km laterally at this point.

To the south, Cascadia Channel is deeply incised into the abyssal plain; the absence of olive green silts on the channel banks and the lack of levees demonstrate no overflow has occurred (Profiles F-G). Holocene turbidity current deposits on the western wall of the channel show that the flows were at least 4 m high here. Hemipelagic sediments on the eastern wall demonstrate that the flows did not rise more than 8 m above the floor on this side of the channel (Profiles F-G). As the sediments were funneled into Blanco fracture zone, they were deposited as high as 54 m above the channel floor (Profile H). The flows continued through the fracture zone and onto Tufts Plain for an unknown distance. The maximum known dimensions of Holocene turbidity currents in Cascadia Channel are believed to be: length--650 km, width--17 km, height--117 m.

#### Geometry of Deposits

Sediments deposited by Holocene turbidity currents along Cascadia Channel have taken the form of sedimentary wedges. Longitudinally, the deposits become thicker in the lower channel (Figure 26); laterally they thin on the walls and levees. The

approximate volume of sediment in an average flow can be computed by summing the amount of material along the various segments of the channel. Neglecting any sediment on the eastern walls and levees, and beyond the outermost core and assuming uniformity between cores a volume of 525 million cubic meters of material results from an average flow ( $5.25 \times 10^7 \text{ m}^3$ ). A number of world-wide marine slumps, which produced or were capable of producing turbidity currents, had volumes of  $10 \times 10^4$  to  $7 \times 10^{10} \text{ m}^3$  (Menard, 1964).

#### Velocity Determinations

Turbidity current velocities have previously been determined in other areas by actual measurement and by the timing of submarine cable breaks (Gould, 1951; Heezen, 1963; Menard, 1964) (Table 6). Within Cascadia Channel estimates of flow velocities have been made by use of a modified Chezy equation, which yields average velocities of uniform flow. Hurley (1964), using what appear to be reasonable assumptions for the density difference between the flow and sea water and for the channel roughness, arrived at average velocities of 5.2 to 7.8 m/sec for the entire channel. Middleton (1966a, b; 1967), however, after numerous laboratory experiments, states that uniform flow theory (Chezy equation) is not applicable to turbidity currents. Bank overflow (i. e., height of flow) will be determined by the

thickness of the head, not by the thickness of uniform flow. The velocity of a turbidity current head on a slope up to about 1:30 is adequately expressed by Keuligan's (1957, 1958) formula

$$V = 0.75 \sqrt{(\Delta \rho / \rho) g d_2}$$

where  $V$  = velocity of the head,  $\Delta \rho$  is the difference between the density of the current ( $\rho$ ) and that of the overlying water,  $d_2$  is the thickness of the head and  $g$  is the acceleration due to gravity. The density difference measured for Lake Mead turbidity currents (Gould, 1951) and commonly used in flow calculations (Hurley, 1964; Wilde, 1964) is 0.05 gms./cc. The thickness of the head can be determined from the sediment distribution and levee dimensions, which record the height of individual flows. This formula also has the advantage over the modified Chezy equation that fewer assumptions need to be made regarding the resistance coefficients.

Velocities determined from this formula decrease from a high of 5.8 m/sec in the upper channel to a low of 3.3 m/sec along the lower channel (Table 6). These are somewhat lower than those values determined by Hurley (average 5.2 to 7.8 m/sec), but considerably less than the maximum values obtained from cable breaks off the Grand Banks and Orleansville (Menard, 1964; Heezen, 1963). A turbidity current with velocities of 3.3 to 5.8 m/sec would certainly be capable of erosion, but perhaps the fine-grained nature of the

Table 6. Holocene turbidity current velocities

Location	Method	Velocity (m/sec)	Reference
Laboratory flume	Visual measurement	0.20-0.36	Middleton (1966)
Colorado River, Lake Mead	Visual observation	0.25	Gould (1951)
Orleansville, Algeria	Cable breaks	2.6 - 20.6	Heezen (1963)
Grand Banks, Newfoundland	Cable breaks	19.1	Menard (1964)
Monterey Canyon	Chezy formula	1.0 - 8.5	Wilde (1964)
Cascadia Channel	Chezy formula	5.2 - 7.8	Hurley (1964)

Cascadia Channel (using formula from Middleton , 1966)

Distance from head of Willapa Canyon (km)	Maximum height (m)	Velocity (m/sec)
131 Upper channel	117	5.8
153 Middle channel	108	5.7
237 Middle channel	80	4.7
337 Lower channel	37	3.3
483 Lower channel	54	3.8

sediments composing the Holocene flows curtailed any such erosion. A turbidity current with an average velocity of 4 m/sec would take about two days to travel the entire length (735 km) of the surveyed portion of Cascadia Channel.

### Pleistocene Turbidity Currents

The turbidity current deposits of the Pleistocene are distinctly different from those of the Holocene (Table 7). The older sediment is generally coarser and cleaner, but may occur in thicker or thinner beds. The sand varies from fine- to medium-grained, and has a coarse fraction dominated by detrital grains (Figure 15). The gradation in grain size and composition (Figure 14), the displaced Foraminifera and distorted clay clasts, and the sharp, often irregular, basal contacts are all suggestive of turbidity current origin. In contrast to the Holocene sequences, lamination, cross-lamination, and clay clasts are much more abundant in the Pleistocene, while burrowing and the fine-grained "tails" are much less abundant. Plant fragments and the organic carbon content of the Pleistocene coarse layers are very low. These differences indicate Pleistocene turbidity currents had a much greater traction load and contained much less suspended material than the Holocene flows. Consequently, more erosion and a more complete development of sedimentary structures characteristic of the lower flow regime of turbidity currents apparently occurred (Walker, 1965). The Pleistocene

Table 7. Comparison between Pleistocene and Holocene turbidity current deposits in Cascadia Basin

	Pleistocene	Holocene
Maximum thickness of an individual deposit	150 cm	225 cm
Maximum grain size	gravel	fine sand
Average sand-silt-clay content of entire deposit	50%-45%-5%	5%-55%-40%
Sorting	moderate to poor	poor to extremely poor
Composition	detrital grains, mica	detrital grains, mica, plant fibers
Sedimentary structures	irregular basal contacts, parallel and cross lamination, distorted clay clasts, graded bedding	irregular basal contact, graded bedding, parallel and cross lamination, extensive burrowing
Locations	all abyssal plain, fan, canyon and channel environments	Cascadia Channel and northern tributaries, Astoria and Willapa Canyons, upper Astoria Fan

flows were also much more extensive as indicated by their deposits in Vancouver Sea Valley, the channels on outer Astoria Fan, and on the abyssal plain, where only hemipelagic clays have been deposited in Holocene time. Pleistocene overflow along upper and middle Cascadia Channel appears to have been almost entirely responsible for the development of levees in those areas.

Coarse granular material, usually designated gravel or pebbles, has only been found in canyons or channels on the deep sea floor. Gravel was cored in the axis of a channel on Monterey Fan about 300 km from shore (Menard, 1964), and at the mouths of Hueneme, Mugu, Dume, and Redondo submarine canyons (Emery, 1960). In the Atlantic Ocean, cores taken from the bottom of Hudson Canyon in water 3820 m deep and up to 220 km from shore contain gravel (Ericson et al., 1952). Granular material up to 3 cm in diameter has been cored at three locations in Cascadia Channel, from 280 to 680 km from possible sediment sources on the continental margin and in water as deep as 3300 m. Thick angular molluscan fragments and rounded pebbles of diverse lithology suggest that the material originated in shallow water. In addition, the foraminiferal fauna consists of 80 percent displaced forms, 25 percent of which came from the inner shelf. A crude grain size gradation, lumps or clasts of clay, and sharp basal contacts suggest transportation by turbidity currents. The occurrence of these deposits at great distances from

shore within a deep-sea channel lend more support to a deposition by turbidity current than by slumping or sliding. The most puzzling aspect of these gravels is their moderate to poor sorting and low clay contents (1-4 percent). It is difficult to imagine a turbidity current consisting almost entirely of sand and gravel, flowing at least 680 km over slopes as low as 1:2000. Winnowing during or after deposition may have removed much of the clay, although in the case of core 6509-14, it seems unlikely that winnowing could have occurred to a depth of 180 cm below the top of the layer.

#### Ice Rafting

Glacial drift is widespread on the seafloor, probably underlying more than 2,500,000 sq. km. of the Arctic, North Atlantic, and northeast Pacific Oceans (Flint, 1967). The distribution of glacial marine sediments indicates that during the last glaciation, ice shelves and bergs together dropped sediment over the floor of the Gulf of Alaska and the adjacent Pacific from the coast of Washington westward at least as far as the Alaska Peninsula (Flint, 1967). The boundaries of glacial marine sediment in the Gulf of Alaska were delineated by Menard (1953) who believed that most bergs from the ice shelves of the Cordilleran Piedmont Glaciers were carried westward, and only a few floated south. Pebbly clays cored in the floor and wall of Cascadia Channel are believed to represent ice



rafted debris. Many of the larger pebbles appear faceted and some are striated. They commonly are oriented with their long axis vertical or oblique (Figure 16). Zones of high pebble concentration may be interspersed with zones completely devoid of pebbles.

Thin sand or silt interbeds also interrupt the sequence. Planktonic Foraminifera are scarce and the benthic species are predominantly deep water forms. The grit or sand and granule sized material that occurs within the clay is fresh and generally angular to sub-angular.

Many pebbly mudstones have been attributed to viscous submarine mudflows, slumps, and turbidity currents (Crowell, 1957). However, the great distance to a possible source area for the pebbly clays, their occurrence well above the channel bottom, and the interbeds and laminations within the sequence seem to rule out these types of depositional processes. The depression of silt laminae beneath pebbles in the wall and levee of Astoria Channel is also evidence of ice rafting in this area (Nelson, 1968).

The thickness of the deposits (up to 570 cm) and the Carbon-14 date of 37,000 years B.P. beneath the glacial marine sediment in one core (Figure 23) indicate that deposition occurred relatively rapidly. The interbedding of layers with and without coarse debris in the upper part of the section indicates intermittent deposition (Figure 16). The layers with coarse material imply the presence

of ice bergs and, hence, either climatic or surface current fluctuations. The closest source area for floating berg ice appears to be the Puget Lowland, 280 to 440 km to the northeast, where extensive glaciation occurred during the Pleistocene (Flint, 1967). Menard (1964) states "in the Gulf of Alaska, Pleistocene bergs deposited sediment at least as far south as Vancouver Island but probably not much farther, for glacial marine sediments are not found on seamounts farther north". The debris laden berg or shelf ice of the Puget Lowland, which deposited the extensive glaciomarine drift in that area (Easterbrook, 1963), must have moved seaward as the glaciers advanced, melting and leaving trails of drift in their wake. Rapid Holocene sedimentation rates in eastern Cascadia Basin have probably buried most of this material. In areas where erosion has occurred or deposition has been minor, the glacial marine sediments have been found close to the surface. These sediments have been found as far south as  $44^{\circ}10'N$ . latitude, 500 km south of Vancouver Island which was believed to be the southern limit of glacial marine deposits (Menard, 1953, 1964). Pleistocene sediments cored to the south in the basins of the Blanco fracture zone do not contain any rafted material (Duncan, 1968).

### Eolian Transportation

The presence of very thin (1 mm) laminae of very clean quartz silt within an otherwise homogeneous Pleistocene gray clay section (6509-15) is suggestive of eolian transport. This sequence occurs in a stiff clay which appears to constitute the wall of Cascadia Channel, about 260 km from shore. Laminations which occur in other clays are coarser, thicker, not as well sorted, and usually are slightly graded. Rex and Goldberg (1958) found a regional regularity in the quartz distribution of pelagic sediments in the northeast Pacific which they interpreted as fallout of dust from high altitude jet streams. Cascadia Basin falls within their area of highest quartz abundance. The extensive eolian deposits of the southern Oregon coast may have provided a local source for the clean fine-grained quartz silt.

### Slumping and Sliding

Although sediment slumping is often difficult to distinguish from deformation due to the coring operation itself, slumping apparently occurred within a tributary entering Cascadia Channel from Astoria Fan (6609-28). A thick section (75 cm) of distorted layers, lenses, and patches of coarse and fine material occurs between two extensive horizontally bedded sections. The seamount adjacent to this tributary

rises over 550 m above the abyssal plain and is very likely the source of this slumped material.

### Pelagic and Hemipelagic Deposition

Sediments which accumulate from the slow settling of fine terrigenous material and skeletal remains through the water column are known as pelagic sediments. Closer to shore where fine terrigenous silts and clays predominate and sedimentation rates are greater than several cm/1000 years, the deposits are usually designated as hemipelagic. The gray clays of Cascadia Basin with their biogenous coarse fraction and decreasing grain size offshore represent hemipelagic deposits. Sedimentation rates vary from 2 to 14 cm/1000 yrs. Although planktonic constituents dominate the coarse fraction, these clays are composed primarily of terrigenous clay derived from the continent. The large suspended sediment load discharged by the Columbia River is transported seaward and settles slowly over Cascadia Abyssal Plain. The foraminiferal oozes with their abundant Globigerina tests and low sedimentation rates represent pelagic deposits which accumulated during periods of low terrestrial runoff, or in areas where terrestrial material was not deposited.

## MINERALOGY, PETROLOGY AND PROVENANCE OF SEDIMENTS

### Clay Mineralogy

#### Olive Green Silts

The mineralogy of the clay fraction of the olive green silts is remarkably uniform along the entire length of Cascadia Channel from Willapa Canyon to beyond the Blanco fracture zone (Figure 35). Montmorillonite is the most abundant constituent making up 52 percent, on the average, of the clay fraction; chlorite and illite constitute 25 and 23 percent, respectively. These sediments fall directly into Facies I of Duncan (1968), which includes all Holocene material deposited in Astoria and Willapa Canyons, Cascadia Channel, and on upper and middle Astoria Fan. These clays originate in the Columbia River drainage and represent the first of three facies which radiate outward from the river mouth. With increasing distance from the Columbia River, the montmorillonite content of the clays decreases, while chlorite and illite increase in abundance. The high montmorillonite content is believed to be due to weathering of a terrane consisting chiefly of volcanic rocks (Duncan, 1968).

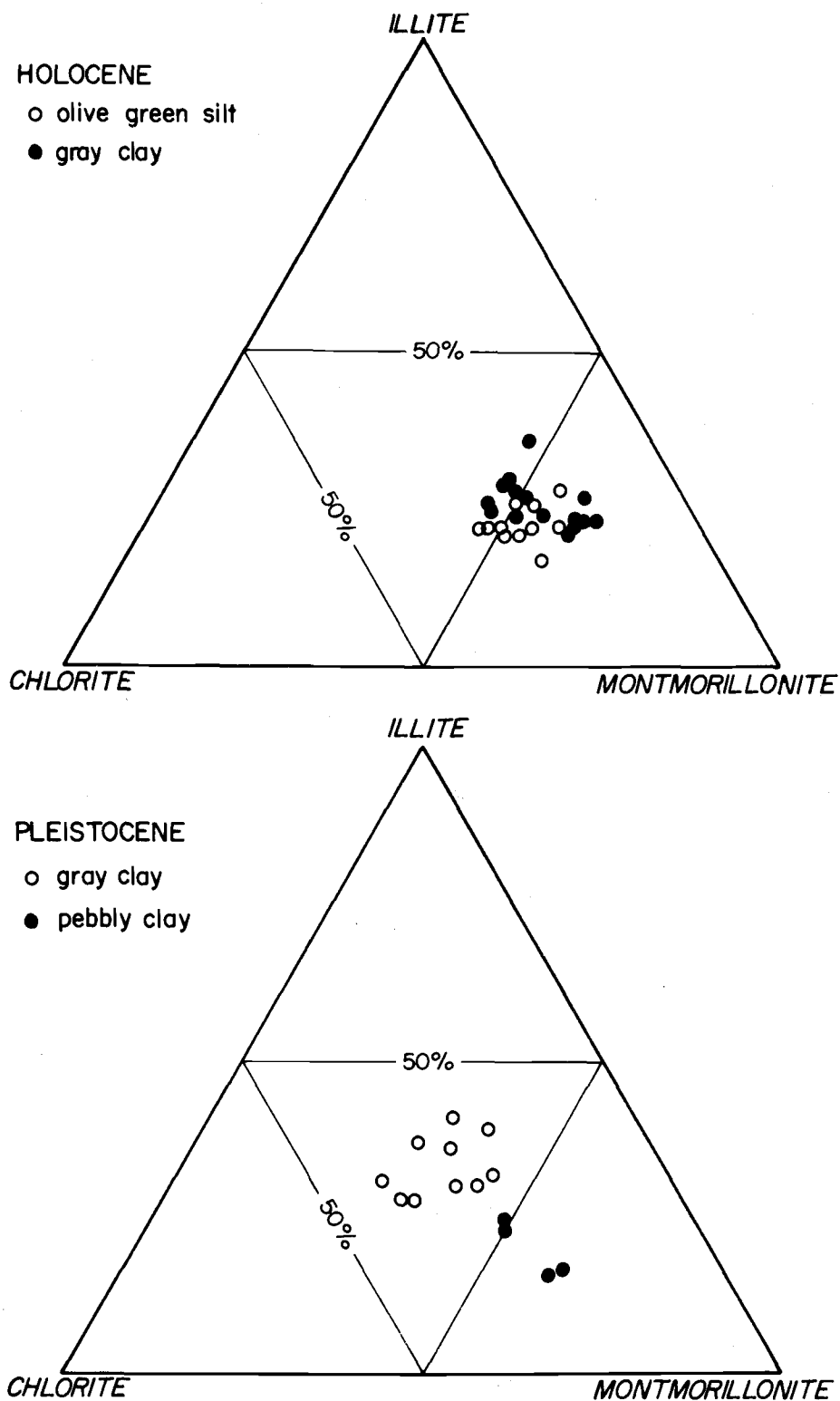


Figure 35. Clay mineral composition of Holocene and Pleistocene sediments

## Gray Clays

The Holocene gray clays are widely distributed and represent pelagic and hemipelagic sedimentation in Cascadia Basin. In the abyssal areas unaffected by turbidity currents since the Pleistocene, such as eastern Cascadia Abyssal Plain and Vancouver Sea Valley, the entire Holocene section consists of gray clay. Cascadia Channel and its active tributaries contain thin gray clay layers interbedded with the olive green silts. The clays vary slightly in composition, probably due more to the inaccuracies of the semiquantitative determination methods, than to areal differences (Figure 35). The clay mineral composition of the gray clays is very close to that of the olive green silts, but, on the average, they have a slightly lower chlorite content. Griffin and Goldberg (1963) found that the chlorite content of clays in the northeastern Pacific Ocean increased towards the coastal areas of Canada, Alaska, and the Aleutian Islands. Duncan (1968) believed that chlorite from these northern source areas and also from the Rogue River to the south might partially account for the relative increase in chlorite and decrease in montmorillonite which he observed with increasing distance from the Columbia River. However, sediment from northern Vancouver Sea Valley (6610-2-1, and 4, Figure 25), 350 km. northwest of the Columbia River mouth, contain only 14 percent chlorite, or the

lowest content of any sediments analyzed.

The Pleistocene gray clays also have a fairly uniform composition (Figure 35). Montmorillonite, on the average, only constitutes 37 percent of the clay fraction while chlorite and illite make up 29 and 34 percent, respectively. These clays are consistent in their composition over a large area which suggests that hemipelagic sediments were uniformly distributed over Cascadia Basin during the Pleistocene, perhaps due to a much larger Columbia River discharge.

Chlorite and illite are more abundant and montmorillonite is less abundant in the Pleistocene gray clays compared to those of the Holocene (Figure 36). This difference in clay mineral composition has been noted by both Russell (1967) and Duncan (1968). The abrupt change in the clay mineral composition at the Pleistocene-Holocene boundary led Russell (1967) to conclude that the difference in clay mineralogy was not due to marine diagenesis. The Columbia River was presumably the source for the Pleistocene as well as the Holocene clay, and changes in weathering processes or relative contributions of different rocks within the Columbia River drainage may have been responsible for the stratigraphic changes in clay mineral composition (Russell, 1967; Duncan, 1968).

Recent investigations of the clay mineralogy of the Columbia River sediments shows significant differences among the various sub-basins (Knebel, Kelley, and Whetten, 1968). The Snake River



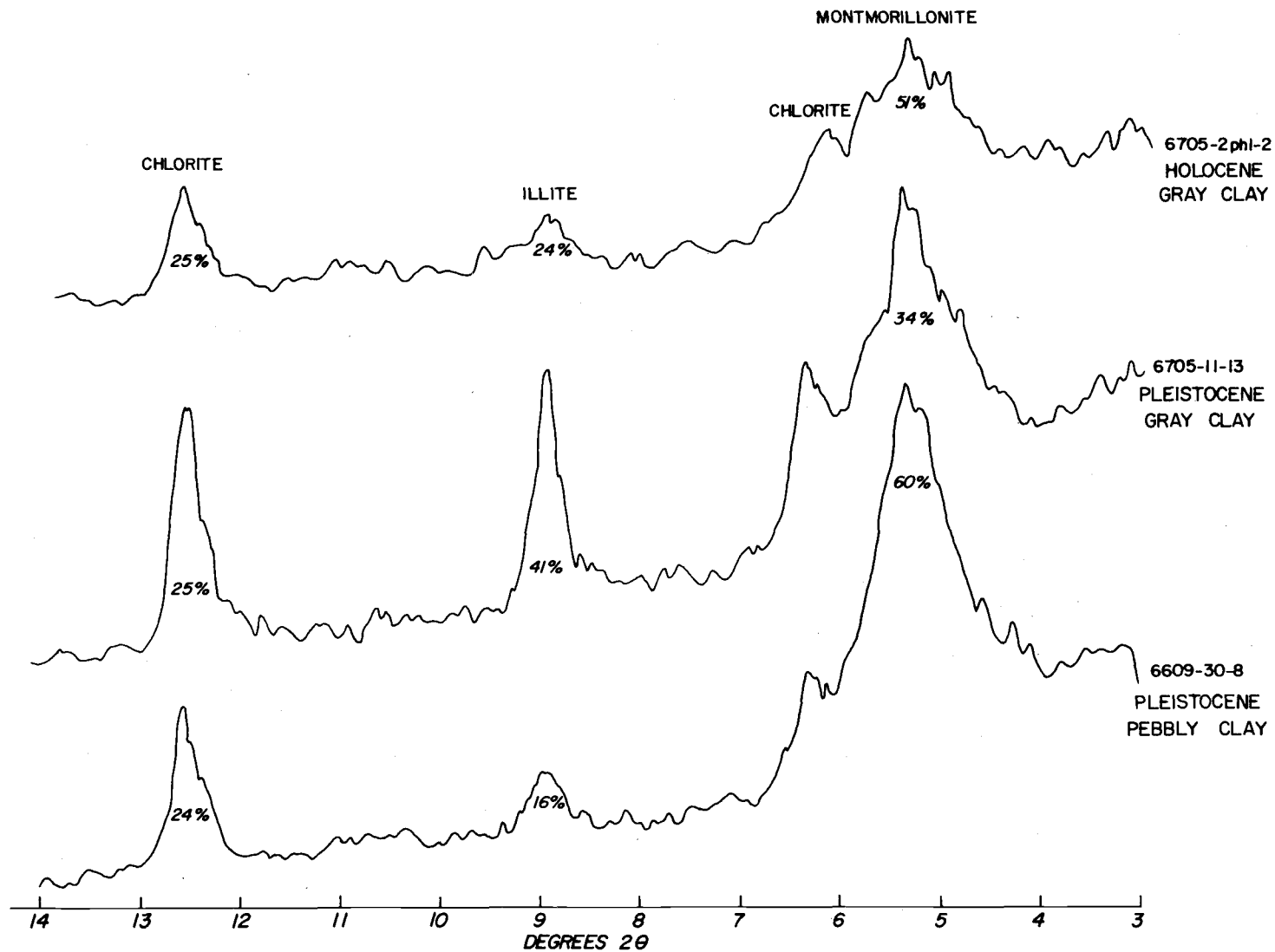


Figure 36. X-Ray diffraction patterns of Holocene and Pleistocene clays showing variation in abundance of chlorite, illite, and montmorillonite

presently carries several times the amount of suspended material as the upper Columbia River (i.e., above the juncture with Snake River) and greatly influences the relative percentages of the clay minerals in sediments of the lower Columbia River (i.e., below the juncture with Snake River). The relative percentages of the clay minerals in the sediments of the lower Columbia Basins, the Snake River, and the Holocene sediments of Cascadia Channel are almost identical (Table 8). The arid to semi-arid climate, plateau or foothill topography, poor water circulation, and meager accumulation of organic matter and acids, in the lower Columbia and Snake River sub-basins give rise to clays high in montmorillonite (Knebel, Kelley and Whetten, 1968). On the other hand, the clays of the upper Columbia sub-basin, are characterized by low montmorillonite and high illite contents, identical to the Pleistocene clays of Cascadia Basin (Table 8). The cool sub-humid to humid climate, bold and rugged topography, active water circulation, and an accumulation of organic litter and acids in this sub-basin have produced a different clay mineral composition (Knebel, Kelley and Whetten, 1968).

These data strongly suggest that the Snake River Basin is presently the major contributor to the suspended load of the Columbia River, whereas during the Pleistocene the upper Columbia River was of major importance. The presence of ice dams and lakes, and the periodic flooding in the channel scabland area of the upper Columbia

Table 8. Comparative clay mineralogy of Cascadia Basin and Columbia River sub-basin sediments.

PHYSIOGRAPHIC ENVIRONMENT	MEAN VALUES		
	% Montmorillonite	% Illite	% Chlorite + Kaolinite
Cascadia Channel (Holocene clays)	52	23	25 (no kaolinite)
Lower Columbia River Bonneville Dam*	55	24	21
The Dalles Dam*	57	27	16
Snake River*	55	28	17
Cascadia Basin (Pleistocene gray clays)	37	34	29 (no kaolinite)
Upper Columbia River Basin*	35	33	32

\*Data from Knebel, Kelley and Whetten (1968)

River during the Pleistocene (Bretz, Smith and Neff, 1956) would have produced a greater Pleistocene contribution from this area.

### Pebbly Clays

The pebbly clays and associated laminated clays are distinctly different from the other Pleistocene clays of Cascadia Basin and are closer in composition to the Holocene sediments (Figures 35 and 36). Montmorillonite constitutes 55 percent of the clay fraction, on the average, and chlorite and illite make up 25 to 20 percent, respectively. The difference in clay mineral composition implies a different source area. If the clays have been ice rafted as other data indicate, the most probable source area is the Puget Lowland and the adjacent mountains of Washington and British Columbia. Much of the terrane scoured by the Pleistocene glaciers (i. e., the Cascades of Washington and British Columbia) consist of volcanic rocks (Easterbrook, 1963). This type of terrane characteristically produces clays high in montmorillonite (Biscaye, 1965; Duncan, 1968).

### Sand Mineralogy

The heavy minerals in a sand are usually characteristic of certain source rock lithologies, and can be used in the determination of the provenance and dispersal patterns of the sediments. In order to study these patterns and their areal and temporal variations,

Holocene and Pleistocene sand from the different depositional environments was examined. Heavy mineral assemblages from these environments and the different sediment units can be divided into three suites (Table 9). Suite I contains only the Pleistocene pebbly clays from Cascadia Channel. The second suite includes all of the remaining Pleistocene and Holocene sediments from Cascadia Channel and the Pleistocene sands of Nitinat Fan and lower Vancouver Sea Valley. Suite III is made up of Pleistocene sand from upper Vancouver Sea Valley and western Cascadia Abyssal Plain.

#### Suite I

The sand fraction of the pebbly clays is characterized by a high hornblende and low clinopyroxene content. The blue-green hornblende and the epidote group are major constituents, resulting in the highest metamorphic mineral content (includes actinolite-tremolite, blue-green hornblende, epidote group, garnet, kyanite, andalusite, staurolite, wollastonite, and sillimanite) of any of the suites (19 to 24 percent). The distinctive clay mineral composition of these sediments, in addition to their sand mineralogy, indicate a source area other than the Columbia River. The Coast mountains of British Columbia, north of the Puget Lowland, consist largely of granitic plutonic rocks with associated schist and gneiss. The ice moved across these mountains during the Pleistocene and

Table 9. Average percentage composition of heavy mineral suites.

	Suite I	Suite II	Suite III
Amphibole Group			
Actinolite-Tremolite	5	3	2
Blue-Green	15	4	4
Common	26	24	20
Pyroxene Group			
Orthopyroxene	10	14	11
Clinopyroxene	15	26	25
Epidote Group	13	6	6
Garnet Group	1	2	-
Olivine Group	1	1	1
Other Minerals	14	20	31

accumulated detrital material from this terrane, and the schist and gneiss are probably the source rocks for the metamorphic minerals. A high hornblende content is characteristic of detrital material derived from the British Columbia-Puget Lowland area (Easterbrook, 1963).

### Suite II

The Holocene and Pleistocene sands and gravels of Cascadia Channel, Nitinat Fan and lower Vancouver Sea Valley are characterized by a Columbia River heavy mineral assemblage (Duncan, 1968). The dominance of clinopyroxene over hornblende is characteristic of these sands. They also contain nine to 20 percent metamorphic minerals. Most of the Tertiary andesites and Pliocene to Recent basalts of the Cascades and the vast Miocene tholeiitic basalts of the Columbia Plateau region are included in the drainage system of the Columbia River (Waters, 1955). In Washington, Columbia River tributaries drain the metamorphosed sedimentary rocks and granitic batholiths of the northern Cascades.

### Suite III

The third heavy mineral suite occurs in upper Vancouver Sea Valley and on western Cascadia Abyssal Plain. This area was also found to be a distinct province by Duncan (1968) from its relatively

high clinopyroxene/hornblende ratio, and by the occasional presence of glaucophane. A low concentration of metamorphic minerals (six to ten percent) is characteristic of all sands from this area. Vancouver Sea Valley, which heads at the base of the continental slope off Vancouver Island, is the most likely route for sediment moving to the western plain. The detrital material may have come from Vancouver Island during the Pleistocene, or may have moved out through the Straits of Juan de Fuca and down Nittinat Fan. Glaucophane, although only present in trace amounts, is indicative of metamorphic rocks, specifically glaucophane schists (Williams, Turner, and Gilbert, 1954). The Sauk River area of the northern Washington Cascades, which drains into Puget Sound, contains glaucophane and green schist (Vance, 1954). The granite-injected (Cretaceous) metamorphic rocks that crop out on southern Vancouver Island (Goddard et al., 1965) are suggested as a possible source for the glaucophane by Duncan (1968). The low metamorphic mineral content in the sands of western Cascadia Abyssal Plain and northern Vancouver Sea Valley may be due to the limited occurrence of metamorphic rocks on Vancouver Island.

### Pebble Petrology

#### Gravels

The Pleistocene gravels of Cascadia Channel exhibit a variety



of lithologies such as chert, volcanic breccia, quartz monzonite, granophyre, and amphibolite, but basalt is the most common. The granophyre consists of micrographic intergrowths of quartz and altered orthoclase. The intergrowths are linear as well as spherulitic or radial in their orientation. Spherulitic granophyre dikes crop out along the upper Columbia River near the Chelan batholith (Waters, 1927). The granophyres with their intergrowth of quartz and feldspar form resistant pebbles which occur in conglomeratic beds in the Swank Formation along the Columbia River (Waters, 1938). The pebbles commonly occur in the river bed many miles downstream (Waters, 1968, personal communication). Amphibolites have been intruded by the Chelan batholith which consists predominantly of granodiorite and quartz monzonite. The Chelan area of eastern Washington is drained by the Columbia River and may be the original source of the Pleistocene gravels of Cascadia Channel.

#### Pebbly Clays

A complete range of lithologies occurs in the pebbles from the pebbly clays of Cascadia Channel (Table 10). Sedimentary rocks present include mudstone, siltstone, graywacke, limestone, and chert. Quartz-mica schist and quartzite represent the metamorphic rocks. Plutonic and volcanic rocks include quartz diorite, granodiorite, quartz monzonite, andesite, basalt, and volcanic breccia.

Table 10. Comparative lithologies of bedrock in areas scoured by glaciers, and erratics contained in glacial deposits (\* from Easterbrook, 1963)

CASCADIA CHANNEL	PUGET LOWLAND*		WASHINGTON*	BRITISH COLUMBIA*	
PEBBLY CLAY	BELLINGHAM DRIFT	VASHON TILL	CASCADES	CASCADES	COAST RANGE
PLUTONIC					
quartz diorite	quartz diorite	granitic rocks	quartz diorite	granitic rocks	quartz diorite
granodiorite	granodiorite	diorite	granodiorite		granodiorite
meta-gabbro			dunite		diorite
quartz monzonite		pink granite			
porphyry					
VOCANIC					
basalt	basalt	basalt	volcanic rocks	basalt	
andesite	andesite	andesite	andesite	andesite	
volcanic breccia					
METAMORPHIC					
quartz-mica schist		schist			schist
quartzite	quartzite	quartzite		quartzite	gneiss
SEDIMENTARY					
chert		chert	chert	chert	
graywacke	graywacke		graywacke	graywacke	
limestone			limestone		
siltstone			argillite		
mudstone					
	arkose	sandstone	arkose		

The northern Washington Cascades contain argillite, graywacke, chert, limestone, and volcanics (Easterbrook, 1963). In British Columbia the Cascades consist of granitic rocks in addition to andesite, basalt, quartzite, chert, and graywacke. North of the Puget Lowland the Coast Range consists largely of granitic plutonic rocks (granodiorite, quartz diorite, and diorite) with associated gneiss and schist (Easterbrook, 1963). Pleistocene continental ice moving south from these two mountain ranges would have accumulated detrital material from this terrane. The glacial and ice deposited material in the Puget Lowland contains pebbles and cobbles of diverse lithologies (Table 10). The lithologic similarities between the pebbly clays of Cascadia Channel, the bedrock of the Coast and Cascade Ranges, and the clasts contained in the tills and drifts of the Puget Lowland strongly suggest this northern area was the source for the pebbly clays in Cascadia Basin.

## SEDIMENT DISPERSAL

### Pleistocene

Climatic conditions during the Pleistocene created a set of geological conditions on the continent different than those which have been operative in Holocene time. Glaciation in the upper reaches of the Columbia River, periodic flooding from the breakage of ice dams, and the lower sea level stand which resulted in the deposition of large volumes of material on the outer shelf, produced a distinct pattern of sediment dispersal in the deep sea. Large volumes of coarse detrital material were transported to the marine environment by the Columbia River. Sediments transported by turbidity currents passed through Astoria and Willapa Canyons to the deep-sea floor. Pleistocene sediment from the Columbia River moved south along Astoria Channel to Blanco Valley (Duncan, 1968) and along Cascadia Channel, through Blanco fracture zone, onto Tufts Abyssal Plain. Large volumes of coarse material were also deposited on Astoria Fan, both in channel and interchannel areas (Nelson, 1968). The massive floods produced by the breaking of glacial ice dams of Lake Missoula (Bretz, Smith and Neff, 1956) are probably responsible for the transportation of the gravel, derived at least in part from the Chelan area of Washington, down the Columbia River to the marine environment

(Figure 37). The poorly sorted late Pleistocene gravels along the lower Columbia River, which are torrentially bedded and which contain glacial erratics, are evidence of this flooding (Lowry and Baldwin, 1952). Similar deposits occur in the scabland gravels and Touchet deposits along the Columbia River near Pasco and Walla Walla in eastern Washington (Lowry and Baldwin, 1952). The shallow water benthic foraminifera and thick walled molluscan debris found in the gravels suggest that the material remained for some time in a shallow marine environment before being transported to the deep-sea. On the other hand, the massive floods laden with sand and gravel may have accumulated faunal debris as they passed through shallow water environments on their way to Cascadia Channel and the abyssal environment. Turbidity currents, perhaps much larger and denser than those of the Holocene, were active in Cascadia Basin during this time. The coarser material deposited during the Pleistocene and the greater percentage of sand and silt in the sections is evidence of this activity (i.e., outside of Cascadia Channel, the Pleistocene sections consist of 56 percent coarse material, whereas the Holocene sections average only seven percent. See Appendix 8). Duncan (1968), who sampled more of the abyssal environments, arrived at similar conclusions as to turbidity current activity (Pleistocene sections contain 32 percent coarse material; Holocene sections nine percent).

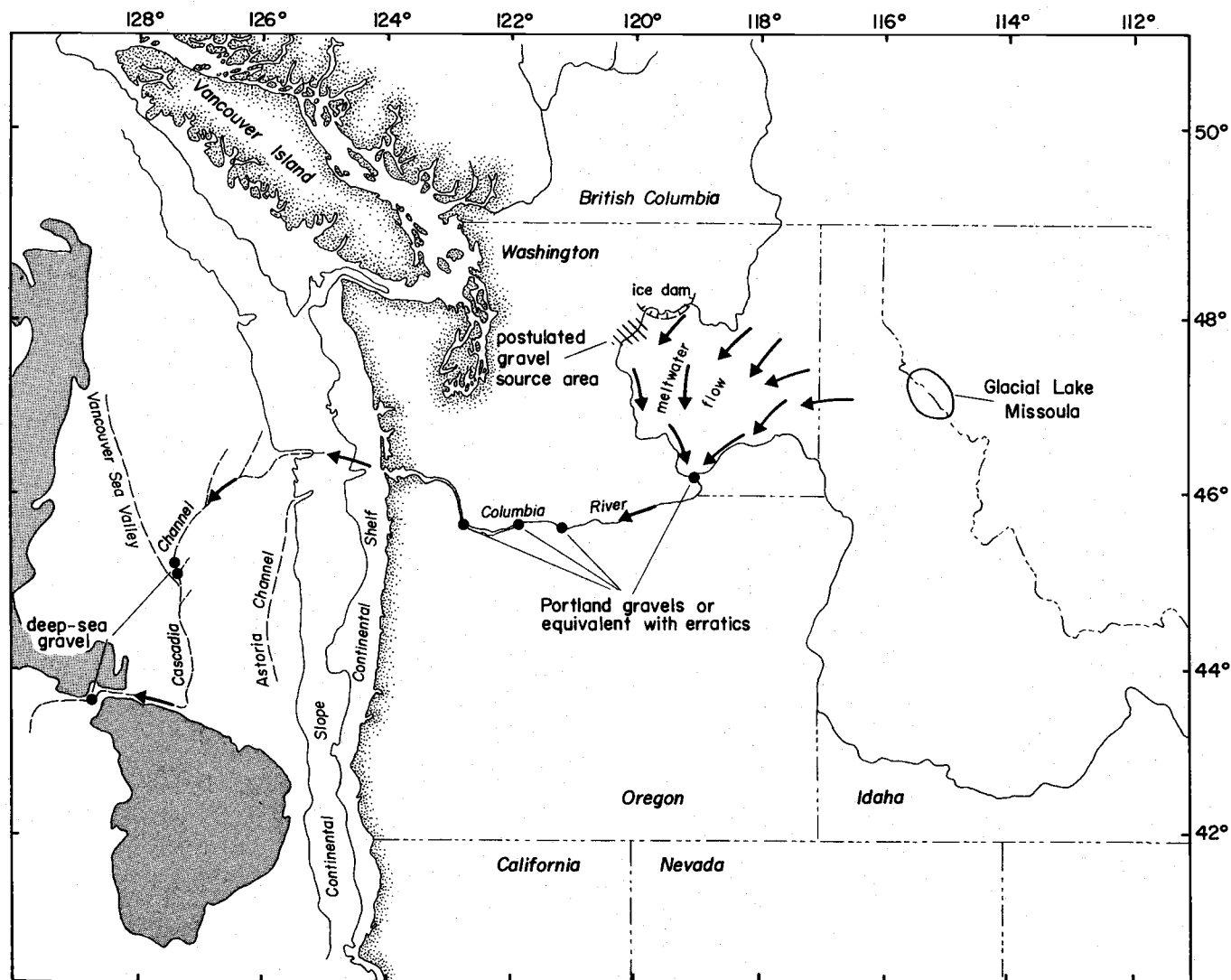


Figure 37. Source, dispersal pattern, and depositional sites for Pleistocene gravels

The Cordilleran Glacier complex, which existed during the last glacial maximum, was a continuous and interconnecting mass of valley glaciers, piedmont glaciers, and an ice sheet. It was centered in British Columbia and stretched northwest to the Aleutian Islands and south to Mt. Adams near the Columbia River (Flint, 1967) (Figure 38). During the maximum advance of the last glaciation, Vashon ice approximately 5000 feet thick flowed south from the Cascades and Coast ranges of British Columbia into the Puget Lowland (Easterbrook, 1963). As the main ice sheet receded, the bergs formed by calving of the nearby ice front melted and dropped their debris, forming a fossiliferous glaciomarine drift. The maximum thickness of the floating ice has been calculated at 220 feet (Easterbrook, 1963). The pebbly clays of Cascadia Channel with their relatively uniform distribution of coarse granular material in a clay-silt matrix suggest a continuous "rain" of unsorted material took place as the sediment accumulated. The only agent capable of depositing this type of material continuously in a marine environment, far from shore, is berg ice. The lithologic similarities between the pebbles and cobbles from Cascadia Channel, the Puget Lowland tills and drifts, and the bedrock of the Coast ranges and Cascades of British Columbia and Washington (Table 10), indicate that the berg ice originated in this area. In order to create the thick uniform sequences of pebbly clay, calving, transportation, and

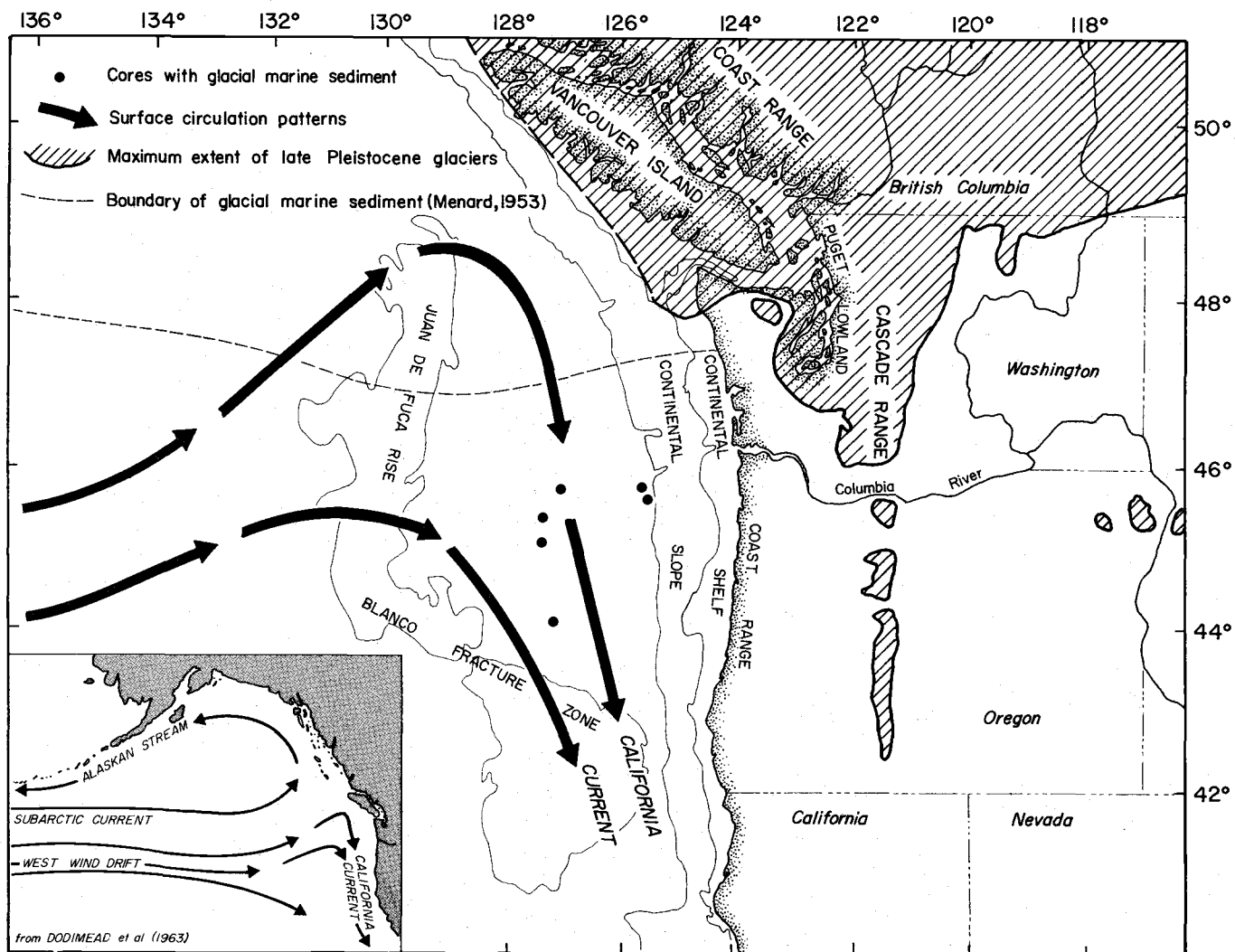


Figure 38. Source areas and depositional sites for glacial marine sediments. Continental areas glaciated in late Pleistocene time and present surface circulation in the vicinity of Cascadia Basin are indicated. Inset illustrates surface circulation of entire northeast Pacific Ocean.



melting of the bergs must have gone on continuously for some time. Stratification with normal marine sediments in the upper part of the sequence (cores 6609-30, 6705-13; Figure 20) infer an intermittent supply of coarse material at the close of the Vashon glaciation.

The areal distribution of the glacial marine deposits can be explained by the present day surface circulation of the northeast Pacific (Dodimead, Favorite and Hirano, 1963). The West Wind Drift (Figure 38) moves eastward across the North Pacific to a point about 500 km off the Oregon-Washington coasts at  $45^{\circ}$  north latitude. Here the water mass divides; part of it turns southward to form the California current; a small part intrudes into the area off the coast of Vancouver Island and then moves southward along the coast; and the remainder flows northward into the Gulf of Alaska (Dodimead, Favorite and Hirano, 1963). The distribution of glacial marine sediments in Cascadia Basin, at least 440 km south of Puget Sound and 175 km from the paleo-shoreline, indicates that the portion of the West Wind Drift which approaches Vancouver Island and then turns southward carried many of the larger bergs to the south during the Pleistocene. Apparently the late Pleistocene surface circulation in this area was similar to the present pattern. The northeast Pacific Gyral may have been farther north during the Pleistocene, but it is very unlikely that it was south of its present position.

Vancouver Sea Valley, which heads near the base of the

continental slope off Vancouver Island, is the most likely route for the bottom transport of the Pleistocene sediments on the western plain. Vancouver Island was also covered by the Cordilleran Glacier complex (Flint, 1967, p. 309) of the late Pleistocene, and the moraines and outwash from these glaciers, or those from the Puget Lowland, probably provided the coarse-grained sediment found in the above mentioned abyssal areas. In addition to Vancouver Sea Valley, some material moved out through canyons and down the flank of Nitinat Fan.

#### Holocene

In response to the world wide melting of glaciers at the end of the Pleistocene epoch, numerous changes occurred which greatly affected sediment dispersal and depositional processes. The rising sea covered the continental shelf, drowned river mouths, and decreased stream gradients. Due to these factors, far less material is presently transported to the abyssal environment. The lower supply of terrestrially derived material to the continental shelf has restricted the generation of turbidity currents which are capable of transporting coarse-grained sediment to the deep-sea. This decrease in terrigenous sand-silt deposition has occurred in Astoria Canyon and on upper Astoria Fan since the Pleistocene (Carlson, 1967; Nelson, 1968). The channels which cross the lower fan and join

Cascadia Channel in the vicinity of Vancouver Sea Valley have received only hemipelagic sediments since the Pleistocene. Prior to this time, large volumes of sand passed through and were deposited in them.

The distribution of Mt. Mazama Ash and Carbon-14 dating demonstrate Cascadia Channel and its northern tributaries have been active during Holocene time (Figure 39). An important factor here is the direction of sediment movement from the Columbia River mouth. A net north and westward transport across the shelf (Figure 39) is indicated by textural studies of northern Oregon and Washington continental shelf sediments (Gross, McManus and Ling, 1967) and by investigations of the radionuclides associated with sediments from the Columbia River (Gross, 1966; Gross and Nelson, 1966).

Much of the material appears to come to rest at the head of Willapa Canyon. The continuity in physiography, gradient, and sedimentation between Cascadia Channel and the Willapa Canyon-Channel system indicate that the Holocene olive green silts originated in Willapa Canyon. The present day Columbia River sediment discharge is 12.2 million  $m^3$ /yr. The bottom load is 1.4 million  $m^3$ , and the suspended load amounts to 10.8 million  $m^3$  (Lockett, 1965; U. S. Army Engineers, 1962). Carlson (1967) computed a littoral current contribution of about 2.4 million  $m^3$ /yr. Most of the suspended material (silt and clay) probably moves offshore with the

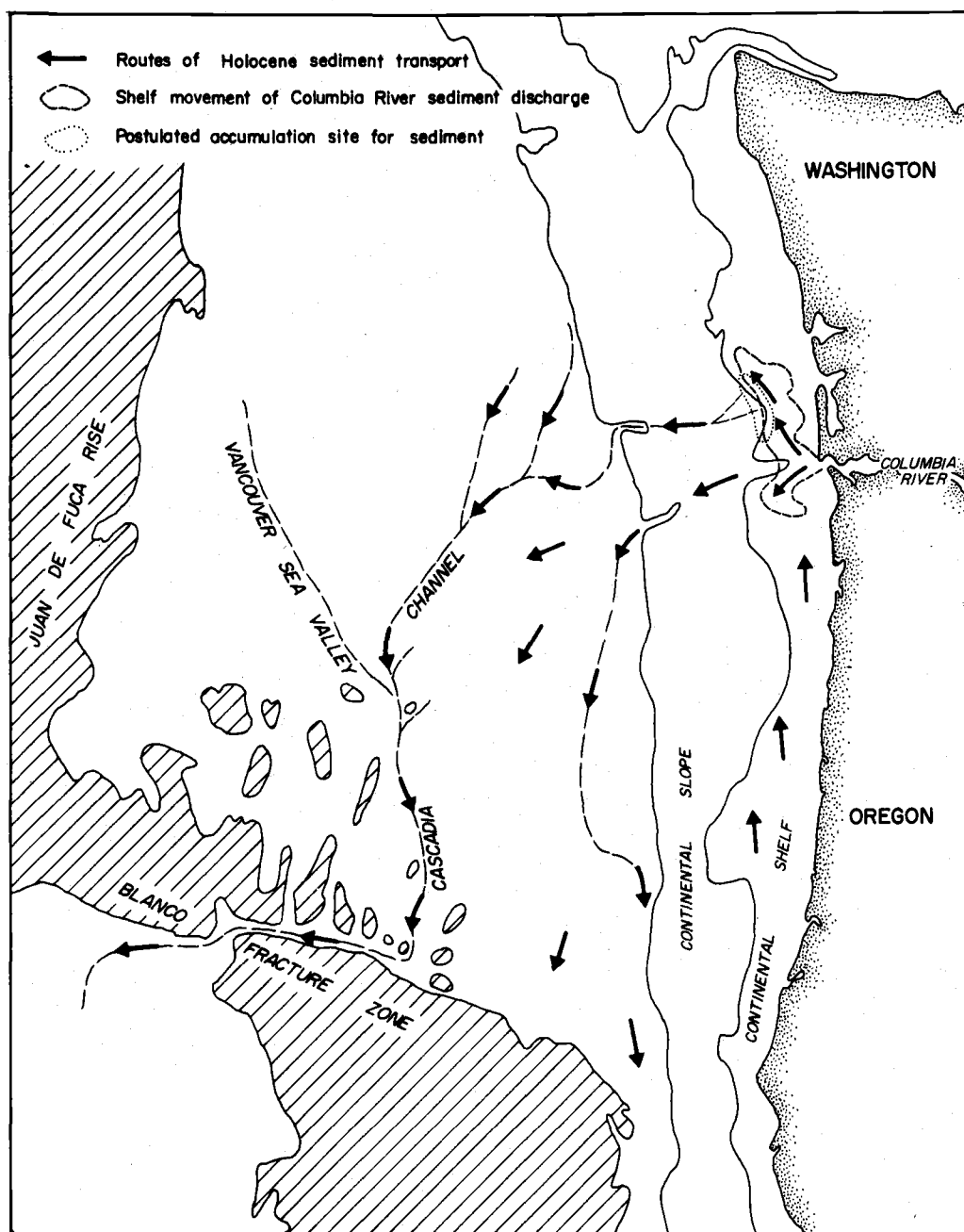


Figure 39. Holocene dispersal pattern and postulated accumulation site for Columbia River sediment discharge (supplemented by data from Duncan, 1968, and Gross and Nelson, 1966)

plume of the river which extends to the southwest during peak discharge (late spring and early summer) and to the north and west for the remainder of the year (Osterberg et al., 1965). The sand, which constitutes much of the bottom load, is presently trapped in the estuary (Carlson, 1967). If only 25 percent of the combined bottom load and littoral drift, or ten percent of the suspended load (one million  $\text{m}^3/\text{yr.}$ ), or some combination totaling this volume, eventually comes to rest in the vicinity of Willapa Canyon, 550 million  $\text{m}^3$  of sediment would accumulate in the recurrence interval (550 years) between turbidity current in Cascadia Channel. This volume is almost identical to that calculated for an average flow (524 million  $\text{m}^3$ ) in Cascadia Channel. There appears to be sufficient silt and clay available from the Columbia River discharge to supply the postulated turbidity currents with sediment. The high seismicity of this area (Berg and Baker, 1963) and the atmospheric conditions of the northeast Pacific provide periodic earthquakes or severe storms capable of generating turbidity currents from this sediment mass. Holocene turbidity currents have also been active in the two tributaries which cross Nitinat Fan, as indicated by the identical sediment sequence found in Cascadia Channel. These sediments must have passed through submarine canyons farther north along the Washington continental slope.

The Holocene sediment sequence in Vancouver Sea Valley and on western Cascadia Abyssal Plain consists only of pelagic and

hemipelagic clays. Turbidity currents have been inactive in this area since the late Pleistocene and all of the sediments have settled through the water column from suspension. Gross, McManus and Ling (1967) have observed that no major local sources are presently contributing sediment to the Vancouver Island shelf. The rivers on the island discharge into long, narrow, glacially scoured inlets which generally have sills at their entrances. The inlets act as settling basins and prevent both suspended and bottom transported sediments from moving seaward. Most of the discharge from the rivers emptying into Puget Sound and the Strait of Georgia would enter the north Pacific Ocean through the Straits of Juan de Fuca. It seems unlikely that much of the sediment would be deposited on the shelf; bottom transported material would move through the trough crossing the shelf and down Juan de Fuca Canyon onto the deep-sea floor (Gross, McManus and Ling, 1967). This may be the source of the Holocene material found in the two northern tributary channels. With the close of the Pleistocene, however, and the retreat of the glaciers, the flow of coarser sediments (sand and silt) to Vancouver Sea Valley and Western Cascadia Abyssal Plain terminated.

## CHANNEL ORIGIN

The early work of Menard (1955) emphasized the "left hook" of all of the deep-sea channels in the northeast Pacific Ocean where they cross deep-sea fans. This characteristic feature was attributed to the "secondary effect of the action of Coriolos force on the turbidity currents which formed the channels" (Menard, 1955, p. 236). The tilting of the turbidity current, so that it rises higher on the right, develops higher levees on this side through deposition. This actually tends to deflect the channels to the left. Deposition by turbidity currents therefore was thought to be an important factor in the development of deep-sea channels. The channel system connecting the Iberia and Biscay abyssal plains was thought to be erosional in origin (Laughton, 1960). Its course was believed to be determined by the original underlying topography. Subsequent photographic evidence of erosion included outcrops of strata, eroded cliffs, steep slopes, and slumping (Laughton, 1968). Recently, subbottom profiles have been obtained for numerous channels in the northeast Pacific by Hamilton (1967). They commonly indicate a depositional origin. Many of the channels originated in low areas in the underlying volcanic topography and subsequently migrated upward and outward, away from the higher levees on the right.

The upper portion of Cascadia Channel extends down the valley

formed between Astoria and Nitinat fans. If this course has always been maintained, then the development of the channel occurred sometime after the initial formation of the two fans. From  $45^{\circ}30'N.$  southward, the channel trends almost north-south and is bordered on the east and west by seamounts which protrude above the abyssal plain. Magnetic anomalies in this area (Raff and Mason, 1961) which reflect the underlying basement topography, also trend almost north-south. The control of the channel course by seamounts and ridges is especially evident within the Blanco fracture zone.

Cascadia Basin represents a flank of the actively spreading East Pacific Rise, the crest of which has been modified and arrested by the encroachment of North America (Vine, 1966). The magnetic anomalies apparently reflect linear bodies of igneous rock derived from the upper mantle, which have been injected into the crust at oceanic rises and subsequently spread away from it at a steady rate (Vine, 1966). The surface expression of these linear bodies has probably been important in influencing sediment transport and deposition. It seems likely that the course of Cascadia Channel was initially determined by the position of several elongate ridges on the flank of the East Pacific Rise which have subsequently been buried. They are presently represented by long, linear magnetic anomalies and chains of partially buried seamounts.

The channels farther north in the Gulf of Alaska have floors



which are above the general level of the flat areas adjacent to the channels (Hamilton, 1967). The elevation of the channels and the presence of levees suggested to Hamilton that turbidity current spillover from the channels covered all the rough topography and formed the flat interchannel areas. Cascadia Channel, on the other hand is incised deeply into the abyssal plain and has no levees south of  $45^{\circ}30'N$ . The confinement of the channel over much of its course between hills and seamounts suggests that it has meandered little, if any, since its formation. The adjacent, flat abyssal plain must therefore have some origin other than Cascadia Channel overflow. The more extensive and competent Pleistocene turbidity currents, both channelized and non-channelized, were probably of major importance in the development of the flat interchannel areas and the deep-sea fans.

## CONCLUSIONS AND GEOLOGIC HISTORY

Cascadia Channel, which is the most extensive deep-sea channel known in the Pacific Ocean, originates off of Oregon and Washington at the base of the continental slope where several other channels have merged. After crossing the southern portion of Cascadia Abyssal Plain it passes through Blanco fracture zone and emerges onto Tufts Abyssal Plain. The channel is believed to be over 2200 km in length. It has a gradually decreasing gradient which averages about 1:1000 (Figure 3). Sections of reversed slope interrupt the gradient several times along the course of the channel and may be due to slumping of sediment from the walls. Near the western end of the fracture zone the channel plunges 130 m into a wide, recently depressed basin. The relief along the upper and middle channel is low, but it increases along the lower portion to a maximum of 300 m on the southern abyssal plain, and 1100 m in the mountains of the fracture zone (Figure 3). The right (west and north) channel bank is consistently about 30 m higher than the left (east and south). Levees are responsible for this difference in height along the upper channel, but their absence along the middle and lower portions imply some other origin, possibly structural. A number of tributaries, of which Vancouver Sea Valley is the largest, enter Cascadia Channel along its course, giving rise to an extensive submarine drainage

system.

Turbidity currents have been actively depositing thick, olive green silt sequences throughout upper and lower Cascadia Channel during Holocene time (Figures 18, 21, and 22). These deposits alternate cyclically with thin layers of hemipelagic gray clay which settles out of suspension during periods of non-turbidity current deposition. The faunal composition of the clay has been used to develop a stratigraphic column for the area (Figure 7). Clays high in Radiolaria characterize the Holocene and previous warm or interglacial periods, while an abundance of planktonic Foraminifera characterizes the cooler, or glacial intervals, of the Pleistocene. Cooling periods at 5000 to 4000 and at 2000 years B.P. have been recognized within the expanded Holocene section.

The rhythmic channel sedimentation of olive green silts and gray clays occurs in the northern tributaries and extends for at least 650 km along the axis of the channel (Figure 26). The Holocene sediment sequence on the walls and levees of the channel shows that turbidity currents have risen high above the floor to deposit the characteristic sediments (Figures 23 and 24). No levees are present along the lower channel and the Holocene section consists only of hemipelagic clay; the turbidity currents were confined to the channel in this area. Erosion or non-deposition has characterized the middle channel during the Holocene. Turbidity currents left

extensive deposits to the north and south but have deposited only a thin surficial covering in this area (Figure 20).

The Holocene sediments deposited within Cascadia Channel by these turbidity currents are graded texturally and compositionally, and contain Foraminifera from neritic, bathyal, and abyssal depths which have been size sorted by the action of the currents (Figures 11 and 27).

A sequence of sedimentary structures occurs in the channel deposits similar to that found in sections of turbidites exposed on the continent (Figure 28). There is a sharp break in the textural and compositional properties of each graded layer (Figure 12). A coarser-grained, more positively skewed, basal zone of each bed represents deposition from the traction carpet which contains a high concentration of coarse material. A finer-grained, organic-rich upper portion of each bed represents deposition from the suspension load or sediment cloud. The thickest turbidity current sequences have been deposited in the lower channel, and the thinner units closer to shore (Figure 30). The successive layers vary uniformly in thickness along the lower channel. Their characteristics, along with those of the interbedded hemipelagic clays, can be correlated over at least 140 km. Recurrence intervals between individual turbidity currents are shorter closer to shore (400 to 500 yrs) than along the lower channel (500 to 600 yrs). The portion of

Cascadia Channel which crosses Tufts Abyssal Plain has recurrence intervals of 825 to 1500 years. All of the flows recorded near the source evidently did not extend the entire length of the channel. Individual flows reached maximum heights of 117 m above the channel bottom and spread laterally as far as 17 km (Figure 34). Calculated velocities range from 5.8 m/sec along the upper channel to 3.3 m/sec along the lower portion. The mineralogy of the sand from Cascadia Channel and the present movement of the sediment at the mouth of the Columbia River, indicate the material in the channel has been derived principally from the Columbia River drainage.(Figure 39).

The Pleistocene sediments of Cascadia Channel and the adjacent areas have recorded a different set of climatic, environmental, and depositional conditions than the Holocene sediments. The Pleistocene turbidity currents deposited sediment which was coarser and cleaner than that of the Holocene flows. These currents were active in all of the canyon, channel, fan, and abyssal plain environments of Cascadia Basin. The pronounced levees along the upper and middle portions of Cascadia Channel are due to overflow from Pleistocene turbidity currents. With the exception of Cascadia Channel, its northern tributaries and upper Astoria Fan, turbidity current activity ceased in Cascadia Basin at the end of the Pleistocene. Pleistocene gravels, which must have been deposited by turbidity currents, have been found as far as 740 km from shore along the axis of Cascadia

Channel. The lithologies of the gravel are similar to the bedrock in eastern Washington in the vicinity of the Chelan batholith. The massive floods produced by the breaking of glacial ice dams of Lake Missoula were probably responsible for transporting the gravel to the marine environment (Figure 37). These floods may have initiated turbidity currents on the upper continental slope which transported and deposited the coarse material along Cascadia Channel.

Glacial marine deposits containing material derived from the Puget Lowland and the adjacent mountains of Washington and British Columbia also were deposited in Cascadia Channel, during the Pleistocene. Ice bergs, which were derived from the Cordilleran glacier complex, melted as they floated south and left a trail of debris as far south as  $44^{\circ}10'N$ . (Figure 38). The distribution of the glacial marine sediments demonstrates that the late Pleistocene surface circulation in this area was similar to the present pattern. The northeast Pacific Gyral may have been farther north during the Pleistocene, but it is very unlikely that it was south of its present position.

In light of the present controversy (ocean bottom currents vs. turbidity currents) over the emplacement of deep-sea sands and silts, the detailed study of Cascadia Channel demonstrates conclusively that turbidity currents are actively transporting and depositing

sediment on the sea floor. Due to the confined and isolated nature of Cascadia Channel the deposits from individual flows have been recognized and correlated, and the dimensions, velocities, and recurrence intervals for the flows have been determined.

## BIBLIOGRAPHY

- Armstrong, J. E., D. R. Crandell, D. J. Easterbrook and J. R. Noble. 1965. Late Pleistocene stratigraphy and chronology in southwestern British Columbia and northwestern Washington. Geological Society of America, Bulletin 76:321-330.
- Arrhenius, G. 1952. Sediment cores from the east Pacific. Swedish Deep-Sea Expedition Reports, 1947-1948. 5:1-227.
- Bandy, Orville L. 1960. The geologic significance of coiling ratios in the foraminifer Globigerina pachyderma (Ehrenberg). Journal of Paleontology 34:671-681.
- Bandy, Orville L. 1967. Foraminiferal definition of the boundaries of the Pleistocene in southern California, U.S.A. In: Progress in Oceanography, ed. by M. Sears. Vol. 4. Oxford, Pergamon. p. 27-49.
- Berg, Joseph W., Jr. and Charles D. Baker. 1963. Oregon earthquakes, 1841 through 1958. Seismological Society of America, Bulletin 53:95-108.
- Biscaye, P. E. 1964. Distinction between kaolinite and chorite in Recent sediments by X-ray diffraction. American Mineralogist 49:1281-1289.
- Biscaye, P. E. 1965. Mineralogy and sedimentation of Recent deep-sea clay in the Atlantic Ocean and adjacent seas and oceans. Geological Society of America, Bulletin 74:803-832.
- Bouma, Arnold H. 1962. Sedimentology of some flysch deposits. A graphic approach to facies interpretation. Amsterdam, Elsevier. 168 p.
- Bretz, J. H., H. T. V. Smith and G. E. Neff. 1956. Bretz's flood hypothesis. Geological Society of America, Bulletin 67:957-1050.
- Carlson, Paul R. 1968. Marine geology of Astoria Submarine Canyon. Ph.D. thesis. Corvallis, Oregon State University. 259 numb. leaves.



- Cifelli, R. and K. N. Sachs, Jr. 1966. Abundance relationships of planktonic Foraminifera and Radiolaria. *Deep-Sea Research* 13:751-753.
- Crowell, John C. 1957. Origin of pebbly mudstones. *Geological Society of America, Bulletin* 68:993-1010.
- Curl, Herbert, Jr. 1962. Analysis of carbon in marine plankton organisms. *Journal of Marine Research* 20:181-188.
- Deevey, E. S. and R. F. Flint. 1957. Postglacial hypsithermal interval. *Science* 125:182-184.
- Dietz, Robert S. 1953. Possible deep-sea turbidity current channels in the Indian Ocean. *Geological Society of America, Bulletin* 64:375-378.
- Dill, Robert F., R. S. Dietz and H. B. Stewart, Jr. 1954. Deep-sea channels and delta of the Monterey Submarine Canyon. *Geological Society of America, Bulletin* 65:191-194.
- Dodimead, A. J., F. Favorite and T. Hirano. 1963. Salmon of the North Pacific Ocean. Part II. Review of Oceanography of the Subarctic Pacific region. *International North Pacific Fisheries Commission, Bulletin* 13:1-195.
- Duncan, John R., Jr. 1966. Microfaunal evidence for differentiating pelagic and bottom-transported deposits in a piston core from Cascadia Channel. Corvallis, Oregon State University. Department of Oceanography. 12 numb. leaves.
- Duncan, John R., Jr. 1968. Late-Pleistocene and postglacial sedimentation and stratigraphy of deep-sea environments off Oregon. Ph.D. thesis. Corvallis, Oregon State University. 222 numb. leaves.
- Easterbrook, Donald J. 1963. Late Pleistocene glacial events and relative sea level changes in the northern Puget Lowland, Washington. *Geological Society of America, Bulletin* 74:1465-1484.
- Emery, K. O. 1960. The sea off southern California. New York, John Wiley. 366 p.

- Emiliani, Cesare. 1966. Paleotemperature analysis of Caribbean cores P6304-8 and P6304-9 and a generalized temperature curve for the past 425,000 years. *Journal of Geology* 74:109-124.
- Ericson, D. B., M. Ewing and B. C. Heezen. 1952. Turbidity currents and sediments in the North Atlantic. *American Association of Petroleum Geologists, Bulletin* 36:489-512.
- Ericson, David B. 1959. Coiling directions of Globigerina pachyderma as a climatic index. *Science* 130:219-220.
- Ewing, Maurice et al. 1953. Exploration of the northwest Atlantic Mid-ocean Canyon. *Geological Society of America, Bulletin* 64:865-868.
- Fairbridge, R. W. 1961. Eustatic changes in sea level. In: *Physics and Chemistry of the Earth*. London, Pergamon. 4:99-185.
- Flint, R. F. 1967. *Glacial and Pleistocene geology*. New York, John Wiley. 366 p.
- Fowler, Gerald A. 1967. Assistant Professor, Oregon State University, Department of Oceanography. Personal communication, Corvallis, Oregon.
- Fowler, Gerald A. and L. D. Kulm. 1966. A multiple corer. *Limnology and Oceanography* 11:630-633.
- Geological Society of America. 1963. Rock color chart. New York. 6 p.
- Gibson, W. M. 1960. Submarine topography in the Gulf of Alaska. *Geological Society of America, Bulletin* 71:1087-1108.
- Goddard, Edwin N., et al. 1965. Geological map of North America. Washington, D. C., U. S. Geological Survey. 1 sheet.
- Gorsline, D. S. and K. O. Emery. 1959. Turbidity current deposition in San Pedro and Santa Monica Basins off southern California. *Geological Society of America, Bulletin* 70:279-290.
- Gould, Howard R. 195 . Some quantitative aspects of Lake Mead turbidity currents. In: *Turbidity currents and the transportation of coarse sediments to deep water*, ed. by J. L. Hough.

- Tulsa, Oklahoma. p. 34-52. (Society of Economic Paleontologists and Mineralogists. Special Publication 2)
- Griffin, J. J. and E. D. Goldberg. 1963. Clay-mineral distribution in the Pacific Ocean. In: The Sea, ed. by M. N. Hill. Vol. 3. New York, Interscience. p. 728-741.
- Griggs, Gary B. 1966. Foraminiferal trends in a Recent turbidite. Corvallis, Oregon State University. Department of Oceanography. 10 numb. leaves.
- Griggs, Gary B., A. G. Carey and L. D. Kulm, 1968. Deep-sea sedimentation and sediment-fauna interaction in Cascadia Channel and on Cascadia Abyssal Plain. Deep-Sea Research: In press.
- Gross, M. Grant. 1966. Distribution of radioactive marine sediments derived from the Columbia River. Journal of Geophysical Research 71:2017-2021.
- Gross, M. Grant and Jack L. Nelson. 1966. Sediment movement on the continental shelf near Washington and Oregon. Science 154:879-881.
- Gross, M. Grant, Dean A. McManus and Hsin-Li Ling. 1967. Continental shelf sediment, northwestern United States. Journal of Sedimentary Petrology 37:790-795.
- Hamilton, Edwin L. 1967. Marine geology of abyssal plains in the Gulf of Alaska. Journal of Geophysical Research 72:4189-4213.
- Heezen, Bruce C. 1963.. Turbidity currents. In: The Sea, ed. by M. N. Hill. Vol. 3. New York, Interscience. p. 742-775.
- Heezen, Bruce C. and D. B. Ericson. 1954. Reconnaissance survey of the abyssal plain south of New Foundland. Deep-Sea Research 2:122-133.
- Heezen, Bruce C., et al. 1964. Congo Submarine Canyon. American Association of Petroleum Geologists, Bulletin 48:1126-1149.
- Heusser, Calvin J. 1965. A Pleistocene phytogeographical sketch of the Pacific Northwest and Alaska. In: The Quaternary of

the United States. ed. by H. E. Wright and D. G. Frey.  
Princeton, Princeton University. p. 469-484.

Hurley, Robert J. 1960. The geomorphology of abyssal plains in the northeast Pacific Ocean. San Diego, California. Scripps Institute of Oceanography. Marine Physical Laboratory, 105 numb. leaves. (SIO reference 60-7)

Hurley, Robert J. 1964. Analysis of flow in Cascadia Deep-Sea Channel. In: Papers in Marine Geology (Shepard Commemorative volume). ed. by R. L. Miller. New York, MacMillan. p. 117-132.

Keulegan, G. H. 1957. Thirteenth progress report on model laws for density currents. An experimental study of the motion of saline water from locks into fresh water channels. Washington, D. C. U. S. National Bureau of Standards. Report 5168.

Keulegan, G. H. 1958. Twelfth progress report on model laws for density currents. The motion of saline fronts in still water. Washington, D. C. U. S. National Bureau of Standards. Report 5831.

Knebel, H. J., J. C. Kelley and J. T. Whetten. 1968. Clay minerals of the Columbia River: a qualitative, quantitative, and statistical evaluation. Journal of Sedimentary Petrology 38: 600-611.

Krumbein, W. C. and F. J. Pettijohn. 1938. Manual of sedimentary petrography. New York, D. Appleton-Century. 549 p.

Kuenen, Ph. H. 1953. Significant features of graded bedding. American Association of Petroleum Geologists, Bulletin 37:1044-1066.

Kuenen, Ph. H. 1964. Deep-sea sands and ancient turbidites. In: Turbidites. ed. by A. H. Bouma and A. Brouwer. Amsterdam, Elsevier. p. 3-33.

Kuenen, Ph. H. 1965. Experiments in connection with turbidity currents and clay-suspensions. In: Submarine geology and geophysics. ed. by W. F. Whittard and R. Bradshaw. London, Butterworths. (Colston Papers no. 17)

- Kuenen, Ph. H. 1966. Experimental turbidite lamination in a circular flume. *Journal of Geology* 74:523-545.
- Kuenen, Ph. H. and C. I. Migliorini. 1950. Turbidity currents as a cause of graded bedding. *Journal of Geology* 58:91-127.
- Laughton, A. S. 1960. An interplain deep-sea channel system. *Deep-Sea Research* 7:75-88.
- Laughton, A. S. 1968. New evidence of erosion on the deep ocean floor. *Deep-Sea Research* 15:21-30.
- Lockett, John B. 1965. Phenomena affecting improvement of the lower Columbia Estuary and entrance. In: *Proceedings of the Federal Inter-agency Sedimentation Conference*, Jackson, Mississippi, 1963. Symposium 3: Sedimentation in estuaries, harbors, and coastal areas. Washington, D.C., p. 626-669.
- Lowry, W. D. and E. M. Baldwin. 1952. Late Cenozoic geology of the lower Columbia River Valley, Oregon and Washington. *Geological Society of America, Bulletin* 63:1-24.
- McBride, Earle F. 1962. Flysch and associated beds of the Martinsburg Formation (Ordovician), Central Appalachians. *Journal of Sedimentary Petrology* 32:39-91.
- McManus, Dean A. 1964. Major bathymetric features near the coast of Oregon, Washington, and Vancouver Island. *North-west Science* 38:65-82.
- McManus, Dean A. 1967. Physiography of Cobb and Gorda Rises, northeast Pacific Ocean. *Geological Society of America, Bulletin*. 78:527-546.
- Matthes, F. E. 1939. Report of committee on glaciers, April, 1939. *Transactions of the American Geophysical Union* 20: 518-523.
- Meischner, K. D. 1964. Allodapische Kalke, Turbidite in riffnahen Sedimentations-becken. In: *Turbidites*. ed. by A. H. Bouma and A. Brouwer. Amsterdam, Elsevier. p. 93-105.
- Menard, Henry W. 1953. Pleistocene and Recent sediment from the floor of the northeast Pacific. *Geological Society of America, Bulletin* 64:1279-1294.

- Menard, Henry W. 1955. Deep-sea channels, topography, and sedimentation. American Association of Petroleum Geologists, Bulletin 39:236-255.
- Menard, Henry W. 1960. Possible pre-Pleistocene deep-sea fans off central California. Geological Society of America, Bulletin 71:1271-1278.
- Menard, Henry W. 1964. Marine geology of the Pacific. New York, McGraw-Hill. 271 p.
- Menard, Henry W., J. M. Smith and R. M. Pratt. 1965. The Rhone Deep-Sea Fan. In: Submarine geology and geophysics. ed. by W. F. Whittard and R. Bradshaw. London, Butterworths. p. 271-285. (Colston papers no. 17)
- Middleton, Gerald V. 1966. Experiments on density and turbidity currents. I. Motion of the head. Canadian Journal of Earth Sciences 3:523-546.
- Middleton, Gerald V. 1966. Experiments on density and turbidity currents. II. Uniform flow of density currents. Canadian Journal of Earth Sciences 3:627-637.
- Middleton, Gerald V. 1967. Experiments on density and turbidity currents. III. Deposition of sediment. Canadian Journal of Earth Sciences 4:475-505.
- Natland, M. L. and Ph. H. Kuenen. 1951. Sedimentary history of the Ventura Basin, California, and the action of turbidity currents. In: Turbidity currents and the transportation of coarse sediment to deep water. ed. by J. L. Hough. Tulsa, Oklahoma. p. 76-107. (Society of Economic Paleontologists and Mineralogists. Special Publication 2)
- Nayudu, Y. R. 1964. Carbonate deposits and paleoclimatic implications in the northeast Pacific Ocean. Science 146:515-517.
- Nelson, C. Hans. 1968. Marine geology of Astoria Deep-Sea Fan. Ph. D. thesis. Corvallis, Oregon State University. 287 numb. leaves.
- Nelson, C. Hans, et al. 1968. Mazama Ash in the northeastern Pacific. Science 161:47-49.

- Nichols, H. 1967. Pollen diagrams from sub-Arctic central Canada. *Science* 155:1665-1666.
- Osterberg, C., N. Cutshall and J. Cronin. 1965. Chromium-51 as a radioactive tracer of Columbia River water at sea. *Science* 150:1585-1587.
- Phleger, Fred. 1951. Displaced Foraminifera faunas. In: *Turbidity currents and the transportation of coarse sediments to deep water.* ed. by J. L. Hough. Tulsa, Oklahoma. p. 66-75. (Society of Economic Paleontologists and Mineralogists. Special Publication 2)
- Pratt, Richard M. 1967. The seaward extension of submarine canyons off the northeast coast of the United States. *Deep-Sea Research* 14:409-420.
- Raff, A. D. and R. G. Mason. 1961. A magnetic survey off the west coast of North America, 40°N to 52½°N. *Geological Society of America, Bulletin* 72:1259-1265.
- Rex, R. W. and E. D. Goldberg. 1968. Quartz contents of pelagic sediments of the Pacific Ocean. *Tellus* 10:153-159.
- Royse, Chester F. 1964. *Sediments of Willapa Submarine Canyon.* Seattle. 62 p. (Washington University, Department of Oceanography. Technical Report No. 111)
- Rubin, M. and C. Alexander. 1958. U. S. Geological Survey radio-carbon dates IV. *Science* 127:1476-1487.
- Russell, Kenneth L. 1967. Clay mineral origin and distribution on Astoria Fan. Master's thesis. Corvallis, Oregon State University. 47 numb. leaves.
- Shepard, Francis P. and Robert F. Dill. 1966. *Submarine canyons and other sea valleys.* Chicago, Rand McNally. 381 p.
- Smith, R. I. 1966. An investigation of upwelling along the Oregon coast. Ph. D. thesis. Corvallis, Oregon State University. 83 numb. leaves.
- United States Army Engineers. 1961. *Sedimentation investigation, lower Columbia and lower Willamette Rivers, July 1959, August 1960.* Portland, Oregon. 17 p.

- Vance, J. A. 1954. Glaucophane schists associated with green schists in the Sauk River area of the northern Cascade Mountains, Washington. Geological Society of America, Bulletin 65:1352.
- Vine, F. J. 1966. Spreading of the ocean floor: new evidence. Science 154:1405-1415.
- Walker, Roger G. 1965. The origin and significance of the internal sedimentary structures of turbidites. Yorkshire Geological Society, Proceedings 35:1-32.
- Walker, Roger G. 1967. Turbidite sedimentary structures and their relationship to proximal and distal depositional environments. Journal of Sedimentary Petrology 37:25-43.
- Waters, A. C. 1927. Concerning the differentiation of a lamprophyric magma at Corbaley Canyon, Washington. Journal of Geology 35:158-170.
- Waters, A. C. 1938. Petrology of the contact breccias of the Chelan Batholith. Geological Society of America, Bulletin 49:763-794.
- Waters, A. C. 1955. Volcanic rocks and the tectonic cycle. In: Crust of the earth, ed. by Arie Poldervaart. New York. p. 703-722. (Geological Society of America Special Paper 62)
- Waters, A. C. 1968. Professor. University of California, Santa Cruz, Division of Natural Sciences. Personal communication, Santa Cruz, California.
- Wilde, Pat. 1965. Recent sediments of the Monterey Deep-Sea Fan. Berkeley. 155 numb. leaves. (California University. Hydraulic Engineering Laboratory. Technical Report Hel-2-13.
- Williams, H., F. J. Turner and C. J. Gilbert. 1954. Petrography. An introduction to the study of rocks in thin sections. San Francisco, Freeman. 406 p.



## APPENDICES

## LEGEND FOR APPENDICES

## Sediment Age

H = Holocene

P = Pleistocene

## Sediment Types

TS = Terrigenous sand-silt

OGS = Olive green silt

GC = Gray clay

PC = Pebbly clay

G = Gravel

FL = Foraminiferal lutite

## Physiographic Environments

CC = Cascadia Channel

WC = Willapa Canyon-Channel

TC = Tributary Channel

V = Vancouver Sea Valley

NF = Nitinat Fan

WP = Western Cascadia Abyssal Plain

Data marked with \* is from Duncan (1968).

p11 - Phleger core

## APPENDIX I. PISTON CORE STATION LOCATIONS

OSU station number	Latitude (north)	Longitude (west)	Water depth (meters)	Physiographic environment	Core length (cm)
6508-K1	46° 14.9'	126° 23.2'	2719	Cascadia Channel Floor	630
6509-10	45° 29.6'	127° 14.5'	2862	Cascadia Channel Floor	243
6509-11	45° 30.9'	127° 30.2'	2801	Nizinat Fan	170
6509-12	45° 25.0'	127° 52.0'	2867	Vancouver Sea Valley	110
6509-13	45° 23.0'	128° 11.0'	2867	Western Cascadia Plain	230
6509-14	45° 15.0'	127° 25.5'	2922	Cascadia Channel Floor	235
6509-15	44° 57.0'	127° 16.4'	2997	Cascadia Channel Wall	243
6509-15A	44° 57.5'	127° 16.0'	3003	Cascadia Channel Floor	367
6509-17	44° 39.8'	127° 21.0'	3038	Cascadia Channel Wall	268
6509-25A	43° 35.0'	129° 12.0'	3334	Cascadia Channel Floor	390
6509-26	43° 44.5'	127° 12.0'	3147	Cascadia Channel Floor	607
6509-27	44° 27.8'	127° 13.6'	3102	Cascadia Channel Floor	580
6509-28	44° 27.0'	127° 19.8'	2838	Cascadia Channel Bank	512
6509-29	44° 29.8'	127° 11.0'	2864	Cascadia Channel Bank	103
6604-1	43° 34.0'	128° 44.5'	3329	Cascadia Channel Floor	50
6604-4	43° 38.5'	127° 58.2'	3244	Cascadia Channel Floor	470
6604-5	43° 33.6'	127° 32.0'	3167	Cascadia Channel Floor	30
6604-30	44° 12.0'	127° 14.0'	2840	Cascadia Channel Bank	348
6604-31	44° 13.5'	127° 06.0'	2880	Cascadia Channel Bank	320
6609-11	43° 31.5'	127° 26.0'	3155	Cascadia Channel Floor	203
6609-19	43° 43.2'	128° 40.9'	3438	Cascadia Channel Floor	860
6609-24	44° 10.0'	127° 11.5'	3126	Cascadia Channel Floor	840
6609-25	44° 09.8'	127° 13.1'	2999	Cascadia Channel Wall	419
6609-26	44° 50.1'	127° 05.5'	2878	Tributary Channel	427
6609-27	45° 02.5'	127° 30.5'	2911	Vancouver Sea Valley	434
6609-28	45° 05.5'	127° 21.1'	2966	Cascadia Channel Floor	572
6609-29	45° 16.0'	127° 19.0'	2889	Tributary Channel	300
6609-30	45° 22.0'	127° 25.5'	2907	Cascadia Channel Floor	388
6609-31	45° 11.5'	127° 48.2'	2884	Vancouver Sea Valley	288
6609-32	44° 57.2'	127° 44.8'	2487	Sea Mount	16
6610-2	46° 24.8'	128° 13.2'	2745	Vancouver Sea Valley	403
6705-1	46° 26.5'	125° 30.1'	2299	Willapa Canyon	320
6705-2	46° 42.7'	126° 03.0'	2622	Tributary Channel	299
6705-4	46° 21.9'	125° 51.9'	2580	Willapa Channel	400
6705-5	46° 10.4'	126° 05.0'	2660	Willapa Channel	593
6705-6	46° 24.8'	126° 23.9'	2688	Tributary Channel	570
6705-7	46° 03.6'	126° 37.9'	2688	Cascadia Channel Bank	574
6705-8	46° 03.5'	126° 37.0'	2774	Cascadia Channel Floor	330
6705-9	46° 01.9'	126° 37.2'	2697	Cascadia Channel Bank	580
6705-10	46° 09.5'	126° 51.9'	2743	Tributary Channel	580
6705-11	46° 09.7'	127° 08.0'	2710	Nizinat Fan	380
6705-12	45° 40.1'	127° 01.1'	2783	Cascadia Channel Bank	414
6705-13	45° 40.0'	127° 02.0'	2842	Cascadia Channel Floor	470
6705-14	45° 41.4'	127° 03.6'	2774	Cascadia Channel Bank	565
6705-15	44° 50.1'	127° 20.0'	3036	Cascadia Channel Floor	50

OSU station number	Latitude (north)	Longitude (west)	Water depth (meters)	Physiographic environment	Core length (cm)
6705-16	44° 50.5'	127° 19.1'	2999	Cascadia Channel Wall	425
6705-17	44° 35.3'	127° 21.3'	3049	Cascadia Channel Wall	81
6705-19	43° 57.7'	127° 09.2'	3147	Cascadia Channel Wall	422
6705-20	43° 27.9'	127° 09.0'	3162	Cascadia Channel Floor	590
6705-21	43° 28.6'	127° 10.3'	3109	Cascadia Channel Wall	542

## APPENDIX II. RADIOCARBON AGE DETERMINATIONS

Sample number	Depth in core (cm)	Material dated	Isotopic age (years BP)
6509-25A-1C14	255-290	total carbon	9,670 $\pm$ 190
6509-27-1C14	485-505	total carbon	4,645 $\pm$ 190
6609-24-1C14	762-807	total carbon	11,040 $\pm$ 160
6609-25-1C14	217-240	total carbon	37,000 $\pm$ 2,900 - 2,200
6705-7-1C14	407-453	total carbon	29,630 $\pm$ 1,400 - 1,200

APPENDIX III. TEXTURAL AND COARSE-FRACTION COMPOSITION OF SEDIMENT SAMPLES

Sample number	Depth in core (cm)	Age	Sediment type	% sand	% silt	% clay	Percent of coarse-fraction by number									
							Detrital grains	Mica	Volcanic glass	Plant fibers	Radiolarians	Diatoms	Planktonic foraminifera	Benthic foraminifera	Fecal pellets	Pyrite
6508-K1-2	17	H	GC	4-53-43			41	10	8	1	14	22	T	1	4	T
-3	43	H	GC	1-44-55			5	6	1	1	26	50	1	1	11	--
-6	104	H	GC	3-45-52			25	3	1	T	21	17	7	2	22	1
-7	121	H	GC	2-49-49			11	14	5	2	21	34	11	T	1	1
-8	131	H	GC	2-46-52			21	2	5	1	16	34	5	1	15	T
-9	138	H	OGS	8-82-10			84	6	9	T	T	1	--	T	--	--
-10	141	H	GC	2-45-53			12	5	8	3	25	37	1	2	7	1
-11	151	H	GC	2-48-50			12	6	8	5	22	35	1	3	7	1
-12	155	H	OGS	13-79-08			68	10	20	1	1	T	--	--	--	--
-13	158	H	GC	2-45-53			22	12	18	4	15	22	4	1	1	T
-16	249	H	GC	3-36-61			39	4	6	T	11	24	5	1	9	T
-19	314	H	OGS	30-52-18			23	16	43	16	1	T	--	1	--	--
-19a	326	H	OGS	35-41-24			44	7	36	10	1	1	--	T	--	--
-21	342	H	GC	5-38-57			15	2	9	1	17	14	8	1	33	--
-22	357	H	GC	1-45-54			5	2	5	1	20	28	2	--	35	T
-26	402	H	GC	1-50-49			8	5	9	--	26	36	1	T	16	T
-27	420	H	OGS	8-67-25			21	15	58	5	T	T	--	--	--	--
-28	433	H	OGS	16-72-12			29	13	51	4	1	1	T	T	--	1
-29	449	H	OGS	25-62-13			40	11	43	5	T	--	--	--	--	--
-30	463	H	OGS	28-41-31			28	7	54	4	1	1	T	4	1	--
-31	466	H	OGS	62-30-08			72	5	20	T	--	T	1	1	--	T
-32	468	H	GC	1-50-49			10	3	8	2	23	39	6	1	6	2
-34	548	H	OGS	1-64-35			8	44	--	43	3	2	T	T	--	--
-35	561	H	OGS	13-73-14			61	26	2	9	T	1	--	1	--	--
-36	575	H	OGS	18-69-13			60	24	2	11	1	1	T	T	--	--

(continued)

Sample number	Depth in core (cm)	Age	Sediment type	% sand % silt % clay			Percent of coarse-fraction by number									
							Detrital grains	Mica	Volcanic glass	Plant fibers	Radiolarians	Diatoms	Planktonic foraminifera	Benthic foraminifera	Fecal pellets	Pyrite
6508-K1-37	597	H	OGS	39-38-23	84	9	1	2	T	1	1	2	--	--		
-38	600	H	OGS	70-21-09	95	3	T	T	--	--	T	1	--	--		
-38a	604	H	OGS	42-44-14	91	4	1	--	1	--	2	1	--	--		
-39	608	H	OGS		46	18	T	26	T	T	1	T	1	--		
-40	610	H	OGS	76-23-01	97	3	T	--	--	--	--	T	--	--		
-41	612	H	GC	1-38-61	11	4	T	T	31	28	10	1	13	2		
6509-10-2	20	H	OGS	1-47-52	42	9	11	32	1	3	--	T	--	1		
-3	25	H	OGS	6-67-27												
-4	31	H	OGS	3-73-24	69	9	16	2	2	T	T	1	--	T		
-6	40	H	GC	0-28-72	4	7	T	4	79	3	1	2	--	--		
-7	73	H	OGS	6-84-10	85	7	7	T	T	T	T	T	--	T		
-8	82	H	OGS	4-54-42	58	14	19	5	2	T	T	T	--	--		
-10	132	H	OGS	3-48-59												
-15	208	H	OGS		48	6	22	17	4	2	T	1	--	2		
-16	213	H	OGS	5-75-20	59	6	32	1	1	T	T	T	T	T		
-17	215	H	GC	1-30-69	38	10	25	4	14	2	5	1	--	--		
6509-11-1	27	P	TS	63-34-03	99	1	--	--	--	T	--	--	--	--		
-3	85	P	GC	2-50-48	3	10	--	--	T	--	87	--	--	--		
-5	158	P	GC	4-38-58	1	3	--	--	--	--	93	1	2	T		
6509-12-1	59	H	GC		17	1	--	1	53	20	6	1	3	--		
-3	152	P	TS	84-14-02	100	T	--	--	--	--	T	--	--	--		
6509-14-1	2	P	TS	79-17-04												
-2	12	P	TS	96-02-02												
-3	22	P	TS	97-01-02												
-5	72	P	TS	95-03-02												
-6a	97	P	TS	95-03-02												
-7	127	P	TS	93-03-04												
-8	158	P	TS	96-02-02												

(continued)

Sample number	Depth in core (cm)	Age	Sediment type				Percent of coarse-fraction by number									
				% sand	% silt	% clay	Detrital grains	Mica	Volcanic glass	Plant fibers	Radiolarians	Diatoms	Planktonic foraminifera	Benthic foraminifera	Fecal pellets	Pyrite
6509-14-9	200	P	TS	97-01-02												
-10	222	P	G	99-00-01												
6509-15-1	2	H	GC	6-45-49			19	2	1	2	18	16	1	1	43	--
-2	43	H	GC	3-37-60			17	5	6	1	27	11	T	T	29	3
-3	54	H	GC				3	1	T	T	18	18	3	3	55	T
-6	74	H	GC				2	T	T	T	16	11	6	1	63	--
-7	82	H	OGS	28-70-02			85	5	10	--	--	--	--	--	--	--
-8	88	H	GC	2-52-46			7	7	12	19	19	24	T	1	9	T
-23	105	H	OGS				72	1	25	1	--	T	--	--	--	--
-24	113	H	OGS				95	1	--	2	T	T	--	1	--	--
-9	143	H	GC	2-36-62			5	1	--	5	16	23	10	T	40	T
-10	146	H	OGS	6-70-24			50	19	1	25	4	2	--	T	--	--
-11	152	H	OGS	39-55-06			90	8	1	T	--	--	--	1	--	--
-12	159	H	OGS	26-70-04			80	17	1	T	--	--	T	T	T	--
-13	163	H	OGS	13-45-42			46	21	1	27	2	2	1	T	--	--
-14	166	H	OGS	38-57-05			89	8	T	1	T	T	--	T	--	--
-15	170	H	OGS	64-33-03			95	4	--	--	--	--	--	1	--	--
-16	179	H	OGS	62-37-01			100	--	T	--	--	--	T	--	--	--
-18	196	P	GC	0-42-58			76	9	1	2	1	T	6	2	--	1
-19	214	P	GC	0-27-73			87	9	1	2	1	--	1	--	--	T
-21	234	P	GC	0-39-61			41	44	4	10	T	T	T	--	--	--
6509-15A-1	37	H	OGS	16-70-14			76	14	3	3	2	2	--	T	--	--
-2	40	H	GC	11-38-51			7	2	T	3	21	13	T	--	54	--
-3	54	H	OGS	1-42-57			T	3	--	71	2	24	--	--	--	--
-4	64	H	OGS	2-76-22			16	27	3	28	2	23	--	T	--	--
-5	68	H	OGS	4-93-03			47	40	5	3	T	5	--	T	--	--
-6	70	H	OGS	6-77-17			22	27	3	30	4	14	--	T	--	--
-8	104	H	OGS	23-63-14			65	12	8	9	1	4	--	T	--	--

(continued)



Sample number	Depth in core (cm)	Age	Sediment type	% sand % silt % clay	Percent of coarse-fraction by number									Pyrite
					Detrital grains	Mica	Volcanic glass	Plant fibers	Radiolarians	Diatoms	Planktonic foraminifera	Benthic foraminifera	Fecal pellets	
6509-15A-9	107	H	GC	7-37-56	--	1	--	5	12	27	--	--	54	--
-10	147	H	OGS	23-63-14	50	17	10	14	3	6	1	1	--	--
-11	150	H	GC	6-37-57	1	1	--	1	20	22	T	T	53	--
-12	200	H	OGS	17-61-22	48	18	18	4	3	6	--	1	T	--
-13	203	H	GC	8-39-53	9	3	2	1	14	16	--	T	53	1
-14	216	H	OGS	1-44-55	--	7	--	65	2	25	--	T	--	--
-15	227	H	OGS	1-47-52	4	13	3	54	1	25	--	--	--	--
-16	237	H	OGS	10-80-10	54	23	16	1	1	4	--	1	--	--
-17	243	H	OGS	19-72-09	54	18	19	3	1	5	T	1	--	--
-18	250	H	OGS	20-58-22	49	17	15	11	4	4	--	1	--	--
-19	252	H	GC	8-40-52	4	2	--	1	27	12	--	--	53	--
-39	255	H	OGS	0-32-68	10	9	5	51	15	10	--	--	--	T
-38	260	H	OGS	1-33-66	2	12	3	62	12	8	--	--	--	T
-37	266	H	OGS	0-34-66	6	6	7	72	4	5	--	--	--	--
-20	270	H	OGS	1-39-60	1	5	3	55	3	25	--	--	6	1
-36	275	H	OGS	1-37-62	2	4	2	67	1	25	--	--	--	2
-35	279	H	OGS	0-39-61	3	6	3	63	1	24	--	--	T	3
-21A	283	H	OGS	1-47-52	4	15	2	52	1	27	--	--	--	--
-34	291	H	OGS	1-49-50	19	13	11	36	3	16	--	--	--	1
-22	297	H	OGS	12-80-08	64	18	10	1	T	3	1	2	--	--
-23	300	H	OGS	11-65-24	35	15	15	22	4	7	--	1	T	--
-24	301	H	OGS	29-66-05	75	8	15	1	1	T	T	T	--	--
-25	303	H	OGS	27-59-13	47	19	23	1	3	3	--	2	--	--
-26	307	H	OGS	63-36-01	92	2	5	--	--	--	--	1	--	--
-27	311	H	GC	4-37-59	1	1	1	1	13	15	--	--	66	2
-28	322	H	OGS	2-46-52	1	10	4	59	2	24	--	--	--	1
-29	339	H	OGS	1-43-56	3	13	3	50	4	26	--	--	T	--
-30	351	H	OGS	2-51-47	24	13	6	36	3	16	--	1	--	--

(continued)

Sample number	Depth in core (cm)	Age	Sediment type	% sand % silt % clay	Percent of coarse-fraction by number									
					Detrital grains	Mica	Volcanic glass	Plant fibers	Radiolarians	Diatoms	Planktonic foraminifera	Benthic foraminifera	Fecal pellets	Pyrite
6509-15A-31	355	H	OGS	16-78-06	84	7	7	1	T	T	--	--	--	--
-32	361	H	OGS	59-40-01	89	6	5	--	--	--	--	--	--	--
-33	364	H	GC	6-33-61	5	--	2	1	23	11	T	--	54	2
6509-17-2	20	H	OGS	3-85-12										
-3	29	H	GC	2-34-64										
-4	31	H	OGS	4-74-22										
-5	36	H	OGS	4-49-47										
-6	47	H	OGS	27-60-13										
-13	110	H	OGS	7-69-24	81	12	1	5	1	--	--	1	--	--
-14	118	H	OGS	18-70-11	92	7	T	T	--	--	T	--	--	--
-15	133	H	OGS	15-75-10	94	5	T	T	--	--	--	--	--	--
-16	152	H	OGS	7-71-22	76	17	2	2	2	--	--	T	--	--
-17	156	H	GC	0-42-58	12	4	T	3	44	6	17	3	2	4
-19	182	H	OGS	3-71-26										
-20	186	H	GC	0-35-65	48	10	2	3	29	--	6	1	T	--
6509-25A-19	8	H	GC	3-44-53	7	14	3	11	57	8	--	T	--	--
-2	41	H	OGS		11	22	24	33	4	3	T	1	--	--
-4	47	H	GC		4	5	1	1	79	T	1	2	--	--
-5	82	H	OGS		22	6	39	25	2	1	1	1	--	--
-7	99	H	OGS	2-84-14	15	15	42	12	13	1	--	1	--	--
-8	104	H	GC		3	4	1	2	75	1	--	3	10	--
-9	235	H	OGS	2-80-18	32	31	T	28	5	1	--	1	--	--
-11	258	H	OGS		24	24	2	40	2	5	T	2	--	--
-12	310	H	OGS		29	24	3	24	7	5	2	2	--	--
-14	318	H	GC		3	1	--	2	63	1	9	4	14	--
-15	351	H	OGS		16	41	2	28	3	2	3	3	--	--
-16	355	H	GC		11	3	--	2	37	1	9	3	27	--
-17	380	H	OGS	4-73-23	42	29	1	22	4	T	T	T	--	--

(continued)

Sample number	Depth in core (cm)	Age	Sediment type				Percent of coarse-fraction by number									
							% sand	% silt	% clay	Detrital grains	Mica	Volcanic glass	Plant fibers	Radiolarians	Diatoms	Planktonic foraminifera
6509-26-36	0	H	OGS	1-41-58			3	6	T	60	9	21	--	1	--	--
-20	42	H	OGS	1-54-45			47	7	9	27	2	5	--	1	--	--
-21	50	H	OGS	3-77-20												
-22	54	H	GC				7	3	1	9	38	7	T	6	25	1
-26	142	H	OGS	0-37-63												
-27	177	H	OGS	0-42-58												
-28	181	H	OGS	2-80-18												
-29	182	H	OGS	6-76-18												
-30	186	H	OGS	6-84-10												
-31	188	H	GC	0-32-68			11	1	2	9	44	8	4	3	7	9
-33	263	H	OGS	22-69-09			87	10	3	--	--	--	--	--	--	--
-34	267	H	GC	1-26-73			22	2	4	2	41	2	10	3	4	9
-35	296	H	OGS	0-38-62												
-1	312	H	OGS	0-42-58												
-2	320	H	OGS	1-67-32												
-3	324	H	GC	0-36-64			6	4	6	6	54	2	1	3	15	1
-4	342	H	OGS	0-39-61												
-5	362	H	OGS	0-39-61												
-8	392	H	GC	0-31-69			3	6	2	11	54	1	1	5	12	2
-11	461	H	OGS	0-47-53			18	13	18	36	3	7	T	1	--	--
-12	465	H	OGS	1-89-10												
-13	471	H	GC	0-32-68			5	5	3	9	50	1	1	4	16	2
-14	487	H	OGS	0-37-63			9	3	5	63	3	9	T	1	--	--
-15	542	H	OGS	1-43-56												
-17	545	H	OGS	10-79-11			56	21	22	T	T	T	--	T	--	--
-16	548	H	GC	1-28-71												
6509-27-1	3	H	OGS	1-40-59												
-2	40	H	OGS	6-69-25												

(continued)

Sample number	Depth in core (cm)	Age	Sediment type				Percent of coarse-fraction by number									
				% sand	% silt	% clay	Detrital grains	Mica	Volcanic glass	Plant fibers	Radiolarians	Diatoms	Planktonic foraminifera	Benthic foraminifera	Fecal pellets	Pyrite
6509-27-3	52	H	OGS	58-33-09												
-4	55	H	GC	1-27-72												
-6	97	H	OGS	3-61-36												
-5	103	H	OGS	3-67-31												
-7	107	H	GC	0-26-74			14	12	12	10	40	10	--	--	--	--
-8	128	H	OGS	1-37-62												
-9	155	H	OGS	24-53-23												
-10	177	H	OGS	0-43-57												
-11	263	H	OGS	6-58-36			31	22	14	18	6	6	T	1	--	--
-12	281	H	OGS	6-72-22			44	9	30	4	--	5	2	1	2	--
-13	283	H	GC	0-34-66			20	2	2	6	36	T	--	1	31	2
-14	292	H	OGS	0-41-59												
-15	333	H	OGS	3-51-46												
-16	360	H	OGS	12-46-42			49	14	20	8	2	2	--	1	--	--
-17	367	H	OGS	15-62-23			72	5	18	3	1	--	T	1	--	--
-18	461	H	OGS	22-51-27			59	11	20	4	2	1	T	1	--	--
-19	469	H	OGS	29-50-21			76	4	19	1	--	T	T	T	--	--
-20	471	H	GC	0-34-66			4	1	1	1	5	2	T	1	83	1
-21	482	H	OGS	0-42-58			10	8	16	56	2	2	--	1	--	5
-22	522	H	OGS	1-45-54												
-23	576	H	OGS	23-42-35												
-33	580	H	OGS	29-44-27			69	11	10	7	2	T	--	T	--	T
6509-28-11	2	H	GC	1-20-79			4	2	1	1	87	T	--	3	--	--
-12	14	H	GC	1-25-74			2	1	2	3	84	T	3	1	--	--
-13	43	P	GC	0-33-67			3	4	T	2	6	--	77	5	1	T
-14	48	P	TS				23	28	1	10	9	T	24	2	1	T
-15	53	P	GC	0-35-65			4	3	1	1	1	--	84	5	T	--
-17	167	P	GC	1-26-73			2	1	T	1	--	--	90	2	--	--

(continued)

Sample number	Depth in core (cm)	Age	Sediment type	Percent of coarse-fraction by number										
				% sand % silt % clay	Detrital grains	Mica	Volcanic glass	Plant fibers	Radiolarians	Diatoms	Planktonic foraminifera	Benthic foraminifera	Fecal pellets	Pyrite
6509-28-2	307	P	TS		63	19	10	3	T	--	4	T	--	--
-7	383	P	GC	1-47-52	2	2	--	1	T	--	91	2	T	1
-3	424	P	GC		4	11	1	--	--	--	75	1	--	--
-4	436	P	GC		2	T	--	3	T	--	91	3	T	--
-6	515	P	GC	0-30-70	T	3	T	1	T	T	94	1	--	--
6509-29-2	26	H	GC	1-27-62	23	2	2	4	34	T	22	4	4	--
-4	66	P	TS		66	16	18	T	T	T	T	T	--	T
-5	78	P	TS	2-90-08	54	23	20	2	--	--	T	T	--	--
6604-31-4	131	P	TS	0-85-15	13	57	--	26	--	--	3	T	--	--
-5	133	P	TS	0-54-56	26	18	--	11	--	T	44	--	--	--
-6	137	P	GC	1-36-63										
6609-24-1	20	H	OGS	40-46-14	60	14	14	1	3	8	--	2	--	--
-2	24	H	GC	0-38-56	1	1	--	1	39	21	--	--	35	--
-3	70	H	OGS	5-72-23	8	30	3	43	9	7	--	--	--	--
-4	73	H	GC	3-41-56	1	1	--	1	52	24	--	2	18	--
-5	110	H	GC	2-43-55	--	T	--	1	51	38	1	1	7	--
-6	157	H	OGS	56-41-03	84	7	4	T	1	3	T	1	--	--
-7	160	H	GC	2-38-60	1	1	T	1	70	16	5	1	5	--
-8	217	H	OGS	8-67-25	2	19	5	51	14	9	--	--	T	--
-9	221	H	GC	3-39-58	T	1	--	1	44	27	--	3	24	--
-10	270	H	OGS	25-64-11	46	18	25	3	6	3	--	--	--	--
-11	272	H	GC		12	6	10	2	39	7	2	1	20	3
-12	334	H	OGS	44-55-01	73	8	17	1	--	--	--	T	--	--
-13	337	H	GC	5-37-58	4	1	2	T	46	8	T	T	37	1
-14	345	H	OGS	1-39-60	5	6	--	60	22	5	1	1	T	--
-15	355	H	OGS	1-42-57	3	4	--	60	18	13	--	--	4	--
-16	364	H	OGS	2-46-52	2	9	--	71	4	13	--	--	--	1
-17	374	H	OGS	3-52-45	11	16	10	56	3	5	--	--	--	--

(continued)

Sample number	Depth in core (cm)	Age	Sediment type				Percent of coarse-fraction by number								
							Detrital grains	Mica	Volcanic glass	Plant fibers	Radiolarians	Diatoms	Planktonic foraminifera	Benthic foraminifera	Fecal pellets
6609-24-18	387	H	OGS	22-58-20	33	18	33	9	3	3	--	T	--	T	
-19	394	H	OGS	33-60-07	55	13	29	3	1	2	T	--	--	--	
-20	397	H	GC	4-35-61	T	1	--	T	50	16	2	T	30	T	
-22	447	H	GC	4-34-62	4	2	T	1	48	10	11	2	21	2	
-23	486	H	OGS	87-11-02	98	1	1	--	--	--	--	--	--	--	
-24	488	H	GC	3-35-62	2	2	--	1	48	15	13	1	18	1	
-25	560	H	OGS	76-22-02	93	1	6	--	--	--	--	--	--	--	
-26	563	H	GC		29	4	10	2	29	5	1	1	17	2	
-28	603	H	GC		7	2	--	1	66	5	1	2	19	1	
-29	634	H	OGS	92-07-01	96	1	3	--	--	--	--	--	--	--	
-30	641	H	GC	2-33-65	2	1	--	--	58	10	20	1	6	3	
-31	680	H	OGS	94-05-01	100	--	--	--	--	--	--	--	--	--	
-32	682	H	GC	2-33-65	5	T	--	--	60	6	16	1	8	3	
-33	713	H	OGS	95-04-01											
-34	716	H	GC	4-34-62	4	1	--	--	46	7	20	2	14	5	
-35	721	H	OGS	0-35-65											
-36	732	H	OGS	1-38-61											
-37	745	H	OGS	4-44-52											
-38	754	H	OGS	47-47-06											
-39	758	H	OGS	79-20-01											
-40	762	H	GC		2	1	--	--	38	4	32	2	11	9	
-41	810	H	OGS	50-45-05											
-42	812	H	OGS		46	21	T	1	13	1	10	1	6	--	
-44	826	H	OGS	0-56-44	8	48	T	23	8	3	5	1	--	1	
6609-25-22	195	P	PC	22-39-39											
-23	201	P	FL	24-46-30	2	--	--	--	--	--	93	1	3	--	
-24	250	P	FL	21-24-55	--	--	--	--	1	--	98	2	--	--	
-25	299	P	FL		1	--	--	--	--	--	97	2	--	--	
-26	350	P	FL		--	--	--	--	--	--	99	1	--	--	

(continued)

Sample number	Depth in core (cm)	Age	Sediment type				Percent of coarse-fraction by number								
				% sand	% silt	% clay	Detrital grains	Mica	Volcanic glass	Plant fibers	Radiolarians	Diatoms	Planktonic foraminifera	Benthic foraminifera	Fecal pellets
6609-26-11	109	P	TS	1-93-05			83	16	--	--	T	--	T	--	--
-12	118	P	TS	2-91-07			34	56	--	5	1	--	2	2	--
-13	136	P	TS	42-54-04			85	14	--	1	--	--	--	--	--
-14	150	P	TS	81-17-02			96	4	--	--	--	--	--	--	--
-18	261	P	GC	11-28-61											
6609-28-5	152	P	PC	59-22-19			99	1	--	--	--	--	--	--	--
-6	200	P	PC	43-30-27			98	2	--	--	--	--	--	--	--
-9	350	P	PC				89	10	T	--	--	--	--	--	--
-13	400	P	PC				98	2	--	--	--	--	--	--	--
6609-29-1	1	H	GC				--	2	--	--	84	8	1	4	--
-2	10	H	GC				1	1	--	1	76	11	3	--	6
-3	20	H	GC				2	T	--	--	69	11	9	1	7
-4	30	H	GC				7	9	--	1	59	8	10	--	6
-5	40	H	GC				4	2	--	--	45	6	22	1	21
-6	50	H	GC				15	10	--	T	54	1	12	1	8
6609-30-6	109	P	TS				67	20	--	11	--	--	T	1	--
-7	129	P	TS				42	39	--	16	--	--	2	--	--
-8	150	P	TS	1-41-58			14	50	--	32	--	T	3	T	--
-9	176	P	TS				72	23	--	4	--	--	2	--	--
-12	250	P	PC	39-34-27			98	2	--	--	--	--	--	--	--
-16	367	P	PC	60-22-18			98	2	--	--	--	--	--	--	--
6609-31-12	170	P	GC	4-29-67											
-13	202	P	TS	2-24-74			62	26	--	9	T	--	T	T	--
-14	223	P	TS	25-36-39			89	10	--	1	--	--	--	--	--
-15	235	P	TS	71-24-05			92	7	--	T	--	--	--	--	--
-16	258	P	TS	81-17-02			95	5	--	T	--	--	--	--	--
-17	271	P	TS	83-16-01			99	1	--	--	--	--	--	--	--

(continued)

Sample number	Depth in core (cm)	Age	Sediment type	Percent of coarse-fraction by number												
				% sand	% silt	% clay	Detrital grains	Mica	Volcanic glass	Plant fibers	Radiolarians	Diatoms	Planktonic foraminifera	Benthic foraminifera	Fecal pellets	Pyrite
6609-32-1	1	P	FL				6	--	T	--	4	--	89	4	--	--
-2	30	P	FL				5	--	1	--	1	--	86	7	--	--
6610-2-1	1	H	GC	21-38-41			16	2	--	--	30	12	7	1	32	--
-3	60	P	GC	20-33-47												
-4	106	P	GC	8-40-52												
-5	203	P	TS	89-10-01												
-6	207	P	GC	6-29-65												
-10	306	P	TS	28-71-01			89	10	1	--	--	--	--	--	--	--
-11	326	P	TS	37-63-00			89	10	1	--	--	--	--	T	--	--
-12	347	P	TS	56-44-00			90	8	T	--	T	--	T	T	--	--
-13	357	P	TS	53-37-10			89	8	1	--	--	--	2	1	--	--
-14	359	P	TS	69-29-02			92	6	1	--	--	--	1	T	--	--
6705-1-1	4	H	OGS	2-50-48			4	10	--	22	10	50	T	1	--	--
-2	16	H	OGS	3-49-48			29	12	3	19	10	28	--	--	--	--
-3	23	H	OGS	3-61-36			17	16	T	35	12	19	--	T	--	--
-4	35	H	OGS	18-54-28			70	10	2	6	5	6	T	1	--	--
-6	49	H	OGS	66-29-05			89	6	T	2	1	1	T	1	1	--
-7	57	H	OGS	35-45-20			70	8	1	12	3	2	--	1	--	--
-8	63	H	OGS				85	6	3	4	--	1	--	1	--	--
-9	72	H	OGS	56-31-13			87	6	4	T	1	T	--	2	--	--
-10	76	H	OGS	51-30-19			83	4	5	4	1	T	T	3	--	--
-11	136	H	GC	2-43-55			10	6	T	15	19	48	1	1	--	--
-12	184	H	OGS	69-18-13			95	1	1	1	T	1	T	1	--	T
-13	221	H	OGS				92	4	2	1	T	--	T	1	--	--
-14	317	H	OGS				89	7	2	1	--	--	--	1	--	T
6705-2-1	5	H	GC	2-43-55			1	2	--	2	54	38	1	3	--	--
-2	49	H	GC				T	4	--	4	40	46	2	2	1	--
-3	83	H	GC	1-40-59			3	2	--	1	57	31	4	1	--	--

(continued)



Sample number	Depth in core (cm)	Age	Sediment type	% sand % silt % clay	Percent of coarse-fraction by number									
					Detrital grains	Mica	Volcanic glass	Plant fibers	Radiolarians	Diatoms	Planktonic foraminifera	Benthic foraminifera	Fecal pellets	Pyrite
6705-2-4	123	H	GC		7	6	1	5	49	21	5	4	2	1
-5	159	H	GC	4-34-62	15	3	3	1	44	18	3	1	13	T
-7	211	H	GC		5	4	--	1	57	22	4	2	4	1
-8	231	H	GC		6	8	2	6	49	13	11	2	3	--
6705-4-5	139	H	OGS		94	2	1	--	1	T	--	2	--	--
-1	181	H	OGS		92	4	3	1	--	--	--	T	--	--
6705-5-9	356	H	GC	7-40-53										
-12	384	H	GC	12-34-54										
6705-6-1	8	H	GC		5	3	--	5	61	18	1	2	4	--
-6	82	H	OGS	25-54-21	78	6	12	2	1	--	--	1	--	T
-7	91	H	OGS	39-48-13	72	10	14	2	T	T	--	2	T	--
-8	96	H	OGS	21-53-26	45	14	23	12	3	2	--	--	--	--
-24	314	H	GC		18	4	--	--	29	3	16	1	28	--
6705-7-7	369	P	GC		T	36	--	14	10	--	34	6	--	--
-11	408	P	TS	0-43-57	23	18	--	40	5	--	13	T	--	--
-16	485	P	TS		1	65	--	23	--	T	10	--	--	--
-19	529	P	TS		27	61	--	9	--	T	2	1	--	--
6705-8-10	267	P	TS	80-18-02										
-11	284	P	TS	82-17-01										
6705-9-1MC	1	H	GC		1	2	--	T	76	9	3	3	5	--
-2MC	13	H	GC		4	1	T	1	76	7	7	2	3	--
-25	68	H	GC		3	1	4	1	62	13	6	5	6	T
-26	83	H	GC		1	1	--	--	59	7	26	2	4	--
-28	131	H	GC		2	3	--	1	43	6	31	4	11	T
-3	325	P	GC		4	20	--	12	1	--	59	4	--	--
-7	348	P	GC	1-39-60	12	7	--	6	2	--	72	1	--	--
-8	351	P	TS	1-51-48	12	63	--	16	T	1	1	1	--	--
-11	389	P	GC		12	3	--	2	T	--	80	1	1	--

(continued)

Sample number	Depth in core (cm)	Age	Sediment type				Percent of coarse-fraction by number									
							Detrital grains	Mica	Volcanic glass	Plant fibers	Radiolarians	Diatoms	Planktonic foraminifera	Benthic foraminifera	Fecal pellets	Pyrite
6705-9-16	476	P	GC				--	2	--	1	T	--	94	2	T	--
-20	545	P	GC				2	6	--	4	T	--	87	1	--	--
6705-10-25	11	H	GC				6	2	--	1	60	13	11	1	6	--
-24	44	H	GC				13	2	--	2	50	21	5	1	5	T
-23	79	H	GC				3	1	--	1	50	28	9	1	6	T
-21	158	H	GC				2	2	--	1	50	13	25	2	8	T
-1	325	H	GC				2	1	--	T	49	3	32	4	7	3
-2	334	H	TS	0-30-70			3	5	--	32	4	54	1	--	--	1
-3	343	H	TS	2-39-59			36	14	--	30	1	15	--	3	--	--
-4	356	H	TS				22	13	--	37	2	22	1	2	--	--
-5	371	H	TS	1-40-59			28	10	--	40	2	14	1	6	T	T
-6	385	H	TS	4-43-53			43	19	--	26	3	6	1	2	--	--
-7	392	H	TS	19-76-05			77	18	--	3	--	T	1	2	--	--
-9	457	H	TS				94	5	--	--	T	--	T	--	--	--
-12	520	P	TS				4	60	--	22	T	9	2	1	--	--
-18	568	P	GC	7-49-44			1	--	--	--	6	--	45	T	47	2
6705-11-7	194	P	TS	0-54-46												
-8	200	P	GC	1-43-56												
-16	314	P	GC	0-27-73												
6705-13-5	43	P	PC				21	23	--	48	7	--	1	--	--	--
-6	91	P	TS	16-44-40												
-8	131	P	TS	1-32-67												
-10	266	P	TS				35	22	--	25	--	1	13	4	--	--
-11	293	P	TS	12-87-01			88	11	--	1	--	--	--	--	--	--
-12	295	P	TS	0-44-56			81	9	--	8	--	--	2	T	--	--
6705-14-9	93	H	GC				2	4	--	1	67	3	7	5	16	--
-27	519	P	GC	0-37-63			14	9	--	12	2	T	60	2	1	--
-28	521	P	TS	0-39-61			9	49	--	34	4	1	4	T	--	--

(continued)

Sample number	Depth in core (cm)	Age	Sediment type	% sand % silt % clay	Percent of coarse-fraction by number									
					Detrital grains	Mica	Volcanic glass	Plant fibers	Radiolarians	Diatoms	Planktonic foraminifera	Benthic foraminifera	Fecal pellets	Pyrite
6705-16-8	74	P	GC	0-17-83	21	2	--	17	--	--	60	--	--	--
-12	238	P	TS	55-38-07										
-13	247	P	TS	73-24-03										
-14	259	P	TS	68-28-04										
-15	276	P	TS	72-24-04										
6705-20-1	150	H	OGS	1-43-56										
-2	170	H	OGS	1-43-56										
-3	190	H	OGS	1-42-57										
-4	210	H	OGS	1-43-56										
-5	230	H	OGS	1-44-55										
-6	250	H	OGS	1-48-51										
-7	270	H	OGS	2-47-51										
-8	290	H	OGS	2-49-49										
-9	310	H	OGS	21-66-13										
6705-21-2	110	H	GC	4-46-50										
-8	70	H	GC	8-46-46										
-12	123	H	GC	1-44-55										
-15	196	H	GC	3-42-55										

APPENDIX IV. PERCENT BY WEIGHT OF ORGANIC CARBON  
AND CALCIUM CARBONATE IN SEDIMENT SAMPLES

Sample number	% Calcium carbonate	% Organic carbon	Lithology	Age
6508-K1-6	1.24	1.20	GC	H
-8	0.25	1.40	GC	H
-9	1.17	2.26	OGS	H
-16	1.15	0.58	GC	H
-26	1.03	0.67	GC	H
-33	2.17	2.27	OGS	H
-39	3.25	1.93	OGS	H
6509-11-3	7.41	0.33	GC	P
6509-15-2	0.58	0.94	GC	H
-18	0.33	0.41	GC	P
-19	0.66	0.35	GC	P
6509-15A-14	0.48	2.47	OGS	H
-15	0.00	2.39	OGS	H
-16	0.96	0.47	OGS	H
-17	0.88	0.69	OGS	H
-20	0.42	2.46	OGS	H
-21	0.33	2.17	OGS	H
-22	1.08	0.80	OGS	H
-24	1.08	0.49	OGS	H
-25	1.17	0.67	OGS	H
-26	0.75	0.23	OGS	H
-28	0.56	2.41	OGS	H
-29	0.88	2.19	OGS	H
-30	0.72	2.13	OGS	H
-31	1.20	0.30	OGS	H
-32	0.96	0.19	OGS	H
-34	0.42	2.07	OGS	H
-35	0.67	2.46	OGS	H
-36	0.92	2.55	OGS	H
-37	4.08	1.97	OGS	H
-38	0.50	2.19	OGS	H
-39	0.33	2.31	OGS	H
-40	1.17	2.32	OGS	H
6509-25A-11	0.17	0.85	GC	H
6509-26-3	1.60	1.86	GC	H
-4	0.46	2.30	OGS	H
-5	0.68	2.52	OGS	H
-6	0.97	2.05	OGS	H
-8	1.17	1.06	GC	H
-13	1.50	0.90	GC	H
-14	0.30	2.31	OGS	H
-15	0.60	2.01	OGS	H
-16	0.83	0.86	GC	H
-25	0.90	1.17	GC	H

(continued)

Sample number	% Calcium carbonate	% Organic carbon	Lithology	Age
6509-26-32	0.00	2.81	OGS	H
-36	0.17	2.89	OGS	H
6509-27-20	2.33	0.77	GC	H
6509-28-5	1.92	0.34	TS	P
-6	6.52	0.40	GC	P
-8	1.75	0.39	TS	P
6609-28-1	0.50	0.38	PC	P
6609-31-1	2.17		GC	H
-2	3.17		GC	H
-3	2.83		GC	H
-4	1.83		GC	H
-5	0.92		GC	H
-6	1.00		GC	H
-7	2.42		GC	H
-8	3.17		GC	H
-9	1.17		GC	H
-10	2.50		GC	P
6609-32-B	41.4		FL	P
-E	42.8		FL	P
6609-25-	31.4		FL	P
6609-25-	25.3		FL	P
6705-5-22a	1.17	1.91	OGS	H
-22b	1.17	1.68	OGS	H
-24	1.08	1.67	OGS	H
-25	1.00	2.20	OGS	H
6705-13-7	0.83	0.35	PC	H

APPENDIX V. HEAVY MINERAL COMPOSITION FOR THE SAND FRACTION OF SEDIMENT SAMPLES  
(Mineral quantities expressed as percent of total counts;\*\* only pyroxenes and amphiboles counted)

Sample number	6509-11-1	6509-14-1	6509-14-4	6509-15A-26	6509-25A-17*	6509-26-12*	6509-26-38*	6509-27-32*	6509-27-33*	6609-24-43	6609-27-8	6609-28-6	6609-28-10	6609-30-13	6609-30phl-2	6609-31-11	6609-31-17**	6610-2-5	6610-2-12	6705-6-31-	6705-8-5	6705-8-9	6705-11-4**	6705-14-14**	6705-16-9**	6705-16-16
AGE	P	P	P	H	H	H	H	H	H	P	P	P	P	P	P	P	P	P	H	P	P	P	P	P	P	P
SEDIMENT TYPE	TS	G	G	OGS	OGS	OGS	OGS	OGS	OGS	OGS	TS	PC	PC	PC	G	TS	TS	TS	TS	OGS	TS	TS	TS	TS	TS	TS
PHYSIOGRAPHIC ENVIRONMENT	WP	CC	CC	CC	CC	CC	CC	CC	CC	CC	V	CC	CC	CC	CC	V	V	V	V	TC	CC	CC	WP	WP	CC	CC
Actinolite-Tremolite	1.9	1.5	1.4	4.4	1.2	3.9	1.2	2.0	3.4	4.0	3.3	1.4	1.5	5.4	3.4	1.5		0.9	1.9		1.0	1.0				0.9
Andalusite	1.9	---	---	1.0	0.3	---	0.6	---	---	---	1.9	1.0	---	0.5	---	1.4		---	0.5		1.5	1.0				1.4
Apatite	---	---	---	2.4	---	---	---	---	---	1.5	---	---	---	---	---	---		---	---		---	0.5				---
Basaltic Hornblende	---	---	0.9	1.9	0.9	0.9	1.6	1.9	0.7	1.5	0.5	---	0.5	---	0.5	2.4		1.4	1.4		0.5	1.0				2.9
Biotite	2.4	2.0	1.4	2.4	3.2	3.6	1.6	0.3	0.3	4.5	0.5	1.0	1.4	1.0	0.5	0.5		2.3	8.5		5.0	2.0				12.1
Chlorite	2.4	---	0.4	1.4	---	---	---	---	---	4.5	---	0.5	1.0	1.0	---	0.5		1.9	9.5		5.0	2.5				6.8
Clinopyroxene	16.7	11.5	13.4	12.1	22.5	19.6	30.9	27.5	31.6	10.9	11.1	11.0	7.6	9.8	14.5	14.2	16	18.1	10.9	34	14.0	16.0	43	32	31	12.1
Clinzoisite-Zoisite	4.3	2.5	3.7	2.9	2.3	2.1	1.6	1.3	2.7	3.0	3.8	6.2	2.4	2.0	2.4	2.4		3.2	3.3		2.5	2.0				4.8
Enstatite	0.5	0.5	0.4	2.9	0.3	0.9	---	---	1.0	0.5	0.5	1.4	0.5	1.0	---	1.0	1	0.9	1.9	4	1.0	3.5	1	4	1	0.5
Epidote	2.9	1.5	0.4	---	1.2	0.6	1.9	1.9	1.7	2.5	1.4	3.4	5.3	4.4	1.9	1.9		3.2	0.9		4.5	1.0				2.9
Garnet	1.0	---	0.4	0.5	2.0	0.6	3.4	1.0	1.3	---	---	---	0.5	---	0.5	1.0		---	---		0.5	1.0				---
Hematite	2.4	1.0	0.9	---	---	---	---	0.6	---	2.5	---	1.0	1.0	---	---	0.5		0.5	2.4		0.5	---				1.4
Hornblende																										
blue-green	2.9	1.0	4.2	1.0	4.4	3.3	5.0	4.2	5.3	1.0	8.7	11.9	8.1	8.8	2.4	4.7	36	1.4	2.4	24	4.5	3.0	8	25	26	8.7
brown	---	0.5	1.4	0.5	0.6	2.1	0.9	0.3	1.7	2.0	1.0	1.9	1.4	1.0	---	1.9	3	0.5	0.5	2	0.5	0.5	2	2	2	---
common	12.8	9.0	14.0	16.5	21.0	16.5	19.9	17.4	20.1	12.4	14.9	9.6	20.1	14.1	7.8	12.3	35	13.4	12.3	22	10.5	13.5	26	29	32	13.5
Hypersthene	3.3	10.5	11.6	5.8	8.4	4.9	10.6	11.0	8.3	4.5	5.3	6.7	2.9	5.8	7.8	11.4	9	7.9	3.3	14	4.5	7.5	20	8	8	1.9
Kyanite	---	---	---	0.5	0.3	---	0.3	---	---	---	0.5	0.5	---	---	0.5	---		---	---		---	---				---
Muscovite	1.0	---	0.4	1.0	14.2	16.1	---	1.0	---	4.0	---	1.4	1.0	1.0	---	0.5		---	1.4		1.0	1.0				2.9
Olivine	---	---	0.4	3.9	0.3	---	---	0.3	0.3	1.0	1.4	0.5	0.5	---	0.5	0.5		0.5	---		0.5	0.5				---
Sillimanite	---	1.0	0.9	---	---	---	0.3	---	0.7	---	---	---	---	---	---	---		---	---		---	---				---
Sphene	0.5	0.5	---	---	1.5	0.3	1.2	0.3	1.0	1.0	0.5	---	---	0.5	---	0.5		---	---		0.5	2.5				0.5
Spinel	---	3.0	---	1.0	---	---	---	---	---	0.5	1.4	---	0.5	0.5	0.5	0.5		1.9	---		1.0	2.5				0.5
Tourmaline	0.5	---	---	0.5	0.6	---	---	---	---	---	0.5	---	1.4	---	---	---		---	---		0.5	0.5				---
Wollastonite	1.0	0.5	0.4	---	---	---	---	---	---	0.5	---	---	1.0	---	---	---		---	---		---	---				---
Zircon	---	---	---	---	---	---	0.3	---	---	0.5	---	1.4	0.5	0.5	---	1.0		---	---		---	---				---
Opagues	5.7	13.5	7.8	4.8	0.6	0.9	2.5	1.0	0.3	3.5	3.4	6.2	7.6	6.3	7.3	6.6		7.4	2.4		4.5	7.5				0.9
Rock fragments	9.1	2.0	7.9	5.8	0.6	6.7	---	7.4	6.0	8.9	6.7	3.8	3.8	4.4	7.3	4.3		4.6	9.0		4.0	2.5				7.7
Weathered grains	22.4	39.0	27.9	20.3	11.9	15.8	12.8	19.0	12.3	21.8	29.3	24.0	25.4	30.3	39.3	26.0		27.3	24.1		24.5	18.0				15.5
Others	3.4	1.5	1.9	6.8	1.7	1.2	2.5	1.0	1.0	3.5	3.4	5.3	5.3	2.0	2.9	1.9		2.3	4.4		7.0	3.5				1.8

APPENDIX VI. QUANTITATIVE ANALYSES OF CHLORITE, ILLITE AND MONTMORILLONITE  
FROM X-RAY DIFFRACTION RECORDS

Sample number	Depth in core	Physiographic environment	Age	Sediment type	% Chlorite	% Illite	% Mont- morillonite
6508-K1-4*	170	CC	H	OGS	28	21	51
6508-K1-6	104	CC	H	GC	18	22	60
6508-K1-17*	278	CC	H	OGS	26	21	53
6509-10PHL-2	110	CC	H	OGS	24	26	50
6509-10PHL-4	21	CC	H	GC	17	23	60
6509-11-3	85	NF	P	GC	21	39	40
6509-15-18	196	CC	P	GC	30	30	40
6509-15-21	235	CC	P	GC	28	36	36
6509-17PHL-3	11	CC	H	GC	16	23	61
6509-25A-6*	85	CC	H	OGS	28	22	50
6509-26-24*	115	CC	H	OGS	24	22	54
6509-27PHL-2	5	CC	H	OGS	20	22	58
6509-27-24*	529	CC	H	OGS	31	22	47
6509-27-25*	370	CC	H	OGS	25	17	58
6509-27-27*	7	CC	H	OGS	30	22	48
6609-24-9	221	CC	H	GC	23	30	47
6609-24-24	488	CC	H	GC	26	28	46
6609-25-20	310	CC	P	GC	32	37	31
6609-26-27	370	TC	P	GC	27	30	43
6609-28-1	2	CC	P	PC	28	24	48
6609-28-3	50	CC	P	PC	21	18	61
6609-28-4	100	CC	P	PC	27	23	50
6609-30-8	150	CC	P	PC	24	16	60
6609-31PHL-1	6	V	H	GC	23	28	49
6610-2-1	2	V	H	GC	14	23	63
6610-2PHL-4	14	V	H	GC	14	27	59
6705-1PHL-2	4	WC	H	GC	21	24	55
6705-2PHL-2	12	TC	H	GC	25	24	51
6705-5-6	351	WC	H	GC	19	21	60
6705-5-7	353	WC	H	OGS	17	28	55
6705-6-20	257	TC	H	OGS	22	26	52
6705-10-13	530	TC	P	GC	24	32	44
6705-11PHL-4	4	NF	H	GC	24	29	47
6705-11-12	240	NF	P	GC	39	28	33
6705-11-13	245	NF	P	GC	25	41	34
6705-12PHL-5	4	CC	H	GC	22	27	51
6705-13-12	295	CC	P	GC	36	28	36
6705-16PHL-1	9	CC	H	GC	17	36	47
6705-21PHL-1	30	CC	H	GC	26	27	47

## APPENDIX VII. CHANNEL DIMENSIONS ON CROSS-SECTIONAL PROFILES

Distance from head of Willapa canyon(km)	Core	Depth (M)	Height of west bank	Height of east bank	Maximum channel relief	Bank relief	Top width	Bottom width
80	6705-1	2308	Seamount	Seamount				
116	6705-4	2582	2494	2516	88	22	2700	650
131		2640	2523	2564	117	40	2000	750
138	6705-5	2662	2564	2573	99	9	2500	1000
153		2713	2606	2637	107	31	2500	1000
157	6508-K1	2706	2609	2648	93	39	1250	750
165		2728	2618	2679	110	61	2000	1000
166		2741	2651	2706	90	55	1500	7750
172		2752	2662	2682	90	20	2900	800
185	6705-8	2770	2684	2701	86	17	2500	1250
201		2794	2712	2721	82	9	2000	1000
205		2791	2712	2734	79	22	2750	1000
220		2818	2749	2767	69	18	3500	1500
237	6705-13	2847	2767	2785	80	18	3000	2000
248		2864	2781	2803	83	22	3250	1250
257		2867	2827	2834	40	7	2000	1300
263	6509-10	2862	2823	2829	39	6	3500	2250
265		2871	2811	2844	60	33	5300	3500
277		2913	2815	2858	98	43	3600	1250
281	6609-30	2909	2807	2853	102	46	4200	1250
292	6509-14	2922	2842	2834	88	8	2000	1200
303		2937	2817	2817	120	0	2500	750
307		2964	2834	2834	130	0	4500	1500
310	6609-28	2966	2845	2834	132	11	4000	1500
324	6509-15A	3001		2853			3000	2000
333		3012	2893	Seamount			6000	4250
337		3036	2867	2822	214	45	6500	4000
339		3028	2856	2864	172	8	6500	4500
340		3028	2844	2856	184	12	7000	4250
348		3038	2853	2893	185	40	7500	1250
357	6509-17	3039	2853	2926	186	73	5000	1500
367	6705-17	3054	2853	2871	201	18	6500	2500
373		3058	2844	2884	214	40	6500	1250
377		3069	2853	2875	216	22	7500	2500
381	6509-27	3102	2847	2882	255	35	6250	1000
392		3109	2889	2919	220	30	4000	1500
397		3122	2882	2908	240	26	4750	1000
406		3129	2862	2908	267	46	5000	750
415	6609-24	3124	2862	2889	262	27	5250	1100
417		3131	2860	2895	271	35	5250	750
422		3140	2853	2869	287	16	5000	1250
432		3138	Seamount	2935	---	---	3500	1000
435	6705-19	3149	2867	2926	282	59	4000	750
440		3146	2862	2926	284	64	4750	1000

(continued)



Distance from head of Willapa canyon(km)	Core	Depth (M)	Height of west bank	Height of east bank	Maximum channel relief	Bank relief	Top width	Bottom width
448		3149	2889	2926	260	47	6000	750
460	6509-26	3147	2891	2926	256	45	7500	1000
478		3151	2853	2889	298	36	8000	1500
483	6705-20	3162	Seamount	2884	---	--	6500	1200
490		3153	2454	2878	699	424	13000	1500
505	6609-11	3155	2725	2926	430	201	11000	1850
517		3155	2898	2935	257	37	7500	1800
522		3164	2889	2917	275	28	9300	1400
530	6604-5	3167	2780	2908	387	128	16500	1300
540		3206	2437	2932	779	495	7500	1300
552		3222	2880	2926	342	46	13000	1300
565		3224	2432	2963	792	531	8300	930
583		3241	2944	2944	297	--	9700	550
592	6604-4	3246	2926	2963	320	37	9300	300
613		3252	3008	2377	875	931	10200	3370
622		3259	2459	2345	814	114	16000	V
630		3274	2395	2761	879	366	9500	V
637		3307	2844	2532	765	312	13700	500
652		3307	2642	2715	665	73	11200	200
657		3307	3005	2743	564	262	7400	450
659		3438	3164	3063	375	101	8300	2800
660		3442	3237	3063	379	174	7400	2800
662	6609-19	3444	2360	3146	1084	786	28000	4600
684	6604-1	3325	3069	3100	256	31	6500	2200
700		3332	3091	3118	241	27	9340	3050
717		3334	3131	3182	203	51	6100	2300
735	6609-25A	3336	3151	3188	185	37	5560	2700
754		3343	3182	3204	161	22	6280	2870
767		3356	3177	3213	179	36	6470	2150

APPENDIX VIII. SEDIMENTATION RATES AND PERCENTAGE OF CORE  
CONSISTING OF COARSE MATERIAL

Core number	Percent of section consisting of coarse material		Postglacial sedimentation rates (cm/1000 years)	
	Postglacial	Pleistocene	Pelagic	Over-all
6508-K1	96		6	71
6509-10	94			> 37
6509-12		99		
6509-14		98	<0.5	< 1
6509-15	88	1	2	16
6509-15A	93		4	78
6509-17	96			13
6509-25A	91		3	26
6509-26	95		6	118
6509-27	97		4	125
6509-28	5	12	6	
6509-29	3		6	
6604-4	97			> 70
6604-30	2	38	5	
6604-31	15	40	6	
6609-11	100			> 33
6609-19	98			>131
6609-24	92		9	92
6609-25	3		13	
6609-26	7	45	7	
6609-27	24	34	5	7
6609-28			<0.5	
6609-29	9	91	6	
6609-31	3	88	8	
6610-2	0	93	2	
6705-1	97			>26
6705-2	69		>14	>24
6705-4	99			>32
6705-5	93		> 7	>47
6705-6	81	89	5	>46
6705-7	47	11	8	13
6705-8	76	99	4	14
6705-9	63	41	7	14
6705-10	92		3	45
6705-11	11	61	4	
6705-12	8	32	4	
6705-14	56	24	4	11
6705-16	3	93	6	
6705-17	3		6	
6705-20	100			>90
6705-21	40			27

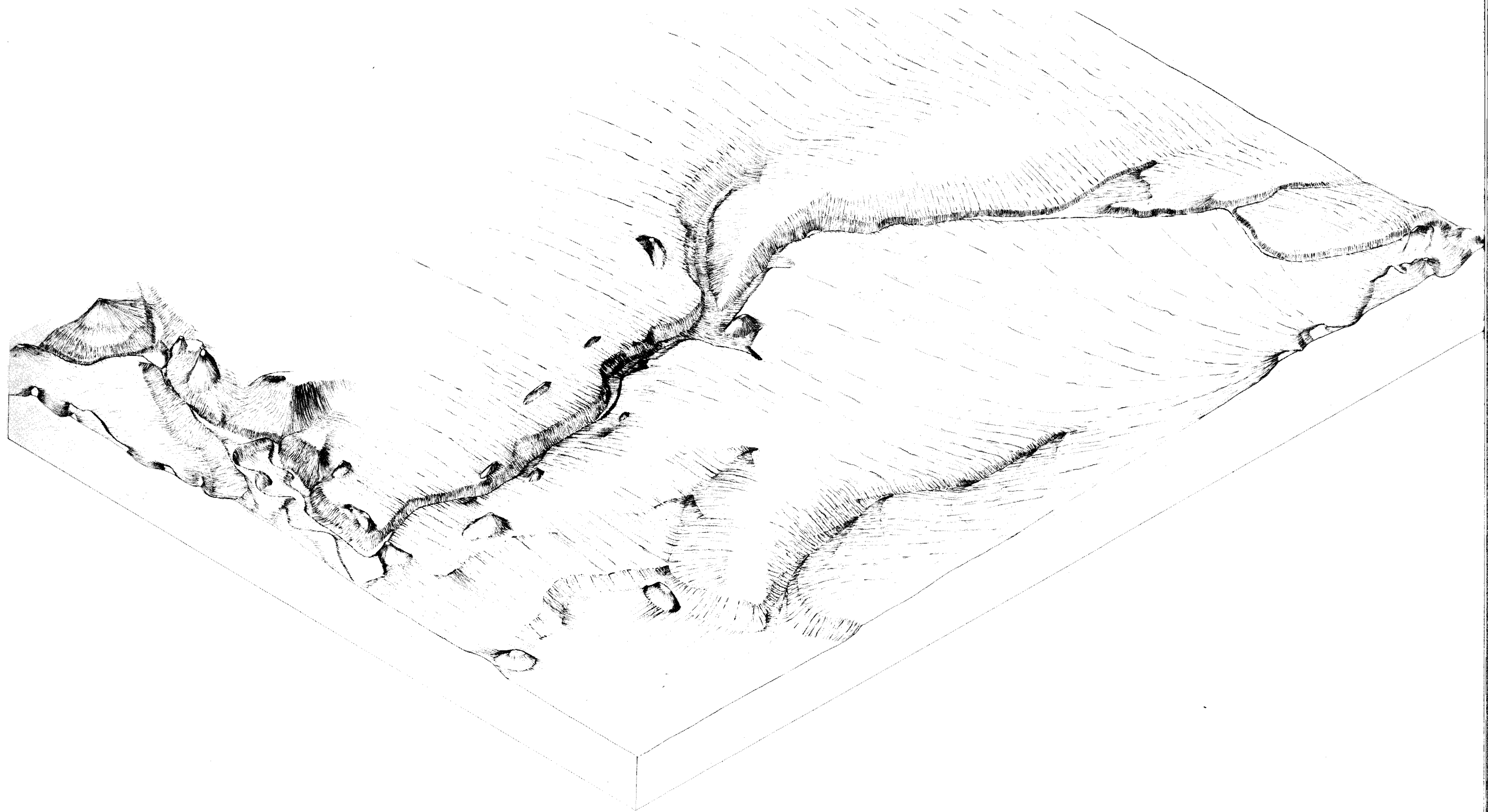


Plate 2. Physiography of Cascadia Channel and vicinity (vertical exaggeration 20 X)

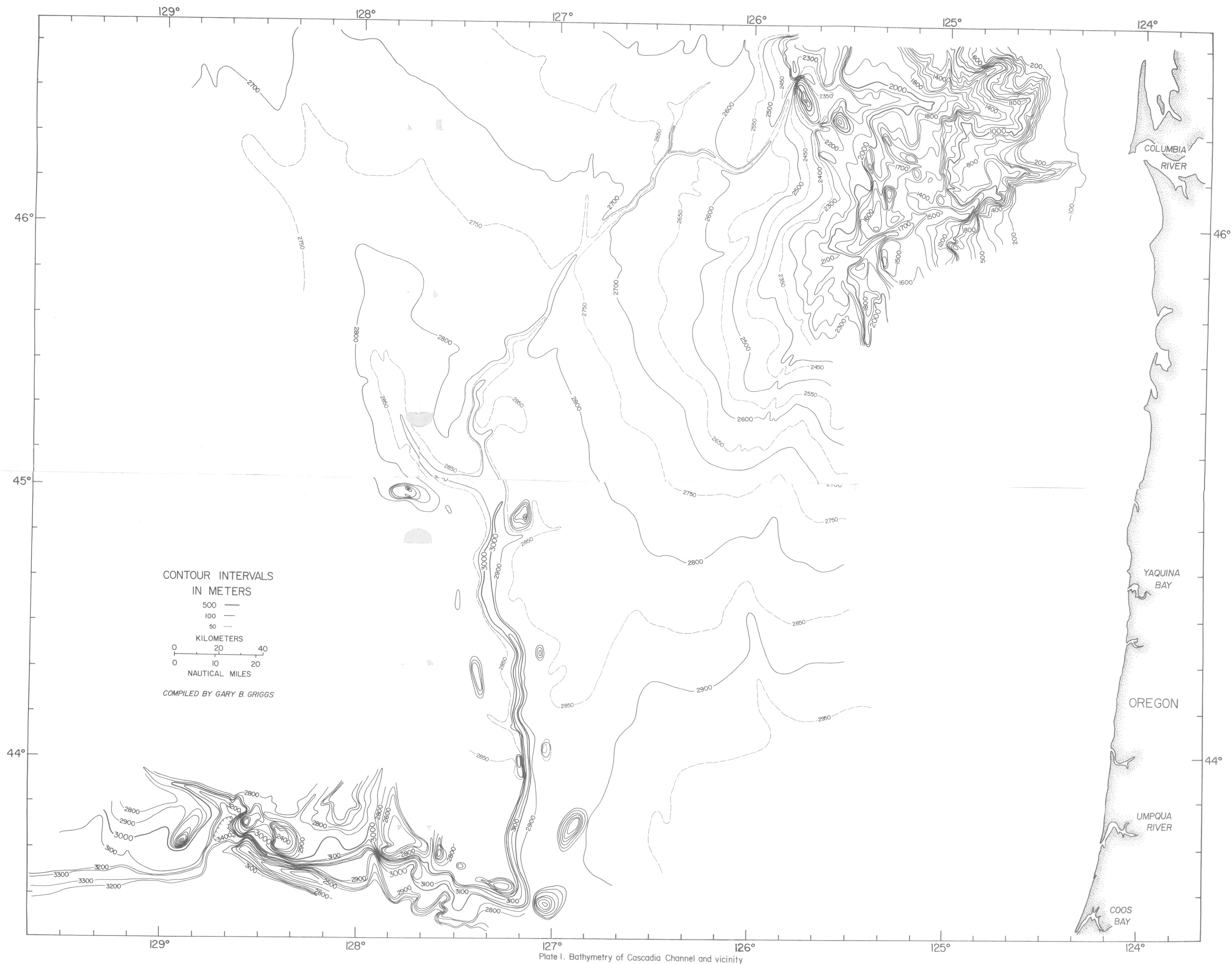


Plate I. Bathymetry of Cascadia Channel and vicinity